

Identification and functional characterisation of three novel
Proline Rich Proteins that are Mitogen Activated Protein
Kinase substrates

Dissertation

zur Erlangung des
Doktorgrades der Naturwissenschaften (Dr. rer. nat.)

der

Naturwissenschaftlichen Fakultät I – Biowissenschaften –

der Martin-Luther-Universität
Halle-Wittenberg,

vorgelegt

von Herrn Mieder A. T. Palm-Forster
geb. am 08.03.1982 in Johannesburg

Gutachterin bzw. Gutachter:

1. Prof. Dr. Dierk Scheel
2. Prof. Dr. Sacha Baginsky
3. Prof. Dr. Wolfgang Dröge-Laser

Dissertation defence: Halle (Saale), 26th February 2013

Acknowledgements

I earnestly thank Prof. Dr. Dierk Scheel and Dr. Justin Lee for the opportunity to undertake my Ph.D. in the department of Stress and Developmental Biology at the Leibniz Institute of Plant Biochemistry.

I would also like to thank Dr. Justin Lee for the critical reading of this dissertation and his supervision and assistance during my Ph.D.

I would like to acknowledge the funding received from the international graduate program Exzellenznetzwerk Biowissenschaften “Strukturen und Mechanismen der biologischen Informationsverarbeitung” and that received from the Leibniz Institute of Plant Biochemistry, which made this dissertation possible.

I would like to thank the following people for all the expert assistance and encouragement during my time at the Leibniz Institute of Plant Biochemistry: Dr. Marcel Quint, Dr. Caroline Delker, Dr. Bettina Hause, Dr. Thomas Vogt, Dr. Douglas Grubb, Dr. Kai Naumann, Dr. Marco Trujillo and Dr. Lore Westphal. I would also like to acknowledge the technical assistance provided by Nicole Bauer, Sylvia Kruger, and the highly skilled team of horticulturalists, especially Thomas Franz and Alice Bühring.

I hereby proclaim that I had the best crew in the entire Germany. Thank you to all my friends for the support and understanding, the work-related discussions, the non-work-related discussions, and the memorable moments. This applies especially to Lennart Eschen-Lippold, Michaela Kopischke, Pascal Pecher, Kati Mielke, Martin Stegmann, and Martin Nin Brauer.

A special mention to Dr. Lennart Eschen-Lippold for the unwavering support and encouragement he provided. It was great.

To my significant other, Leah, thank you for being there for me not only through the best times, but most importantly, the tough times. You are an incredible individual and I consider myself exceptionally privileged to be your partner. LLV!

Last, but certainly not least, I have the utmost gratitude and respect for my mother, Therza. I would not be at this point in my life if it had not been for her sacrifice and determination. The cliché of words not being able to convey the true depth of thanks and appreciation holds true now more than ever. So I shall simply say “Thank you Mom!”

Abstract

Plants are surrounded by a complex, ever changing environment. The MAPK signaling cascade is central to conveying the perceived signals of pathogen presence to downstream substrates through phosphorylation events. These modifications lead to modulation of various defence related responses. A small number of these MAPK substrates have been identified to date. Three proteins, Proline Rich Protein (PRP), PRP Homolog 1 (PH1) and PRP Homolog 2 (PH2), are *in vitro* kinase substrates of MPK3 and MPK6. Targeted mutagenesis revealed that the PRP-like proteins possess a MAPK docking domain that is required for the interaction with MAPKs and revealed that MPK3 and MPK6 target a conserved phospho in all three proteins. Both PRP and PH1 are transcriptionally activated by the MAMPs flg22 and elf18. Co-expression of the PRP-like proteins augment the promoter activities of the defense related genes, *FRK1* and *NHL10*. Finally, transgenic lines over-expressing PRP displayed an increased resistance to *Pseudomonas syringae*. This study identified the PRP-like proteins as a novel class of MAPK substrates that may have a role in defence related responses in Arabidopsis.

Keywords: MAPK, MAMP, flg22, elf18, MAPK substrates, *Pseudomonas syringae*, FRK1, NHL10, MPK3, MPK6

Pflanzen leben in einer komplexen wechselhaften Umgebung. Zentraler Bestandteil der Abwehrantwort sind MAPK Signalkaskaden, die nach Pathogenerkennung durch Phosphorylierung von Substratproteinen eine Signalweiterleitung ermöglichen. Diese Phosphorylierung führt zur Modulation verschiedener Abwehrantworten. Nur eine geringe Zahl an MAPK-Substratproteinen ist beschrieben. Diese Arbeit identifiziert eine neue Klasse von MAPK-Substraten, Proline Rich Protein (PRP), PRP Homolog 1 (PH1) und PRP Homolog 2 (PH2). Diese Proteine sind *in vitro* Kinase-Substrate von MPK3/6. Gezielte Mutagenese-Experimente zeigten, dass PRP-ähnliche Proteine eine *MAPK docking domain* besitzen sowie eine konservierte Phosphorylierungsstelle vorliegt. Flg22 und elf18 können PRP und PH1 transkriptionell aktivieren. PRP-ähnliche Proteine können die Promoteraktivität der Abwehr-relevanten Gene *FRK1* und *NHL10* erhöhen. In PRP-Überexpressionslinien wurde eine erhöhte Resistenz gegen *P. syringae* nachgewiesen. Diese Arbeit identifizierte PRP-ähnliche Proteine als neue MAPK-Substratklasse, die eine Rolle in der Abwehrantwort Arabidopsis spielen.

Keywords: MAPK, MAMP, flg22, elf18, MAPK substrat, *Pseudomonas syringae*, FRK1, NHL10, MPK3, MPK6

Table of Contents

I. Introduction	1
1. Plant-microbe/parasite interactions	1
2. Plant Immunity	1
2.1 Receptor-like protein kinases (RLKs)	3
2.2 PAMP triggered immunity (PTI)	4
2.3 Effector triggered immunity (ETI)	5
2.4 Systemic acquired resistance (SAR)	7
3. Mitogen activated protein kinases (MAPKs)	7
3.1 MAPKs signalling in <i>Arabidopsis thaliana</i>	8
3.1.1 MAPK signalling and Biotic stimuli	9
3.1.2 MAPK signalling and Abiotic stimuli	13
3.1.3 Roles of MAPK cascades in plant development	14
4. Aim of study	16
II. Materials and Methods.....	19
1. Consumables	19
2. Molecular biological techniques	19
2.1 Polymerase Chain Reaction (PCR)	19
2.2 Cloning	19
2.3 Plasmid preparation	19
2.4 Restriction analysis and Sequencing	20
2.5 RNA extraction, cDNA synthesis and Quantitative Real time PCR	20
2.6 Site directed mutagenesis	20
2.7 Electrophoretic analysis	21
2.8 Primers	21
2.9 Transformation	21
2.9.1 <i>Escherichia coli</i>	21
2.9.2 <i>Saccharomyces cerevisiae</i>	21
2.9.3 <i>Nicotiana benthamiana</i>	22
2.9.4 <i>Arabidopsis thaliana</i>	22
2.9.5 Mesophyll protoplasts	22
3. Protein biochemical techniques	23
3.1 Recombinant protein expression	23

3.2	Recombinant protein purification	23
3.3	Protein extraction from plant material.....	24
3.4	SDS-PAGE electrophoresis and Western blot analysis	24
3.5	Electrophoretic Mobility Shift Assay (EMSA) analysis	25
3.6	Promoter activity analysis	25
4.	Plant analysis	25
4.1	Seedling assays	25
4.2	Root growth inhibition assays	26
4.3	Pathogen assays	26
5.	Microscopy.....	27
6.	Statistical analysis	27
7.	Online Resources.....	27
III.	Results.....	29
1.	Evaluation of MAPK interaction	29
1.1	Analysis of PRP-like proteins as MAPK interactors by a Yeast-two-hybrid screen 29	
1.2	Bimolecular Fluorescence Complementation (BiFC).....	29
1.3	<i>In vitro</i> phosphorylation assay	31
1.4	<i>In silico</i> sequence analysis of PRP and its homologs	33
1.4.1	Substrate analysis by targeted site directed mutation.....	34
2.	Gene expression profile of <i>PRP</i> , <i>PH1</i> and <i>PH2</i> in <i>A. thaliana</i>	38
2.1	Effect of MAMP treatment on expression of <i>PRP</i> -like genes	40
2.2	Effect of abiotic stresses on expression of <i>PRP-like</i> genes	43
3.	Promoter Analysis	43
3.1	Analysis of <i>PRP</i> , <i>PH1</i> and <i>PH2</i> promoter activity in response to flg22 or elf18 treatments.....	43
3.2	Effect of PRP-like proteins on the MAMP-responsive promoter <i>FRK1</i>	44
3.3	Effect of PRP-like proteins on the <i>NHL10</i> MAMP-responsive promoter.....	48
3.4	Are PRP and PH1 able to augment their promoter activity?.....	52
3.5	Are PRP-like proteins able to bind the investigated promoters?	55
4.	Effects of MAMP-treatments on the stability of PRP-like proteins	57
5.	Subcellular localization of PRP-like proteins	58
5.1	Subcellular localization of PRP-like proteins after MAMP treatment	60
6.	Phenotypic Analysis	61
6.1	Developmental effects of overexpressing PRP-like proteins.....	61

6.2	Root growth inhibition assay of PRP-like overexpressing lines.....	61
6.3	<i>Pst</i> DC3000 growth assay with PRP-like overexpressing lines	64
IV.	Discussion	67
1.	PRP-like proteins interact with stress-activated MAPKs	67
2.	Post-translational modification by MAPKs and target specificity for PRP-like proteins	69
3.	Potential functions of PRP-like proteins in innate immunity	73
4.	The localisation of the PRP-like proteins.....	75
5.	Potential functions inferred from the expression patterns of <i>PRP</i> -like genes.....	76
6.	Resistance phenotype of PRP-overexpressing plants.....	78
V.	Summary	81
VI.	Appendix.....	83
VII.	References.....	87
VIII.	Erratum.....	96
IX.	Curriculum Vitae.....	98

List of Abbreviations

°C	degrees Celsius
µg	Microgram
µl	Microliter
µM	Micromolar
<i>A. thaliana</i>	<i>Arabidopsis thaliana</i>
<i>A. tumefaciens</i>	<i>Agrobacterium tumefaciens</i>
ABA	Abscisic acid
ABI3VP1	ABA INSENSITIVE 3/V-PPASE 1
ACS6	1-AMINOCYCLOPROPANE-1-CARBOXYLIC ACID SYNTHASE 6
Ade	Adenine
Ala	Alanine
AS2	ASSYMMETRICAL LEAVES 2
Avr	Avirulence
AvrB	Avirulence protein B from <i>Psg</i>
AvrPto	Avirulence protein from <i>Pto</i>
AvrPtoB	Avirulence protein from <i>Pto</i> with functional similarity to AvrPto
<i>B. cinerea</i>	<i>Botrytis cinerea</i>
BAK1	BRI1-ASSOCIATED RECEPTOR KINASE 1
bZIP	Basic leucine-zipper
CAT1	CATALASE 1
CC	Coiled coil motif
CDC4	CELL DIVISION CONTROL 4
cDNA	copy DNA
CDPK	CALCIUM DEPENDENT PROTEIN KINASE
CERK1	CHITIN ELICITOR RECEPTOR KINASE 1
CFP	CYAN FLUORESCENT PROTEIN
Col-0	<i>Arabidopsis</i> accession Columbia
CTR1	CONSTITUTIVE TRIPLE RESPONSE 1
CYP	Cytochrome P450
DAMP	Damage-associated molecular pattern
DEX	Dexamethasone
DNA	Deoxyribonucleic acid
dpi	Days post infection
DTT	Dithiothreitol
<i>E. coli</i>	<i>Escherichia coli</i>
e.g.	Example
EDS1	ENHANCED DISEASE SUSCEPTIBILITY 1
EDTA	Ethylenediaminetetraacetic acid
EFR	EF-Tu receptor
EF-Tu	Prokaryotic elongation factor
EGTA	Ethylene glycol tetraacetic acid
EIN3	Ethylene-insensitive 3

elf18	18 amino acid domain in EF-Tu
EMSA	Electrophoretic mobility shift assay
ERF104	ETHYLENE RESPONSE FACTOR104
ET	Ethylene
et al.	<i>et alteri</i>
ETI	Effector triggered immunity
ETS	Effector-triggered susceptibility
flg22	22 amino acid domain in flagellin
FLS2	FLAGELLIN-SENSING 2
FRK1	flg22- INDUCED RECEPTOR LIKE KINASE1
g	Grams
GFP	GREEN FLUORESCENT PROTEIN
GST	Glutathione-S-transferase
GUS	β -glucuronidase
H ₂ O ₂	Hydrogen peroxide
His	Histidine
HR	Hypersensitive response
HRP	HYPERSENSITIVE REACTION AND PATHOGENICITY
HSF	HEAT SHOCK FACTOR
HSP90	HEAT SHOCK PROTEIN 90
i.e.	<i>Id est</i>
IPTG	Isopropyl β -D-1-thiogalactopyranoside
ISR	Induced systemic resistance
JA	Jasmonic acid
L	Liter
LC-MS/MS	Liquid chromatography Tandem Mass Spectrometry
Leu	Leucine
LFY	LEAFY
LiAc	Lithium acetate
LOX	Lipoxygenase
LUC	Luciferease
M	Molar
MAMP	Microbe-associated molecular pattern
MAP2K/MKK	MAP kinase kinase
MAP3K/MKKK	MAP kinase kinase kinase
MES	2-(N-morpholino)ethanesulfonic acid
min.	Minute
MKP2	MAPK phosphatase 2
MKS1	MAP kinase substrate 1
ml	Millilitre
mM	Millimolar
mm	Millimetre
MAPK/MPK	MITOGEN ACTIVATED PROTEIN KINASE
<i>N. benthamiana</i>	<i>Nicotiana benthamiana</i>
NB-LRR	Nucleotide binding leucine-rich repeat

NDR1	NON-RACE SPECIFIC DISEASE RESISTANCE1
NHL10	NDR1/HIN1-like 10
NIA2	NITRATE REDUCTASE 2
nm	Nanometer
NO	Nitric oxide
OD	Optical density
OXR	FAD-binding oxidoreductase
<i>P. syringae</i>	<i>Pseudomonas syringae</i>
PAD3	PHYTOALEXIN-DEFICIENT3
PAD4	PHYTOALEXIN DEFICIENT
PAMP	Pathogen-associated molecular pattern
PBS	Phosphate buffered saline
PCD	Programmed cell death
PCR	Polymerase chain reaction
PDF1.2	PLANT DEFENSIN 1.2
PER	Peroxidase
PH1	PRP Homolog 1
PH2	PRP Homolog 2
<i>Pma</i>	<i>Pseudomonas syringae</i> pv. <i>maculicola</i>
PMSF	Phenylmethanesulfonylfluoride
PP2A	PROTEIN PHOSPHATASE 2A
PP2C	PROTEIN PHOSPHATASE 2C
<i>Pph</i>	<i>Pseudomonas syringae</i> pv. <i>phaseolicola</i>
<i>PR1</i>	PATHOGENESIS RELATED 1
PRP	Proline rich protein
PRR	Pattern recognition receptor
<i>Psg</i>	<i>Pseudomonas syringae</i> pv. <i>glycinea</i>
<i>Pst</i>	<i>Pseudomonas syringae</i> pv. <i>tomato</i>
PTI	PAMP triggered immunity
<i>Pto</i>	<i>Pseudomonas syringae</i> pv. <i>tomato</i>
PUB	Plant U-box E3-ligase
pv.	Pathovar
R	Resistance
RAR1	REQUIRED FOR MLA12 RESISTANCE 1
RIN4	RPM1 INTERACTING PROTEIN 4
RLK	Receptor-like kinase
RNA	Ribonucleic acid
ROS	Reactive oxygen species
rpm	Revolutions per minute
RPM1	Resistance to <i>Pma</i> 1
RPS2	Resistance to <i>Pseudomonas syringae</i> expressing avrRpt2
RPS5	Resistance to <i>Pseudomonas syringae</i> expressing avrPphB
RT-PCR	Reverse transcriptase polymerase chain reaction
SA	Salicylic acid
SAG101	SENESCENCE ASSOCIATED GENE 101

SAR	Systemic acquired resistance
SD	Selective dropout
SDS-PAGE	Sodium dodecyl sulfate polyacrylamide gel electrophoresis
sec	Seconds
Ser	Serine
SIC1	CDK INHIBITOR p40
SPCH	SPEECHLESS
SUBA	Arabidopsis subcellular database
TAE	Tris-Acetate-EDTA
TBST	Tris-Buffered Saline and Tween 20
T-DNA	Transferred DNA of the tumor-inducing (Ti) plasmid
TF	Transcription factor
Thr	Threonine
TIR	Toll and interleukin transmembrane receptor
TLR	Toll-like receptor
Trp	Tryptophan
TTSS	Type III secretion system
UBQ	Ubiquitin
v/v	Volume per volume
VIP1	VirE2-interacting protein 1
w/v	Weight per volume
Xa21	Resistance to <i>Xanthomonas oryzae</i> pv. <i>oryzae</i>
xg	x gravity
Y2H	Yeast-two-hybrid
YFP	YELLOW FLUORESCENT PROTEIN

List of Tables

Table 1: List of online tools	27
Table 2: Vector list	83
Table 3: Primer and probe list	84
Table 4: Site directed mutagenesis primer list	85

List of Figures

Fig. A: Zigzag model illustrating the quantitative output of the plant immune system.	3
Fig. B: MAPK networks in MAMP perception downstream of receptors.	10

Fig. 1: Yeast-2-Hybrid protein-protein interaction screen of PRP (in pDEST32), PH1 (in pDEST32) and PH2 (in pDEST32) with all 20 MAPKs (in pDEST22) of <i>A. thaliana</i> (Col-0).	30
Fig. 2: BiFC visualization of PRP (in pESPYCE), PH1 (in pESPYCE) and PH2 (in pESPYCE) interaction with MPK3, MPK4, MPK6, MPK8 and MPK11 (in pESPYNE) in mesophyll protoplasts from <i>A. thaliana</i> (Col-0).	31
Fig. 3: In vitro phosphorylation assay of PRP, PH1 and PH2.	32
Fig. 4: Amino acid alignment of PRP, PH1, and PH2 with T-Coffee (.....)	34
Fig. 5: Autoradiographs of PRP (A), PH1 (B) and PH2 (C) after targeted mutagenesis (Ser/Thr mutated to Ala) and subsequent in vitro phosphorylation with MPK3 and MPK6.	35
Fig. 6A: Yeast-2-Hybrid protein-protein interaction screen of PRP (in pDEST32), PH1 (in pDEST32) and PH2 (in pDEST32) docking site mutants with all 20 MAPKs (in pDEST22) of <i>A. thaliana</i> (Col-0).	36
Fig. 6B: Autoradiographs of PRP, PH1 and PH2 wild type proteins along with the docking site mutated versions after in vitro phosphorylation by MPK3 and MPK6.	37
Fig. 7A: Genevestigator and eFP browser pictograph representation of the expression levels of <i>PRP</i> and <i>PH2</i> in various organs in <i>A. thaliana</i> (Col-0) based on the ATH1 microarray data set.	39
Fig. 7B: Real-time qPCR analysis of <i>PRP</i> , <i>PH1</i> and <i>PH2</i> expression in various organs and seedlings of <i>A. thaliana</i> (Col-0). The relative expression of each gene was normalized to the reference gene <i>PP2A</i> (At1g13320).	39
Fig. 8: Relative gene expression of <i>PRP</i> , <i>PH1</i> and <i>PH2</i> in seedlings after treatment with (A) flg22 [100nM], (B) elf18 [100nM] and (C) H ₂ O.....	41
Fig. 9: Relative gene expression of <i>PRP</i> , <i>PH1</i> and <i>PH2</i> in seedlings after treatment incorporating (A) 4°C, (B) 37°C, (C) NaCl [250mM], and (D) desiccation.	42
Fig. 10: Promoter activity of <i>PRP</i> , <i>PH1</i> and <i>PH2</i> after treatment with flg22 [100nM], elf18 [100nM] and dH ₂ O.....	44

Fig. 11: Impact of PRP-like proteins on basal and flg22-induced <i>FRK1</i> expression.	46
Fig. 12: Impact of PRP-like proteins on basal and elf18-induced <i>FRK1</i> expression.	47
Fig. 13: Impact of PRP-like proteins on basal and flg22-induced <i>NHL10</i> expression.	50
Fig. 14: Impact of PRP-like proteins on basal and elf18-induced <i>NHL10</i> expression.	51
Fig. 15: Promoter activity of <i>PRP</i> and <i>PH1</i> after treatment with flg22 [100nM], elf18 [100nM], and dH ₂ O and co-expressing different constructs.	54
Fig. 16A: Electrophoretic mobility shift assay (EMSA) to investigate DNA-protein interactions between PRP-like proteins and their promoters.	55
Fig. 16B: Electrophoretic mobility shift assay (EMSA) to investigate DNA-protein interactions between PRP-like proteins and <i>FRK1</i> or <i>NHL10</i> defence-related promoters.	56
Fig. 17: Influence of MAMP treatment on protein stability.	58
Fig. 18: Subcellular localization of PRP, PH1, and PH2 in <i>Nicotiana benthamiana</i>	59
Fig. 19: Subcellular localization of PRP, PH1, and PH2 in <i>Arabidopsis thaliana</i> (Col-0) protoplasts.	59
Fig. 20: Subcellular localization in response to MAMP treatment of PRP, PH1 and PH2 in <i>Arabidopsis thaliana</i> (Col-0).	60
Fig. 21: Developmental phenotype observed in two independent lines overexpressing PRP-like proteins.	62
Fig. 22: Root length of untreated and flg22 [1 μM] treated PRP-like overexpressing lines at 14 days.	63
Fig. 23: Bacterial growth assay with <i>P. syringae</i> pv. <i>tomato</i> DC3000 (<i>Pst</i>).	65

I. Introduction

1. Plant-microbe/parasite interactions

Plants have developed highly sophisticated defence systems to shield themselves against invading organisms such as fungi, viruses, bacteria, oomycetes, nematodes and insect herbivores. Plant pathogens can be divided into biotrophs and necrotrophs depending on their lifestyle. Biotrophic organisms such as *Blumeria graminis* require living plant hosts to survive and reproduce, whereas necrotrophs like *Botrytis cinerea*, actively kill and thrive on dead tissues. Hemi-biotrophic organisms like *Pseudomonas syringae* and the oomycete *Phytophthora infestans* initially colonize living tissue before necrotising tissue and thereby switching from a biotrophic to a necrotrophic lifestyle (Pieterse et al., 2009).

2. Plant Immunity

The sessile nature of plants demands that they possess the ability to appropriately respond to a large variety of environmental stresses to ensure their continued survival. Every response to stress is initiated by the perception of an extracellular stimulus and transducing the signal through the cell leading to the expression of a variety of genes. One of the most prolific mechanisms of signal transduction is driven by a group of phosphotransferases, namely the mitogen activated protein kinases (MAPK) that propagate the signal through cells *via* transient phosphorylation events.

Plants possess two main forms of immunity to help deal with biotic stresses namely, pathogen-associated molecular pattern (PAMP)-triggered immunity (PTI) and effector triggered immunity (ETI). PAMPs are conserved microbial molecules that are required for the livelihood of the pathogen and hence cannot be easily mutated without compromising its function. As such, it has been proposed that host organisms have evolved mechanisms to detect such PAMP structures of invading parasites. To reflect the fact that these structures

may not be restricted to pathogens, the term microbe-associated molecular pattern (MAMP), replaced the term PAMP to incorporate all microbes that are able to elicit defence responses (Mackey and McFall, 2006). Damage-associated molecular patterns (DAMPs) are another type of molecule that triggers defence responses. Examples of DAMPs include plants cell walls and cutin fragments generated from pathogenic lytic enzymes (Lotze et al., 2007). PTI occurs after MAMPs and DAMPs are recognised by the innate immune system through pattern recognition receptors (PRRs). PRRs resemble *Drosophila melanogaster* Toll and mammalian Toll-like receptors (TLRs) in terms of structure and function (Song et al., 1995). They typically have an extracellular domain for direct MAMP/DAMP binding, transmembrane domain, juxtamembrane domain and intracellular kinase domain.

The plant immune system has been described as a four phased zigzag model as depicted in figure A below (Jones and Dangl, 2006). In the first phase of the model, PAMPs/MAMPs are recognized by PRRs that trigger PTI and that can stop further colonization by pathogens. In the second phase, pathogens that were not stopped deploy effectors that contribute to the pathogens virulence by interfering with PTI, resulting in effector-triggered susceptibility (ETS). The third phase occurs when certain effectors are specifically recognized and targeted by proteins with nucleotide-binding-leucine-rich repeat (NB-LRR) domains, which as a consequence results in (ETI). Effector recognition by NB-LRR proteins can be either direct or indirect. Jones and Dangl (2006) describe ETI as an accelerated and amplified PTI response that gives rise to disease resistance and hypersensitive cell death response (HR) at the infection site. In the fourth phase natural selection pushes pathogens to avoid ETI by removing the effectors that are recognised by the plant or by evolving new effector molecules that the plant does not recognise in order to suppress ETI. This model describes the evolutionary relationship that exists between plants and pathogen and the various zig-zag phases are assumed to occur repeatedly in the on-going quest for survival of both partners.

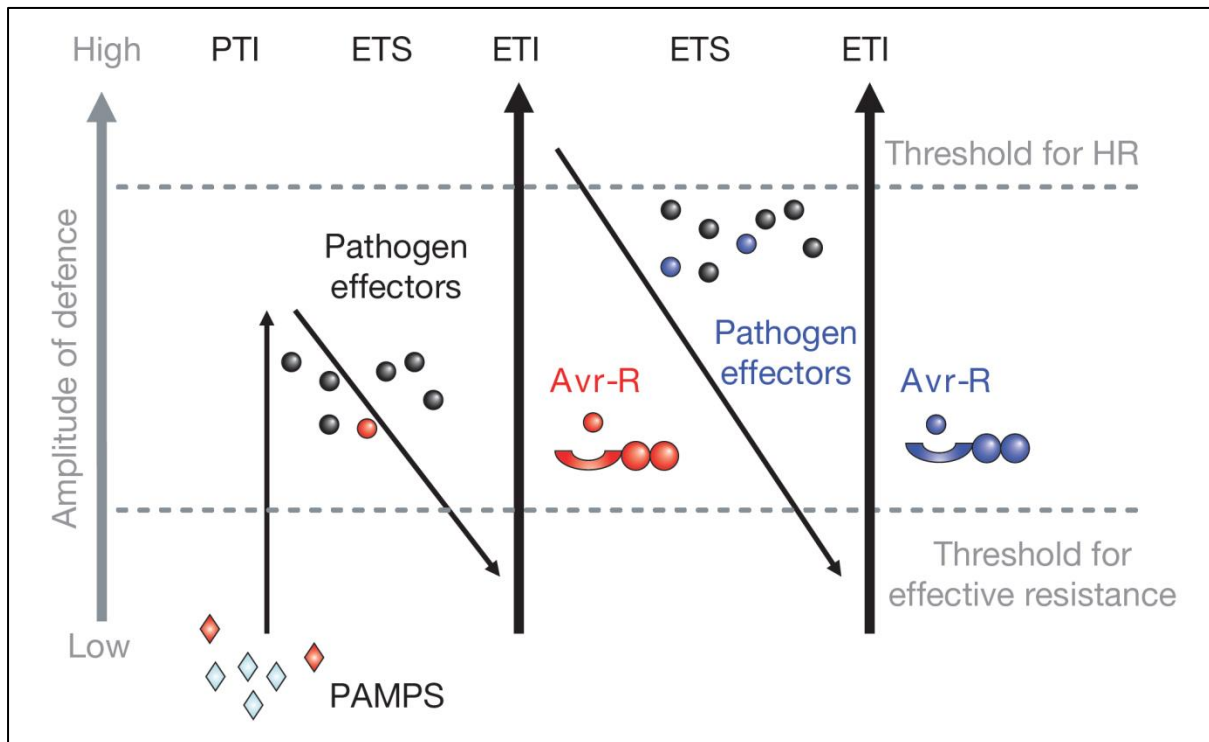


Fig. A: Zigzag model illustrating the quantitative output of the plant immune system. In this scheme, the ultimate amplitude of disease resistance or susceptibility is proportional to $[PTI - ETS + ETI]$. In phase 1, plants detect microbial/pathogen-associated molecular patterns (MAMPs/PAMPs, red diamonds) via PRRs to trigger PAMP-triggered immunity (PTI). In phase 2, successful pathogens deliver effectors that interfere with PTI, or otherwise enable pathogen nutrition and dispersal, resulting in effector-triggered susceptibility (ETS). In phase 3, one effector (indicated in red) is recognized by an NB-LRR protein, activating effector-triggered immunity (ETI), an amplified version of PTI that often passes a threshold for induction of hypersensitive cell death (HR). In phase 4, pathogen isolates are selected that have lost the red effector, and perhaps gained new effectors through horizontal gene flow (in blue) - these can help pathogens to suppress ETI. Selection favours new plant NB-LRR alleles that can recognize one of the newly acquired effectors, resulting again in ETI. **Jones, J.D.G., and Dangl, J.L. (2006).** The plant immune system. *Nature* **444**, 323-329.

2.1 Receptor-like protein kinases (RLKs)

Pattern recognition receptors (PRRs) are responsible for detecting MAMPs from phytopathogenic organisms. One of the first plant PRRs discovered is the receptor-like kinase (RLK), Xa21, which is required for resistance to the bacterial pathogen, *Xanthomonas oryzae* pv. *oryzae* (Song et al., 1995). The RLK gene family has more than 600 members in *Arabidopsis* alone and are transmembrane proteins containing cytoplasmic serine/threonine kinase

domains with divergent extracellular domains. Plant RLKs recognise a multitude of ligands that bind depending on which extracellular domain is present, and therefore have several roles ranging from control of meristem and leaf development, to self-incompatibility and pathogen resistance (Shiu and Bleecker, 2001). Two of the most well studied plant RLKs are FLAGELLIN-SENSING 2 (FLS2) and EF-Tu receptor (EFR) (Gómez-Gómez and Boller, 2000; Kunze et al., 2004; Robatzek et al., 2006; Zipfel et al., 2006).

2.2 PAMP triggered immunity (PTI)

The first level of defence that plants initiate against phytopathogenic organisms is through the perception of MAMPs by PRRs that triggers PTI (Jones and Dangl, 2006). MAMPs are part of or derived from conserved structures from microorganisms. For instance, many plant associated bacteria have surface appendages such as the flagellum that enable them to reach internal spaces within leaves of host plants (Felix et al., 1999). However, this structure also alerts the plant to the presence of invading bacteria. Felix et al. (1999) were able to determine that recognition was specific to a highly conserved domain within the N-terminal domain of flagellin, the protein subunit of flagellum. EF-Tu (prokaryotic elongation factor) is the most abundant protein within a bacterial cell and was discovered to elicit a defence response (Kunze et al., 2004). A major component of fungal cell walls is the N-acetyl-d-glucosamine polymer, chitin, which has also been classified as a MAMP that triggers plant defence responses (Boller, 1995).

PTI is activated by the detection of MAMPs such as flagellin, EF-Tu, and chitin, which are recognized by plant cells through plasma membrane-localized PRRs namely FLS2, EFR, and CERK1 (CHITIN ELICITOR RECEPTOR KINASE 1) (Gómez-Gómez and Boller, 2000; Petutschnig et al., 2010). Flagellin and EF-Tu can be represented by highly conserved N-terminus peptides, 22 amino acids from flagellin (flg22) and 18 amino acids

from EF-Tu (elf18) respectively, and their perception is able to induce PTI (Gómez-Gómez and Boller, 2000; Zipfel et al., 2006; Miya et al., 2007).

BAK1 (BRI1-ASSOCIATED RECEPTOR KINASE1) is able to interact with FLS2 in a ligand-dependent manner after binding of flg22 to FLS2 (Chinchilla et al., 2007). This leads to a variety of defence-related responses such as *PR1* (PATHOGENESIS RELATED 1) gene induction, callose deposition and even inhibition of seedling growth in *Arabidopsis* (Gómez-Gómez et al., 1999). Besides FLS2, BAK1 is also shown to be involved in EFR signalling. Treatment of *Arabidopsis* with elf18 leads to reactive oxygen species accumulation and increases ethylene biosynthesis, which is symptomatic of pathogen attack. Further, only *Brassicaceae* species (*Brassica alboglabra*, *Brassica oleracea*, *Sinapis alba*), and not any other tested plant species (*Solanum tuberosum*, *Cucumis sativus*, *Helianthus annuus*, *Glycine max*), demonstrate responsiveness to elf18 treatment (Kunze et al., 2004).

Elicitation of *Arabidopsis* with chitin oligomers activates defence responses that trigger the MAPK defence signalling pathway (Wan et al., 2004). A mutation in the *CERK1* gene has been demonstrated to lead to enhanced susceptibility of *Arabidopsis* to fungal pathogens (Wan et al., 2008b). Further, there is an overlap between the chitin signalling pathway and that of flg22 and elf18, indicating that plants detect different pathogens through unique receptors that converge on a conserved downstream signalling cascade resulting in PTI (Wan et al., 2008a).

2.3 Effector triggered immunity (ETI)

Evolution of pathogens has endowed them with the ability to suppress PTI through the deployment of effector proteins (Jones and Dangl, 2006). The most well studied plant-pathogen interaction is that between *Pseudomonas syringae* with either *Arabidopsis* or Tomato. Up to 30 effector proteins can be delivered into the plant cell by *P. syringae* to overcome and hijack plant defence systems (Jones and Dangl, 2006). *P. syringae* injects effector

proteins into plant cells through a type III secretion system (TTSS) that is encoded by *hrp* (*hypersensitive reaction and pathogenicity*) genes (Jin et al., 2003).

AvrPto and AvrPtoB are two effector/avirulence (Avr) proteins that have been shown to influence the plant defence response by interfering with PRR defence signalling. AvrPto appears to bind receptor kinases such as FLS2 and EFR in *Arabidopsis* thereby hindering immune responses (Xiang et al., 2008). AvrPtoB specifically targets and associates with FLS2 and BAK1, modifying kinase substrates leading to degradation (Göhre et al., 2008). While effectors have evolved to subvert defence, some plants can recognise effectors through R proteins (Resistance protein) to mount ETI, where the effectors serve as Avr factors (Jones and Dangl, 2006). The R protein Pto (serine/threonine kinase) confers resistance to *Pseudomonas syringae* pv. *tomato* strains that express AvrPto in tomato through direct interaction (Chandra et al., 1996). AvrPtoB has a low sequence similarity to AvrPto but elicits Pto-specific defence responses by direct interaction with AvrPtoB through a conserved amino acid sequence shared with AvrPto (Kim et al., 2002). Pto confers recognition of AvrPto and AvrPtoB through a multimeric protein complex with Prf (NB-LRR protein) and other Pto family members including Fen, Pth2, Pth3 or Pth5 (Gutierrez et al., 2010).

There are two main classes of R proteins that elicit similar responses during ETI, namely CC (coiled coil) and TIR (toll and interleukin transmembrane receptors) NB-LRR proteins (Aarts et al., 1998). NDR1 (NON-RACE SPECIFIC DISEASE RESISTANCE1) is required by the CC-NB-LRR class of R proteins, such as RPS2, RPS5, and RPM1 for resistance towards *Pseudomonas syringae* while EDS1 (ENHANCED DISEASE SUSCEPTIBILITY 1) is required by TIR-NB-LRR proteins (Aarts et al., 1998). EDS1 interacts with PAD4 (PHYTOALEXIN DEFICIENT 4) and SAG101 (SENESCENCE ASSOCIATED GENE 101) forming distinct complexes that are essential for basal resistance against biotrophic pathogens (Feys et al.,

2005; Wiermer et al., 2005). EDS1 and PAD4 also activate SA (salicylic acid) signalling and mediate ET (ethylene) and JA (jasmonic acid) defence signalling pathways (Wiermer et al., 2005).

There are a large number of effector proteins that suppress defence responses of plants and are recognized by R-proteins (Gassmann and Bhattacharjee, 2012). Despite all the research that has been performed and knowledge accumulated in the past decade, many questions still remain pertaining to the mechanistic operations of ETI as a function of plant immunity.

2.4 Systemic acquired resistance (SAR)

Systemic acquired resistance (SAR) is induced by infection with a broad range of pathogens. This leads to an accumulation of SA that activates expression of PR genes leading to broad spectrum resistance (Durrant and Dong, 2004). Unlike PTI or ETI, SAR is not only restricted to the site of infection, but additionally provides long term systemic immunity leading to protection against secondary infections by a range of pathogens. A variation of SAR is induced systemic resistance (ISR), which leads to resistance to fungi and bacteria in the aerial parts of the plant after perception of non-pathogenic root-colonizing bacteria (Durrant and Dong, 2004). ISR does not have as broad a spectrum as SAR and also requires JA and ET signalling (Grant and Lamb, 2006).

3. Mitogen activated protein kinases (MAPKs)

The perception of MAMPs, such as flagellin or EF-Tu by the RLKs FLS2 and EFR, is one of the earliest events that occur after pathogen attack. In order to generate an appropriate defence response, the perceived signal must be effectively and rapidly transduced via signalling networks. A core component of this signalling network is the MAPK signalling cascade that transduces environmental stimuli perceived by RLKs via sequential phosphorylation to effect the appropriate intracellular responses. This signalling cascade consists

of three tiers: MAP kinase kinase kinases (MAP3Ks/MKKKs), MAP kinase kinases (MAP2Ks/MKKs), and MAP kinases (MAPKs) that are evolutionary conserved in all eukaryotes (Jonak et al., 2002). In *Arabidopsis*, 60 MAP3Ks, 10 MAP2Ks, and 20 MAPKs have been identified from the fully sequenced genome (Ichimura et al., 2002).

Perception of external stimuli activates a serine/threonine MAP3K that then phosphorylates the S/T-X₃₋₅-S/T motif present in MAP2Ks. The MAP2Ks then in turn phosphorylate MAPKs with a T-X-Y motif (Chang and Karin, 2001). Thus, MAPK cascades link upstream receptors with downstream targets. MAPKs are proline directed serine/threonine kinases, which means they phosphorylate substrates at serine/threonine residues preceding a proline (S/T-P motif). Approximately 80% of all proteins possess the S/T-P motif and it is unlikely that these proteins are all substrates of MAPKs (Bardwell, 2006). The MAPK kinase signalling cascade is very precise in terms of specificity for its substrate. Typically, the recognition and binding of specific targeted proteins by MAPKs is based on the differential interaction of the catalytic and docking sites present (Yoshioka, 2004).

3.1 MAPKs signalling in *Arabidopsis thaliana*

MAPK signalling plays a pivotal role in the transduction of diverse extracellular signals that allow plants to mount the appropriate physiological responses to help ensure survival. Biotic stresses that are perceived by plants have multiple sources such as bacteria, viruses, fungi, and insects (Fig. B). The manner in which plants are able to detect and defend themselves from pathogen attack has garnered a lot of attention in order to elucidate the mechanistic intricacies of plant defence (Tena et al., 2011). The majority of knowledge of MAPK-mediated signalling has been from the intensive study and characterization of three MAPKs, namely MPK3, MPK4 and MPK6 (Fig. B). All three of these MAPKs have significant roles in multiple cascades activated by biotic, abiotic and developmental cues (Colcombet and Hirt, 2008). Recently, MPK11 was

described as a MAMP-activated MAPK (Bethke et al., 2012; Eschen-Lippold et al., 2012).

3.1.1 MAPK signalling and Biotic stimuli

Flg22 perception initiates defence responses by activating the MAPK signalling pathway MKK4/MKK5-MPK3/MPK6, triggering early defence gene expression of *WRKY29*, *GST1*, and *FRK1* as depicted in figure B below (Asai et al., 2002). The defence response triggered by flg22 perception activates MPK3 that phosphorylates the bZIP transcription factor VIP1 (VirE2-INTERACTING PROTEIN1) that regulates the expression of *PR1*. Upon phosphorylation, the localisation of VIP1 is altered from the cytoplasm to the nucleus. *Agrobacterium tumefaciens* capitalises on the altered localisation of VIP1 in order to deliver its T-DNA complex into the plant cell nucleus by binding VIP1, essentially hijacking the plant's defence response (Djamei et al., 2007).

Ethylene is an important hormone that plays numerous roles in plant development and stress responses. ACS6 (1-Aminocyclopropane-1-carboxylic acid synthase 6) is a rate limiting enzyme that is specific for the ET biosynthetic pathway and has been shown to have an MPK6-dependent increase in response to flg22 treatment of Arabidopsis seedlings (Liu and Zhang, 2004). ACS6 and ACS2 are both substrates of MPK6 (Joo et al., 2008). The phosphorylation of ACS stabilizes the proteins, consequently leading to accumulation of ACS and ET production. The C-terminal non-catalytic domain of unphosphorylated ACS6 is targeted by the 26S proteasome and rapidly degraded (Joo et al., 2008). ACS6 possesses three Ser residues and phosphorylation of one or multiple residues is required for full functionality of regulation that could lead to the fine tuning of ethylene biosynthesis (Joo et al., 2008).

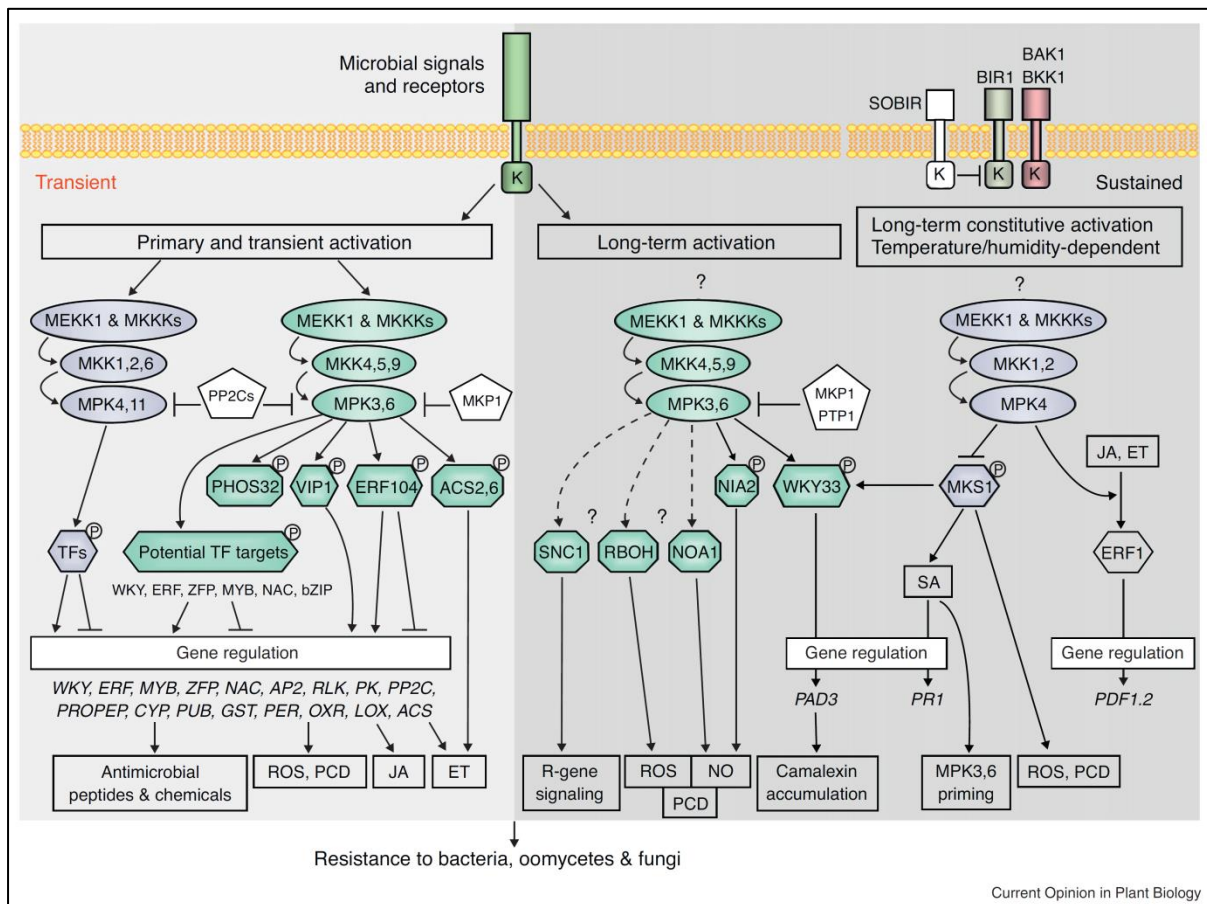


Fig. B: MAPK networks in MAMP perception downstream of receptors. Fast and transient activation of at least two MAPK cascades induces primary responses (left). Direct targets, phosphorylated in minutes, have been identified for MPK3/6. Modulation of transcription factor (TF) activity by MAPKs induces a massive gene expression reprogramming, ultimately leading to increased resistance to pathogens through various biological responses such as synthesis of antimicrobial peptides and chemicals, programmed cell death (PCD), and production of reactive oxygen species (ROS), nitric oxide (NO) and stress hormones. A long-term activation of MAPKs (centre) by microbes also induces biological responses, most notably the accumulation of camalexin through release and direct phosphorylation of WKY33 and modulation of *PAD3* gene expression in leaves. A continuously active MAPK cascade, consisting of MEKK1 and other MKKKs, MKK1/2 and MPK4 (right), has a sustained requirement to control salicylic acid (SA), PCD, ROS and *PR1* gene levels through the direct phosphorylation of MKS1, and to allow JA and ET responses, independently of MAMP perception. Abbreviations: PP2C, protein phosphatase 2C; CYP, cytochrome P450; PUB, plant U-box E3-ligase; GST, glutathione-S-transferase; PER, peroxidase; OXR, FAD-binding oxidoreductase; LOX, lipoxygenase. **Tena, G., Boudsocq, M., and Sheen, J. (2011).** Protein kinase signaling networks in plant innate immunity. *Curr Opin Plant Biol* **14**, 519-529.

Ethylene inactivates the negative regulator CTR1 (CONSTITUTIVE TRIPLE RESPONSE 1) and then EIN3 (ETHYLENE-INSENSITIVE 3) is transcriptionally activated by the MKK9–MPK3/MPK6 signalling cascade. EIN3 possesses two phosphorylation sites, T174 for stabilization and T592 for the degradation of the protein. The MKK9–MPK3/MPK6 cascade targets EIN3 in the nucleus, thereby differentiating this signal from ACS6/MPK6 activity leading to ethylene biosynthesis, which occurs in the cytoplasm (Yoo et al., 2008).

ERF104 (ETHYLENE RESPONSE FACTOR 104) is a transcription factor that is exclusively phosphorylated by MPK6 (Bethke et al., 2009). Bethke et al. (2009) demonstrated that treatment with flg22 disrupted the interaction complex between ERF104 and MPK6 in the nucleus. The disruption of the interaction complex not only required MPK6 activity, but ET signalling as well. MPK6 additionally affects ERF104 stability through phosphorylation. There is speculation that downstream components of the MPK6 pathway may feed into the MPK4 pathway linking two different branches of flg22-regulated signalling pathways leading to defence responses (Bethke et al., 2012).

Nitric oxide (NO) and hydrogen peroxide (H₂O₂) are signalling molecules in plants that respond to a wide variety of stresses and have been implicated in multiple responses including defence gene activation (Neill et al., 2002). MPK6 has been demonstrated to phosphorylate NIA2 (NITRATE REDUCTASE 2), which increases NO production dramatically (Wang et al., 2010). The phosphorylation of NIA2 increases the activity of NIA2 and additionally leads to morphological changes in Arabidopsis root systems. Wang et al. (2010) showed that mutant plants where *mpk6* is silenced displayed longer and more lateral root development than wild type plants did after treatment with H₂O₂ or the NO donor sodium nitroprusside. This supports the conclusion that MPK6 plays a regulatory role in the production of NO induced by H₂O₂.

The nickel-binding protein AtPHOS32 was identified as substrate of MPK3 and MPK6 and was phosphorylated in response to flg22 treatment (Merkouropoulos et al., 2008). The function of this protein is unknown, but the authors speculate that it may have a role that requires ATP, as it contains an ATP-binding domain. Further, they could not deduce the possible function of AtPHOS32 using sequence comparison analysis.

MPK4 targets WRKY25 and WRKY33 transcription factors (TFs), and also MKS1 (MAP kinase substrate 1), which is involved in pathogen response (Andreasson et al., 2005). MKS1 is phosphorylated by MPK4, represses SA signalling, and inhibits downstream production of PR proteins. Therefore MPK4 acts as a negative regulator of SA responses. Interaction of MKS1 with MPK4 is mediated by a domain in the N-terminal region while interaction with WRKY25 and WRKY33 TFs is due to a conserved VQ motif. MKS1 overexpression leads to high levels of SA, which in turn induces *PR1* expression. As a result, MKS1 overexpressing plants have a higher resistance to virulent *Pseudomonas syringae* pv. *tomato* DC3000 than wild type plants do (Andreasson et al., 2005). MPK4, MKS1, and WRKY33 associate in a complex (Petersen et al., 2010). After flg22 treatment, MPK4 is phosphorylated, releasing MKS1 and WRKY33 thereby allowing WRKY33 to target the promoter of *PAD3* (*PHYTOALEXIN-DEFICIENT3*), which encodes a cytochrome P450 monooxygenase required for the production of the antimicrobial compound camalexin (Petersen et al., 2010).

WRKY33 is a pathogen-inducible transcription factor that can bind its own promoter *in vivo* and is phosphorylated by both MPK3 and MPK6 in response to pathogen perception. MPK3 and MPK6 require WRKY33 in order to induce camalexin biosynthesis (Mao et al., 2011). MPK4 is not required for camalexin induction after *Botrytis cinerea* infection even though it is found in a protein complex with WRKY33. MPK4 has instead been associated with camalexin induction after bacterial pathogen infection (Qiu et al., 2008).

The transgenic expression of AvrB suppresses MAMP-induced responses through interaction with RAR1 (REQUIRED FOR MLA12 RESISTANCE 1), a cochaperone of HSP90 (HEAT SHOCK PROTEIN 90) required for ETI (Shang et al., 2006). Disease resistance to *P. syringae* is thought to be positively regulated by MPK3/6, whereas MPK4 is considered to negatively impact *P. syringae* resistance through regulation of multiple hormonal pathways (Petersen et al., 2000). Cui et al. (2010) demonstrated that RAR1 was required for stable AvrB-MPK4 interaction and that the association of RAR1 with AvrB induced the phosphorylation of MPK4. Further, HSP90 was implicated in regulating MPK4 activity and JA signalling.

RIN4 (RPM1 INTERACTING PROTEIN 4) positively modulates JA responses and is required for AvrB to induce JA signalling that leads to plant susceptibility (Cui et al., 2010). Additionally, RIN4 interacts with MPK4 both *in vitro* and *in vivo*, and its phosphorylation by MPK4 places it downstream of MPK4. Therefore AvrB is able to increase the plant susceptibility to *Pseudomonas syringae* by targeting RIN4 through its interaction with MPK4. RIN4 interacts with MPK4 *via* RAR1 and HSP90, leading to the phosphorylation of MPK4 and subsequent phosphorylation of RIN4. The result is that hormone signalling is perturbed by the induction of JA signalling through *PDF1.2* (*PLANT DEFENSIN 1.2*) expression inducing plant susceptibility (Cui et al., 2010).

3.1.2 MAPK signalling and Abiotic stimuli

There are numerous abiotic stresses that have a marked impact on plant growth and possibly their survival. Some of the most common abiotic stresses include osmotic, salt, temperature, and reactive oxygen species (ROS). One such MAPK cascade consists of MEKK1-MKK2-MPK4/MPK6, which plays a critical role in cold and salt stress in Arabidopsis. MKK2 was shown to phosphorylate both MPK4 and MPK6, activated specifically by cold and salt stresses, but not by any other stresses tested such as heat, flg22, laminarin, etc. (Teige et al., 2004).

MPK3 and MPK6 are implicated in oxidative stress signalling and are activated by ozone. Plant cells are more vulnerable to oxidative stress when the activation of MPK3 and MPK6 are lost or unregulated. Further, MKP2 (MAPK phosphatase 2) is responsible for dephosphorylating the TEY motif of MPK3 and MPK6, thereby aiding redox homeostasis (Lee and Ellis, 2007). The *mekk1* mutant plants display chlorotic cotyledons due to misregulation of redox control genes. ROS are negative regulators of auxin responses and *mekk1* and *mpk4* mutant plants demonstrate a reduced expression of auxin-inducible marker genes. MEKK1 activity is induced by H₂O₂ in protoplasts and leads to MPK4 activation. Therefore ROS homeostasis is integrated with hormone signalling and plant development by MEKK1 (Nakagami et al., 2006).

H₂O₂ is a major contributor of ROS and can severely damage cells if unchecked. In Arabidopsis, CAT1 (CATALASE 1) is an enzyme that regulates H₂O₂ by decomposing it to water and oxygen. *CAT1* expression is induced by ABA (abscisic acid), and induction of *CAT1* is abolished in *mpk6* mutant plants, implicating MPK6 as a vital component. MKK1-MPK6 has been implicated as a key module in the ABA dependent signalling cascade resulting in H₂O₂ production (Xing et al., 2008).

3.1.3 Roles of MAPK cascades in plant development

One of the roles of MAPKs in development is the regulation of stomata development, which is specified and positioned by the integration of asymmetric cell divisions and intercellular signalling of the meristemoid guard cell mother cells. The Arabidopsis MAP3K, YODA (YDA), is identified as part of a molecular switch that controls epidermal cell identities. The constitutive activation of YODA compromises stomata development while null mutations within *YODA* have the opposite effect, leading to an excess of stomata (Bergmann et al., 2004).

The MAPK module YDA-MKK4/MKK5-MPK3/MPK6 is a key regulator of stomatal development and patterning. The absence of either MKK4/MKK5 or MPK3/MPK6 results in clustered stomata in seedlings, while the activation of these kinases leads to a lack of stomatal differentiation, due to suppression of asymmetric cell divisions and stomatal cell fate specification (Wang et al., 2007). Further, the transcription factor SPCH (SPEECHLESS) was identified as an *in vitro* substrate of both MPK3 and MPK6 in the YODA pathway. The *spch* loss-of-function mutants cannot produce stomata (Lampard et al., 2008).

MPK6 was shown to affect a variety of plant developmental processes including male fertility, embryo development, anther development, and inflorescence development that is independent of MPK3 (Bush and Krysan, 2007). Both MPK3 and MPK6 influence ovule development. The absence of *mpk6*, combined with a heterozygous copy of *MPK3*, leads to incomplete integument development resulting in an ovule that is not adequately covered at the micropylar end. The result of this is female sterility and therefore making MPK3 haplo-insufficient. Conversely, *mpk3* mutant plants with a heterozygous copy of *MPK6* are able to maintain female fertility, which could be attributed to the enhanced expression of *MPK6* when *mpk3* is absent (Wang et al., 2008).

MAPKs also influence the proper development of pollen. The MAP3Ks, MAP3K ϵ 1 and MAP3K ϵ 2, are required for pollen viability. The double knockout mutant plants of these MAP3Ks result in pollen lethality. Also MAP3K ϵ 1 is required for normal functioning of the plasma membrane during pollen development (Chaiwongsar et al., 2006). The MAPK signalling cascade NACK2/TES/STUD-ANP3-MKK6-MPK4 facilitates male-specific meiotic cytokinesis in Arabidopsis. MPK4 is phosphorylated by MKK6, which is a cytokinesis-related MKK. In *mpk4* null plants, meiotic cytokinesis cannot be completed, due to the failure of normal intersporal wall formation after male meiosis. As a result, a developmental phenotype can be observed in enlarged pollen grains that possess an increased number of tricellular structures (Zeng et al., 2011).

Leaf senescence is another developmental phase that is highly regulated by MAPKs. During senescence, leaves start the process of macromolecule degradation and mobilization of components to other plant tissues. The transcription factor WRKY53 is expressed during early senescence events regulating senescence specific gene expression (Hinderhofer and Zentgraf, 2001). The MAP3K, MEKK1, has been implicated in the transcriptional regulation of senescence by binding specific regions of the *WRKY53* promoter. Phosphorylation of WRKY53 by MEKK1, increases DNA binding activity of WRKY53 *in vitro*, and MEKK1 binds to the promoter of *WRKY53*, which regulates the switch between leaf age-dependent to plant age-dependent expression (Miao et al., 2007). This is a contentious example of how MAPK signalling cascades can regulate events without employing the entire signalling cascade. The MKK9-MPK6 module has also been implicated in senescence. The absence of MKK9 delays the onset of senescence in detached leaves, which is similarly phenocopied by the absence of MPK6 (Zhou et al., 2009a).

4. Aim of study

As introduced above, perception of stress signals by plants and the response generated by them are crucial for mitigating effects of stresses in an attempt to ensure their survival under adverse conditions. These signals are transduced within the plant cell by complex signalling cascades, including elements from the MAPK pathway, which ultimately allow the plant to respond to abiotic and biotic stresses (Pitzschke et al., 2009). MAPKs contribute to plant immunity, development, and abiotic stress responses through the phosphorylation of various substrates such as transcription factors, cytoskeletal components etc. (Suarez-Rodriguez et al., 2010). A prerequisite for dissecting the complex MAPK network is the identification of the plethora of MAPK substrates involved in these various MAPK signalling pathways. A number of techniques, ranging from yeast-two-hybrid screens to protein

microarray analysis (Feilner et al., 2005), have been employed in order to identify potential MAPK interactors and substrates.

The aim of this study is to characterise one such candidate that interacted with MPK6 and MPK11 in a yeast-two-hybrid screen. The screen was performed by Dr. Joachim F. Uhrig of the University of Cologne, Germany, in a collaborative effort to isolate potential interactors of MAPKs. One candidate identified as a possible interactor of MAPKs was a protein of unknown biological function, encoded by the annotated gene At3g23170. The predicted protein has a molecular mass of 11.7 kDa and contains 15.9% prolines. We therefore designated this protein as **Proline Rich Protein (PRP)**. To expand the investigation, BlastP analysis was performed with PRP's amino acid sequence and subsequent sequence alignments were performed using ClustalW. Two homologs, both with 53% sequence identity to PRP, were identified in *A. thaliana* (Col-0). The two PRP homologs were named **PRP Homolog 1 (PH1, At4g14450)** and **PRP Homolog 2 (PH2, At1g04330)** and possessed a proline content of 12.8% and 18% respectively. Hence, in this work, the ability of these three PRP-related proteins to interact with MAPKs and their contribution to MAPK-mediated signalling were examined with respect to plant defence and development.

II. Materials and Methods

1. Consumables

All chemicals and solvents used were of analytical grade or higher and obtained from Serva, Bio-Rad, Merck, Sigma-Aldrich, Promega, Roth, GE Healthcare, Difco, Ducheфа and Calbiochem. Enzymes were obtained from Invitrogen, Fermentas, and New England Biolabs (NEB). Antibodies used were obtained from Sigma, NEB, and Eurogentec. Primers and taqman probes were ordered from Eurofins MWG with flg22/elf18 peptides synthesised in house with an *Economy Peptide Synthesizer EPS221* from Abimed (by Sylvia Kruger, IPB Halle an der Saale).

2. Molecular biological techniques

2.1 Polymerase Chain Reaction (PCR)

The amplification of DNA fragments in a *MyCycler* thermocycler (Bio-Rad) were performed according to standard protocols as described (Sambrook et al., 1989).

2.2 Cloning

PRP (At3g23170), *PH1* (At4g14450) and *PH2* (At1g04330) were amplified by PCR from *A. thaliana* Col-0 cDNA with primers indicated (Table: 2, Appendix) and cloned into the pENTR-D-TOPO entry vector (Invitrogen). All subcloning was performed *via* the Gateway system (Invitrogen) into various destination vectors (Table. 1, Appendix).

2.3 Plasmid preparation

DNA plasmids were isolated from cultures grown overnight at 37°C at 160rpm in Luria Broth media using either the *QIAprep Spin Miniprep Kit* or *QIAGEN Plasmid Maxi Kit* from Qiagen according to the manufacturer's protocols.

2.4 Restriction analysis and Sequencing

Restriction analysis was performed using restriction enzymes from Fermentas according to the manufacturer's protocol. Constructs were sent for sequencing at *Eurofins MWG Operon* (Germany).

2.5 RNA extraction, cDNA synthesis and Quantitative Real time PCR

Total RNA was extracted by the Trizol method as described (Chomczynski and Sacchi, 1987). cDNA was synthesised from 2µg total RNA with *RevertAid™ H Minus First Strand cDNA Synthesis Kit* (Fermentas). cDNA was diluted 1:10 in MilliQ H₂O (Millipore, U.S.A.) before analysis by quantitative Real time PCR. For the PCR, *Maxima™ Probe qPCR Master Mix* (Fermentas), Taqman Probe (Roche), gene specific primers (Table 2, Appendix), were utilised in a 20µl total reaction volume including 3µl of diluted cDNA sample with a *Mx3005P QPCR System* (Stratagene). All data was normalised to the Arabidopsis housekeeping gene PP2A (PROTEIN PHOSPHATASE 2A; At1g13320) (Czechowski et al., 2005). Relative expression was determined with the comparative C(T) method (Schmittgen and Livak, 2008).

2.6 Site directed mutagenesis

Full-length coding sequences for all targeted genes were subcloned in the pENTR-D-TOPO Gateway entry vectors (Invitrogen) that were then used as templates to amplify the entire plasmid with gene specific primers (Table 3, Appendix) and Phusion DNA Polymerase (Finnzymes). Initial denaturation was performed at 98°C for 30sec and fifteen PCR cycles were carried out at 98°C for 10sec, 58°C for 20sec, and 72°C for 90sec. Following a final elongation step at 72°C for 7min, a 20µl aliquot of the PCR was digested with *DpnI* (Fermentas) to remove the parental methylated plasmid and purified by Qiagen-Spin columns to remove remnant enzymes. A combined digestion–ligation approach (*Eco31I* and *T4* DNA ligase, Fermentas) using a thermal

cycler was then applied to generate and ligate the cohesive overhangs (50µl at 37°C for 5min and then 22°C for 5min, 6-10 cycles). An aliquot of the final product was transformed into *Escherichia coli* strain DH5α (Invitrogen). Prior to sequencing, the individual clones were first analysed by restriction digest to determine whether the diagnostic restriction sites were incorporated as described (Palm-Forster et al., 2012).

2.7 Electrophoretic analysis

DNA fragments were run in an agarose gel (SeaKem LE Agarose, Biozym) of varying percentages depending on the fragment size to obtain adequate separation in a TAE buffer system (Tris-Acetate [40mM], EDTA [2mM], pH 8.5). DNA was visualised after staining gel for 5min in an Ethidium bromide bath [0.5µg/ml] with a *Gene Genius* (Syngene) gel documentation system.

2.8 Primers

Standard primers were design using the online software OligoPerfect™ Designer (Invitrogen). Real time primers and Taqman probes were designed with the online software Universal ProbeLibrary Assay Design Centre (Roche). All primers and probes used for the research performed are listed in Table 3 (Appendix).

2.9 Transformation

2.9.1 *Escherichia coli*

Chemically competent cells (Table 4) were transformed with DNA after incubation on ice for 30min, heat shocked at 42°C for 40sec after which the transformed cells were grown while shaking at 160rpm for one hour at 37°C before plating out onto antibiotic selection medium (Sambrook et al., 1989).

2.9.2 *Saccharomyces cerevisiae*

Yeast strain PJ69-4A (James et al., 1996) was transformed with pDEST22 containing the *GAL4* DNA activating domain (Invitrogen) and pDEST32

containing the *GAL4* DNA binding domain (Invitrogen) using the high efficiency LiAc-mediated transformation protocol (Schiestl and Gietz, 1989).

2.9.3 *Nicotiana benthamiana*

Agrobacterium tumefaciens cultures containing the gene of interest in a binary vector were grown overnight in Luria Broth media and resuspended the next day in induction media (1.05% (w/v) K_2HPO_4 , 0.45% (w/v) KH_2PO_4 , 0.1% (w/v) $(NH_4)_2SO_4$, 0.05% (w/v) $C_6H_8O_7Na_2.H_2O$, 0.012% (w/v) $MgSO_4$, 0.1% (w/v) glucose, 0.1% (w/v) fructose, 0.4% (w/v) glycerol and 0.145% (w/v) MES). Cultures were incubated further for five hours before resuspending in infiltration media (MES [10mM] pH 5.5, $MgCl_2$ [10mM] and acetosyringone [150 μ g/ml]) to an $OD_{600}=0.5$. The *Agrobacterium* solution was infiltrated into leaves with a needleless syringe for transient expression (Marois et al., 2002).

2.9.4 *Arabidopsis thaliana*

Stable overexpressing lines were generated by the floral dip method (Logemann et al., 2006). In brief, *Agrobacterium tumefaciens* containing the gene of interest in a binary vector was grown overnight at 28°C in Luria Broth media containing the appropriate antibiotics. The culture was resuspended to an $OD_{600}=0.8$ in a 5% (w/v) sucrose solution and 0.05% (v/v) Silwet L-77 was added prior to dipping the *Arabidopsis* inflorescences. After overnight incubation at high humidity and low light intensity, the plants were placed in the greenhouse. Positive transformants were selected with the appropriate antibiotics or herbicide.

2.9.5 Mesophyll protoplasts

Arabidopsis mesophyll protoplasts were prepared by cutting six week old leaves into fine strips (<0.5 mm) and placing into an enzyme solution (mannitol [0.4M], KCL [20mM], MES [20mM] pH 5.7, 1.5% (w/v) cellulose R10, 0.4% (w/v) macerozyme R10, $CaCl_2$ [10mM], 0.1% (w/v) BSA). The leaf strips were vacuum infiltrated in a dessicator for 30min before digesting further at

22°C for three hours in the dark. Protoplasts were then gently shook before adding 10ml W5 solution (NaCl [154mM], CaCl₂ [125mM], MES [2 mM] pH 5.7, KCl [5 mM]) to every 10ml enzyme solution. Suspension was filtered through a nylon mesh (100µM) and centrifuged at 200xg and 4°C for one minute. Supernatant was removed and the protoplasts resuspended in W5, followed by incubation on ice in the dark for 40min before repeating the wash and allowing to settle once more for 40min. Protoplasts were then resuspended in MMG (mannitol [0.4M], MES [4mM] pH 5.7, MgCl₂ [15mM]) at a density of 2x10⁵/ml and transfected with 10µg plasmid DNA expressing effectors and/or reporters with 1.1x volume PEG solution (mannitol [0.2M], CaCl₂ [0.1M], 4% (w/v) PEG 3000) for 10min. The transformation was stopped by adding 4.4x volume W5 solution, gently mixed and centrifuged at 200xg and 4°C for one min. The supernatant was removed and the protoplasts resuspended in W1 solution (mannitol [0.5M], MES [4mM] pH 5.7, KCl [20mM]) and then incubated overnight in the dark (Yoo et al., 2007).

3. Protein biochemical techniques

3.1 Recombinant protein expression

PRP, PH1 and PH2 were recombinantly overexpressed in KRX cells (Promega). Pc-MKK5DD was recombinantly overexpressed in BL21(DE3) cells while MPK3 and MPK6 were recombinantly overexpressed in BL21 cells (Invitrogen). All cultures were grown at 37°C to the density recommended by the manufacturers before induction, after which cultures were grown 12 hours at 18°C. KRX cells were induced with rhamnose [0.1% w/v] and the BL21-derivative strains with IPTG [0.1mM] final concentration as recommended by the manufacturers.

3.2 Recombinant protein purification

Purification of HIS-tagged proteins was performed *via* affinity chromatography with Ni-NTA agarose (Qiagen) with the under non-denaturing conditions for Pc-MKK5DD (pJC40) and under denaturing conditions for PRP, PH1, and

PH2 (pDEST-N110) according to the manufacturer's recommendations. After purifying PRP, PH1, and PH2, they were refolded at 4°C while still bound on the Ni-NTA agarose in 50mM NaPO₄ buffer pH 8 (for 1 hour), then eluted with 250mM imidazole in 50mM NaPO₄ buffer pH 8.

The GST tagged proteins of MPK3 and MPK6 (pGEX4t-1) via affinity chromatography with Glutathione Sepharose 4 Fast Flow (GE Healthcare) according to the manufacturer's recommendations. Proteins were eluted in 50mM Tris pH 8 containing 10mM reduced Glutathione.

3.3 Protein extraction from plant material

Leaf material was snap frozen in liquid nitrogen and ground at 6200rpm for 20 seconds with a Precellys 24 (Bertin Technologies) homogenizer. Total protein was extracted by adding extraction buffer (Tris/HCl [25mM] pH 7.8; NaCl [75mM]; EGTA [15mM]; MgCl₂ [10mM]; Glycerophosphate [15mM]; 4-Nitrophenylphosphate [15mM]; DTT [1mM]; NaF [1mM]; Na₃VO₄ [0.5mM]; PMSF [0.5mM]; Aprotinin [10µg/ml]; Leupeptin [10µg/ml]; 0.1% (v/v) Tween 20), grinding once more, then placing in a centrifuge for one minute. The supernatant containing the extracted total protein was used for further analysis (Ahlfors et al., 2004).

3.4 SDS-PAGE electrophoresis and Western blot analysis

Protein concentrations were determined with the Bradford assay (Bradford, 1976) to ensure equal loading before SDS-PAGE analysis. The proteins were separated on 15% SDS-PAGE gels (Laemmli, 1970) and transferred to a nitrocellulose membrane (Hybond-ECL; Amersham Biosciences). The blot was incubated in TBST (NaCl [140mM], 0.1% (v/v) Tween-20, Tris HCl [20mM] pH 7.6) containing 5% (w/v) non-fat dry milk (Biorad) at room temperature (RT) for 30min before incubating with the primary antibody for one hour at R. followed by the secondary antibody for another hour at RT. Blots were washed with TBST before incubating with ECL kit reagents (GE

Life Sciences) for five minutes at RT according to the manufacturer's instructions.

3.5 Electrophoretic Mobility Shift Assay (EMSA) analysis

Cloned promoter fragments were cut from vectors by restriction digest with *NcoI* and *BamH1* restriction enzymes at 37°C for one hour. The DNA fragments were separated on an agarose gel and bands for the corresponding promoters excised and purified with a Qiaquick gel extraction kit (Qiagen). For the EMSA assay, 1µl purified proteins [2.5µg/µl] were added to a mixture containing excised 10µl promoter fragments [10ng/µl], sheared single stranded salmon sperm DNA [1µg] in binding buffer (Tris [50mM] pH 8, KCl [750mM], EDTA [2.5mM], 0.5% (v/v) Triton X-100, 62.5% (v/v) glycerol, DTT [1mM]). Samples were incubated for 30 min at 20°C in a thermocycler before running on a 1% (w/v) agarose gel.

3.6 Promoter activity analysis

pPRP::LUC, *pPH1::LUC*, *pPH2::LUC*, *pFRK1::LUC* and *pNHL10::LUC* promoter–luciferase fusion constructs were transfected into Arabidopsis mesophyll protoplast and used as reporters for promoter activity. *pUBQ10::GUS* was co-transfected for normalization. Luminescence of protoplast suspensions containing D-luciferin (200µM; Invitrogen) were recorded in 96-well plates (Luminoskan Ascent 2.1) after treatment with MAMPs (Ranf et al., 2011).

4. Plant analysis

4.1 Seedling assays

Seedlings were grown for 14 days under long day conditions (Ranf et al., 2011) in half MS media (0.245% (w/v) Murashige & Skoog medium (Duchefa), MES [1mM] pH 5.7, 0.25% (w/v) saccharose). MAMP treatment of seedlings was performed with flg22 [1µM] and elf18 [1µM]. Cold stress was induced by adding precooled media (4°C) and incubating on ice. Heat stressed was

induced by adding preheated media (37°C) and incubating in a water bath (37°C). Salt stress was induced by adding media containing NaCl [250mM]. Desiccation stress was induced by removing seedlings from the media and placing on a paper towel to drain excess moisture, allowing them to dry during the time course of the experiment (0-300min).

4.2 Root growth inhibition assays

Seeds from various genotypes were grown vertically on agar plates containing half MS media for 14 days (Ranf et al., 2011). Each plate contained 20 seeds from one line under investigation along with 20 seeds from wild type Col-0 as a control. Untreated plates contained only the media while treated plates were supplemented with flg22 [1µM].

4.3 Pathogen assays

The Arabidopsis plants were grown under short day conditions at 22°C for 5 weeks before leaves were sprayed with *Pseudomonas syringae* pv. *tomato* DC3000 (*Pst*) (Zipfel et al., 2004). *Pst* was grown on plates containing King's B media (proteose peptone [20g/L], anhydrous K₂HPO₄ [1.5g/L], 1% (v/v) glycerol, MgSO₄ [5mM]) with the appropriate antibiotic. *Pst* was resuspended in water to an OD₆₀₀=1 and 0.04% (v/v) Silwet-L77 was added just before spraying. Five plants per line were sprayed and sealed by wrapping parafilm around the clear plastic cover, before placing back into the growth chamber. Sampling was performed at day 0 (4 hours after spraying) and day 3. Day 0 leaves were surfaced sterilised with 70% ethanol before harvesting leaf discs. Leaf discs were harvested in triplicate and collected randomly from leaves, then placed into 2ml tubes containing 100µl water and ground in a Precellys 24 (Bertin Technologies) for 20sec at 6800rpm. Dilution series were plated out with technical duplicates and grown at 28°C before colonies were counted.

5. Microscopy

The detection of intracellular CFP, GFP, and YFP fluorescence was performed with the LSM 710 inverted confocal microscope (Zeiss, Jena). GFP and YFP excitation occurred at 488nm with the argon laser and detection at 490nm-530nm. Excitation of CFP occurred at 425nm and emission detected at 460nm-490nm. Image processing was performed with ZEN 2009 bundled software.

6. Statistical analysis

Analyses of data were performed with the aid of GraphPad Prism 5 (GraphPad Software, Inc., La Jolla, USA).

7. Online Resources

Table 1: List of online tools

CLUSTALW2	Nucleotide and protein alignment	http://www.ebi.ac.uk/Tools/mesa/clustalw2/
eFP browser	Expression database	http://bar.utoronto.ca/efp/cgi-bin/efpWeb.cgi
Genevestigator	Expression database	https://www.genevestigator.com/gv/
NCBI BLAST	Nucleotide and protein homology search	http://blast.ncbi.nlm.nih.gov/
NEB cutter V2.0	Identification of Type II / Type III restriction enzyme target sites	http://tools.neb.com/NEBcutter2/
OligoPerfect™	Primer design	http://tools.invitrogen.com/content.cfm?pageid=9716
Reverse complement	DNA sequence into its reverse, complement, or	http://www.bioinformatics.org/sms/rev_comp.html

	reverse-complement	
SUBA	Subcellular localisation	http://suba.plantenergy.uwa.edu.au/
T-COFFEE	Protein alignment	http://www.tcoffee.org/
TAIR	Arabidopsis genome	http://www.arabidopsis.org/
Universal probe library assay design centre	Real time PCR primer and probe design	https://www.roche-applied-science.com/sis/rtpcr/upl/index.jsp?id=UP030000

III. Results

1. Evaluation of MAPK interaction

1.1 Analysis of PRP-like proteins as MAPK interactors by a Yeast-two-hybrid screen

To examine the specificity of interactions with MAPKs, a yeast-two-hybrid assay was performed with PRP, PH1 and PH2 against all 20 known MAPKs from *A. thaliana* (Col-0). The growth of yeast colonies on selective dropout media lacking the indicated amino acids (SD-Leu-Trp-His) is the indicator that a protein-protein interaction is occurring. From this we observed that PRP interacted with MPK3, MPK4, and MPK6, PH2 with MPK3, MPK4, MPK6 and MPK11, while PH1 interacted with MPK6 and MPK8 (Fig. 1). Upon selection under more stringent conditions (SD-Leu-Trp-His-Ade), PRP interacted with MPK4 and MPK6, PH2 only interacted with MPK6, while no interactions were observed for PH1. This demonstrates that the interaction with the MAPKs not only varies in strength, but more importantly, preference is given to interaction of the three proteins with specific MAPKs that are known to be stress-activated (Takahashi et al., 2011; Bethke et al., 2012).

1.2 Bimolecular Fluorescence Complementation (BiFC)

Bimolecular Fluorescence Complementation (BiFC) is utilised to visualize protein-protein interactions in living plant cells. A fluorescent protein, in this case YFP (YELLOW FLUORESCENT PROTEIN), is split into two fragments and fused to potential interacting partners i.e. protein "X" fused to N-terminal YFP fragment and protein "Y" fused to C-terminal YFP fragment. Interaction of the two protein partners brings the YFP fragments into close proximity allowing them to reconstitute, resulting in YFP fluorescence and thereby confirming a protein-protein interaction of the investigated partners (Walter et al., 2004).

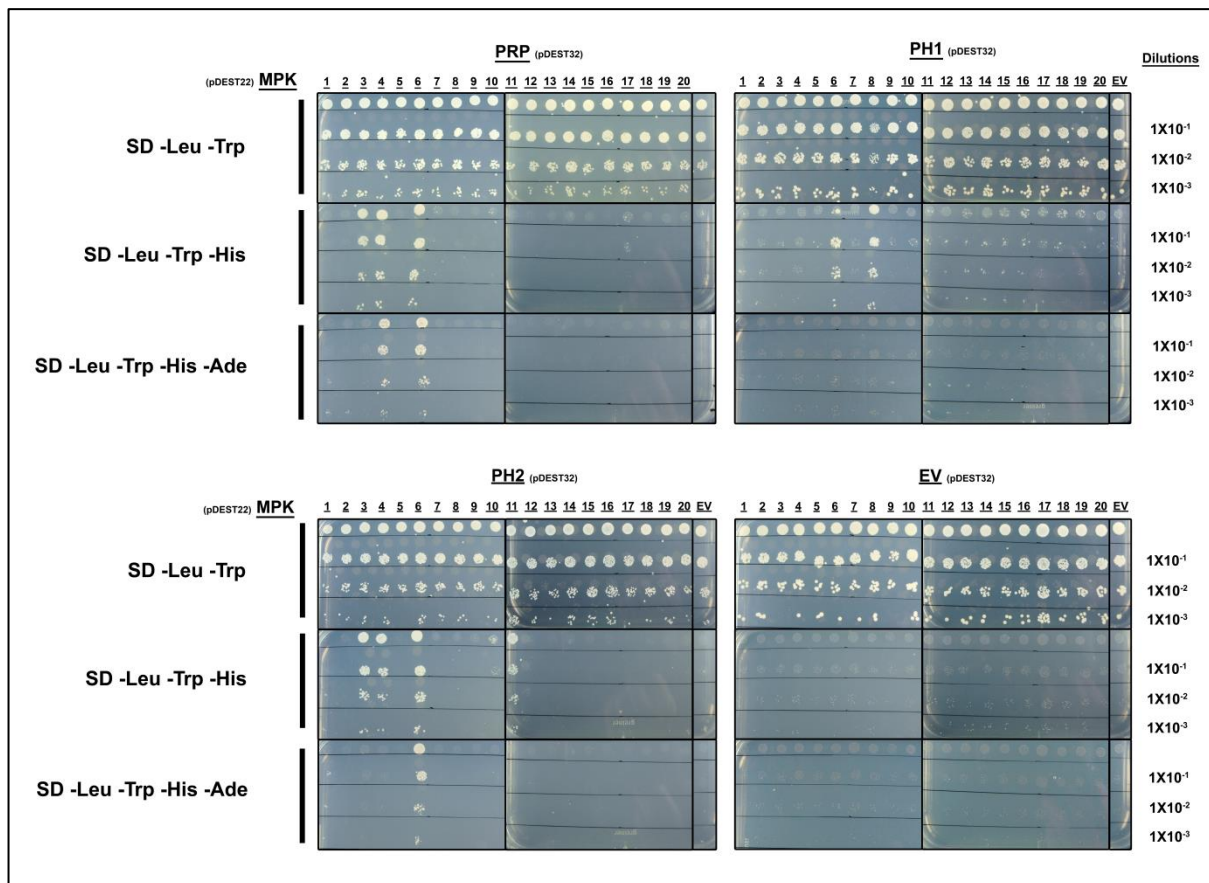


Fig. 1: Yeast-2-Hybrid protein-protein interaction screen of PRP (in pDEST32), PH1 (in pDEST32) and PH2 (in pDEST32) with all 20 MAPKs (in pDEST22) of *A. thaliana* (Col-0). Positive interactions were determined by visualising yeast growth of serial dilutions on the selective dropout medium (SD-Leu-Trp-His and SD-Leu-Trp-His-Ade). pDEST32 was used to generate the GAL4 binding domain fusion product and pDEST22 the GAL4 activating domain fusion product that had been transformed into yeast strain PJ69-4A. EV denotes the empty vector control.

Bimolecular fluorescence complementation (BiFC) was performed using mesophyll protoplasts prepared from *A. thaliana* (Col-0) to determine if the interactions in the yeast-two-hybrid assay could be verified. MPK3, MPK4, MPK6, MPK11, the four best characterised stress-activated MAPKs, as well as the putative PH1 interactor, MPK8 (Fig. 1), were selected to confirm the interactions determined in the yeast-two-hybrid screen. YFP fluorescence was detected (Fig. 2) for PRP and PH2 interacting with MPK3, MPK4, MPK6, and MPK11, but none was observed for MPK8. No YFP signal was detected for PH1 and thus the interaction with MAPKs could not be confirmed in this case.

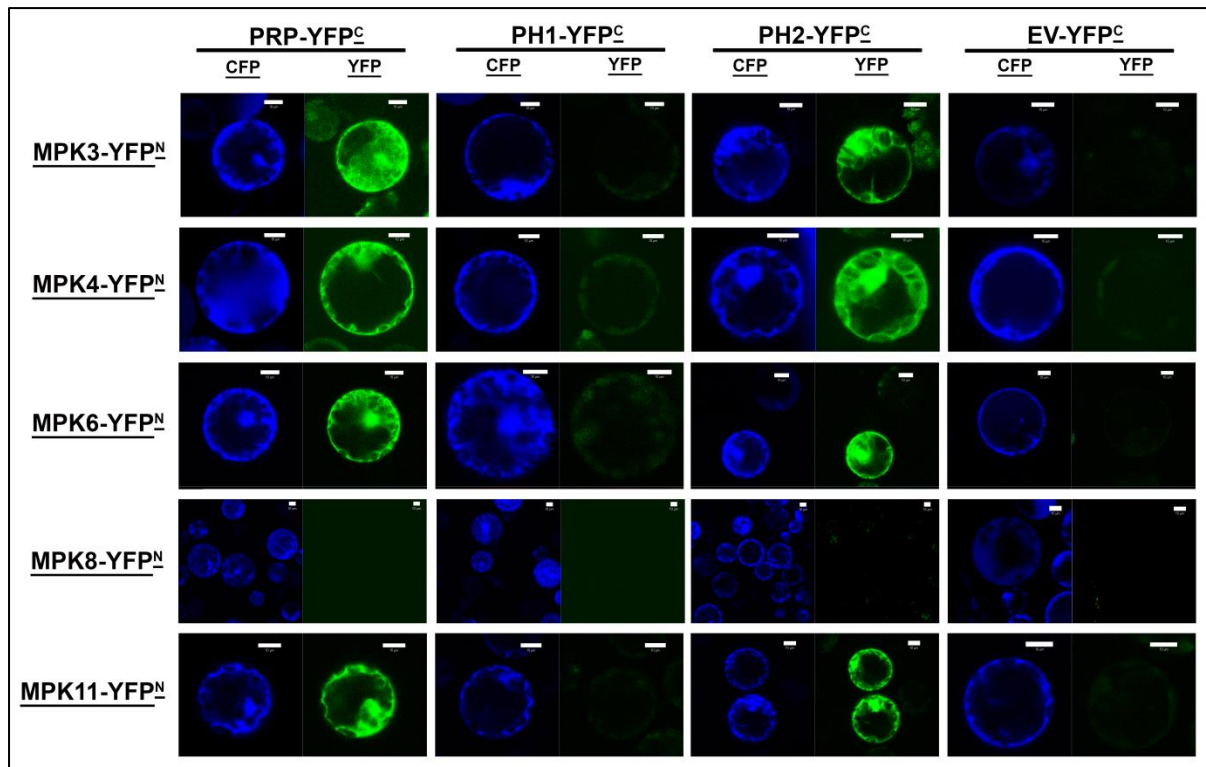


Fig. 2: BiFC visualization of PRP (in pESPYCE), PH1 (in pESPYCE) and PH2 (in pESPYCE) interaction with MPK3, MPK4, MPK6, MPK8 and MPK11 (in pESPYNE) in mesophyll protoplasts from *A. thaliana* (Col-0). Protoplasts were co-transformed with cyan fluorescent protein (CFP; pENSG) as a positive transfection control. Scale bars are 10 μ m. pESPYCE/ pESPYNE vectors contain the C-terminal YFP fragment and N-terminal YFP fragment, respectively. Interaction of the investigated proteins reconstituted a functional YFP, resulting in fluorescence.

1.3 *In vitro* phosphorylation assay

To determine whether PRP, PH1 and PH2 were not only MAPK interactors, but substrates as well, an *in vitro* phosphorylation assay was performed with MPK3 and MPK6 (Fig. 3). Both MPK3 and MPK6 have been shown to be activated by MKK4/5 (Asai et al., 2002). Since MAPKs require activation by their respective MAPK kinases (MKK), MPK3 and MPK6 were selected to be used in the assay since we could activate them both (Bethke et al., 2009) using the constitutively active Pc-MKK5DD from Parsley (Lee et al., 2004). All proteins were recombinantly overexpressed in *E. coli* and purified. The constitutively active Pc-MKK5DD was purified under non-denaturing

conditions on Ni-NTA resin (Qiagen) and MPK3 and MPK6 on Glutathione Sepharose™ 4 Fast Flow (GE Life Sciences).

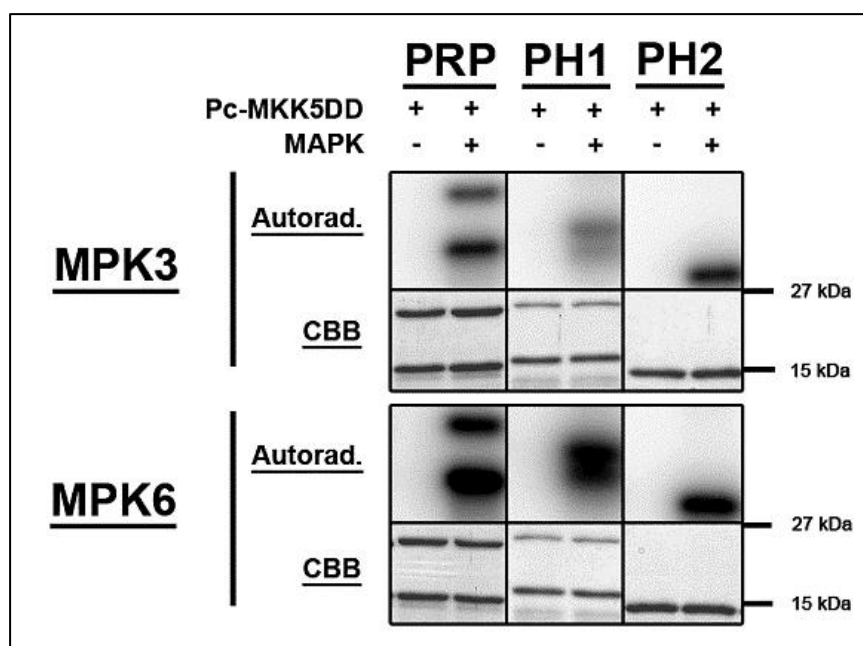


Fig. 3: In vitro phosphorylation assay of PRP, PH1 and PH2. PRP, PH1 and PH2 were purified by denaturing Ni-NTA purification and refolded before assay. MPK3 and MPK6 were activated by incubation with a constitutively active MKK from parsley (Pc-MKK5DD). Equal sample loading was visualised with Coomassie brilliant blue (CBB) staining.

Poly-histidine-tagged PRP, PH1, and PH2 were initially purified by Ni-NTA affinity chromatography (Qiagen) under non-denaturing conditions, but a second band above the expected band was visible in all eluates for PRP and PH1. Even under denaturing purification conditions where potential interacting proteins of *E. coli* origin should be absent, the second band remained in purified eluates of PRP and PH1. The upper bands for both proteins were excised from the SDS-page gel and analysed by Liquid Chromatography/Mass Spectrometry (LC/MS). Since only peptides of the PRP or PH1 could be detected (data not shown), the second band was also the recombinantly expressed protein. These two different forms of bands could be due to alternative folding that are recalcitrant to unfolding under the standard SDS-page conditions or possibly through self-dimerization. However, no

homodimerization could be detected using yeast-two-hybrid analysis (data not shown).

PRP, PH1 and PH2 were phosphorylated by both MPK3 and MPK6 but not the active Pc-MKK5DD, which demonstrated that these proteins are specifically utilised as MAPK substrates. Notably, both PRP bands were phosphorylated while for PH1, only the faster migrating species, i.e. of the expected size of PH1 (16 kDa), was phosphorylated.

1.4 *In silico* sequence analysis of PRP and its homologs

MAPKs are proline directed kinases (Ubersax and Ferrell Jr, 2007) that target serine/threonine preceded by a proline (S/T-P). Five potential target sites were identified in PRP (T37, S51, S56, S60, T80), three sites in PH1 (S65, T98, S109) and two sites in PH2 (S44, S48). Additionally a putative MAPK docking site with $(R/K)_{1-2}-(X)_{2-6}-\Phi-X-\Phi$ consensus sequence (where Φ is a hydrophobic residue) was also identified within the amino acid sequences of PRP (K26, R27, L31, I33), PH1 (R42, R43, L47, I49), and PH2 (R21, R22, L27, I29). The basic residues of $(R/K)_{1-2}-(X)_{2-6}-\Phi-X-\Phi$ bind the corresponding negatively charged area in a region C-terminal to the kinase domain, while the hydrophobic residues bind within a hydrophobic groove present in MAPKs (Ubersax and Ferrell Jr, 2007). Variation and spacing of residues in the docking site combined with the preference of the MAPK catalytic site increases the specificity of the MAPK interaction with substrates (Ubersax and Ferrell Jr, 2007). The aligned amino acid sequences of PRP, PH1 and PH2 (T-Coffee; Di Tommaso et al., 2011) is shown below where the identified potential MAPK targeted phosphosites and docking sites are highlighted (Fig. 4).

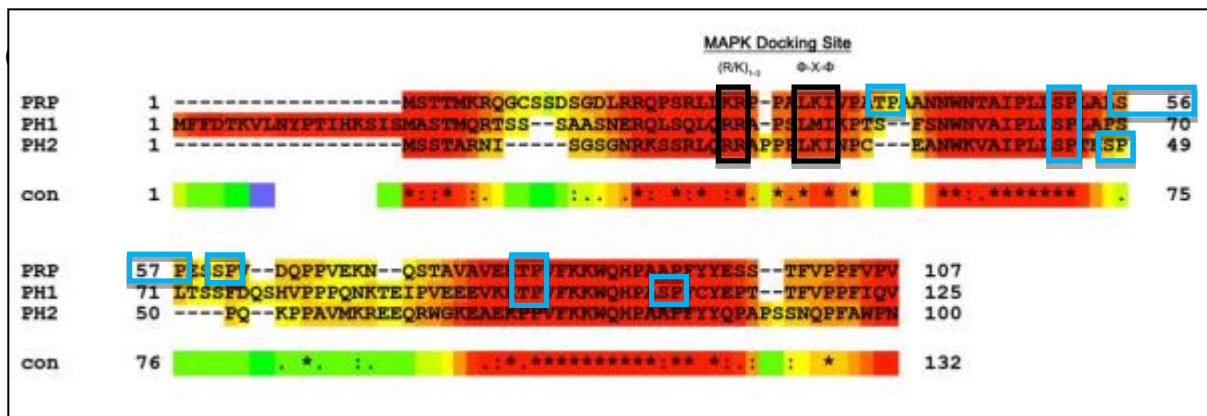


Fig. 4: Amino acid alignment of PRP, PH1, and PH2 with T-Coffee (Di Tommaso et al., 2011). Potential MAPK docking sites are highlighted in black boxes for PRP (K26, R27, L31, I33), PH1 (R42, R43, L47, I49), and PH2 (R21, R22, L27, I29). Five putative MAPK phosphorylation sites were identified in PRP (T37, S51, S56, S60, T80), three sites in PH1 (S65, T98, S109) and two sites in PH2 (S44, S48); which are highlighted in the blue boxes. The alignment colour scheme is named the CORE index and it uses the consistency among pairwise alignments to estimate reliability, ranging from poor (green) to good (red) consensus. An “*” indicates positions that have a fully conserved residue, a “:” indicates conservation between groups of strongly similar properties and “.” indicates conservation between groups of weakly similar properties.

1.4.1 Substrate analysis by targeted site directed mutation

The introduction of mutated phosphosites in proteins can be used to determine exactly which sites are specifically targeted by kinases (Robbins et al., 1993). Phosphosite mutants were created for PRP, PH1 and PH2 by exchanging the serine/threonine with alanine by site-directed mutagenesis. An optimized method for the rapid site-directed mutagenesis of putative MAPK phosphosites was developed and employed (Palm-Forster et al., 2012). Single, double, and complete phosphosite mutants were generated for each protein, and subsequently used in an *in vitro* phosphorylation assay to determine the main phosphosites (Fig. 5).

As illustrated in figure 5A, PRP was phosphorylated by both MPK3 and MPK6. Of all the single phosphosite mutants, only PRP^{S51A} showed a strong reduction in the phosphorylation signal intensity. Double phosphosite mutants, in which S51A was one of the mutated PRP sites, also showed strong reduction in phosphorylation signal. In all cases where S51 was present, phosphorylation signals that are comparable to the wild-type PRP were

The docking site that MAPK substrates possess generally follow the pattern of (R/K)₁₋₂-(X)₂₋₆-Φ-X-Φ (Ubersax and Ferrell Jr, 2007). In order to determine whether this docking site in PRP and its homologs had any effect on the interaction with MPK3 and MPK6, the basic (R/K) and hydrophobic (Φ-X-Φ) region was mutated to contain aspartic/glutamic acid. This resulted in the regions having opposite properties than in the native protein. A yeast-two-hybrid screen was performed with the docking site mutants of PRP, PH1 and PH2 against all 20 MAPKs. All interactions with MAPKs that were previously seen (Fig. 1) on selective media was no longer visible (Fig. 6A).

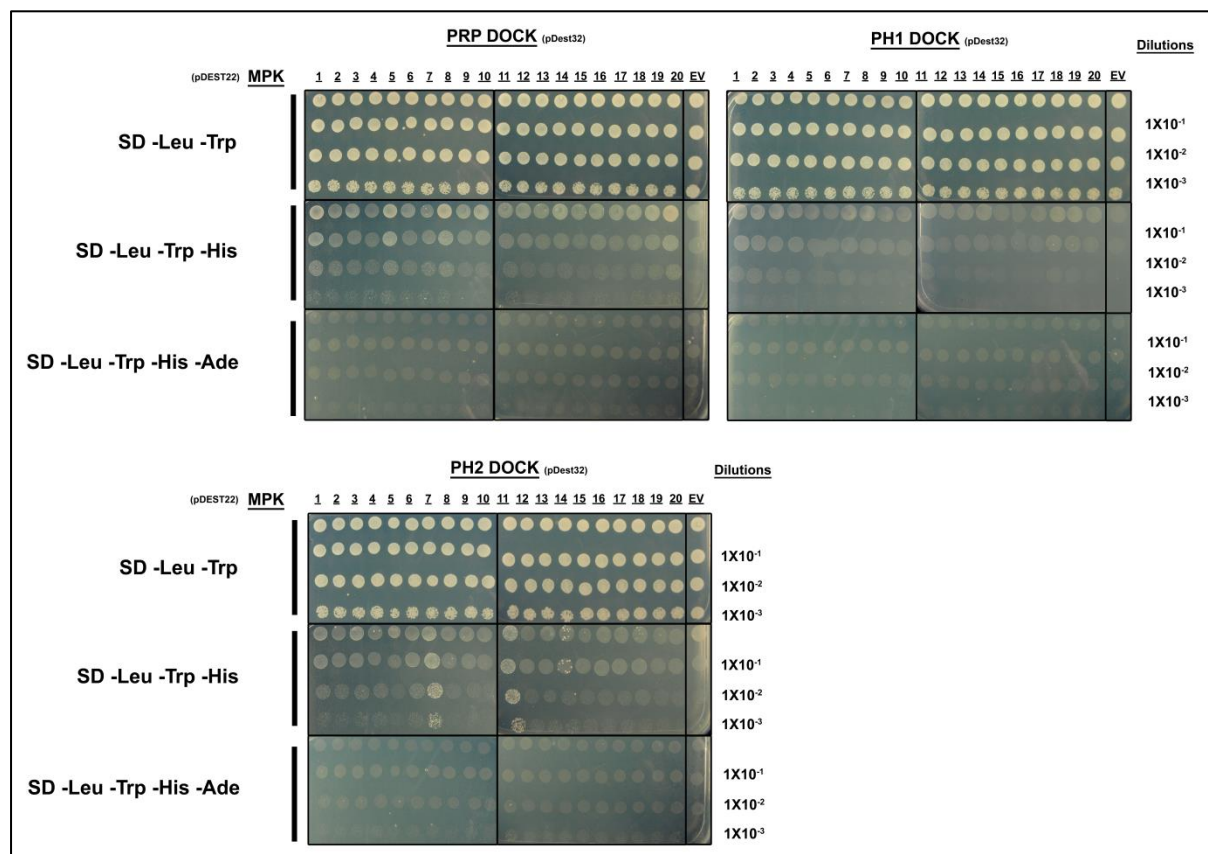


Fig. 6A: Yeast-2-Hybrid protein-protein interaction screen of PRP (in pDEST32), PH1 (in pDEST32) and PH2 (in pDEST32) docking site mutants with all 20 MAPKs (in pDEST22) of *A. thaliana* (Col-0). Interactions were determined by visualising yeast growth of serial dilutions on the selective dropout medium (SD-Leu-Trp-His and SD-Leu-Trp-His-Ade). pDEST32 was used to generate the *GAL4* binding domain fusion product and pDEST22 the *GAL4* activating domain fusion product that had been transformed into yeast strain PJ69-4A.

For the *in vitro* phosphorylation assay, wild type protein along with the mutated version of the docking site (Fig. 6B) was used to determine if any effect of phosphorylation by MPK3 and MPK6 could be observed. In all cases, the wild type protein of PRP, PH1 and PH2 were strongly phosphorylated by both MAPKs while the docking site mutants were phosphorylated to a lesser extent. Taken together, the assays confirmed that PRP and its homologs not only possess a MAPK docking site, but more importantly, it is necessary to aid interaction of MPK3 and MPK6 with PRP, PH1 and PH2.

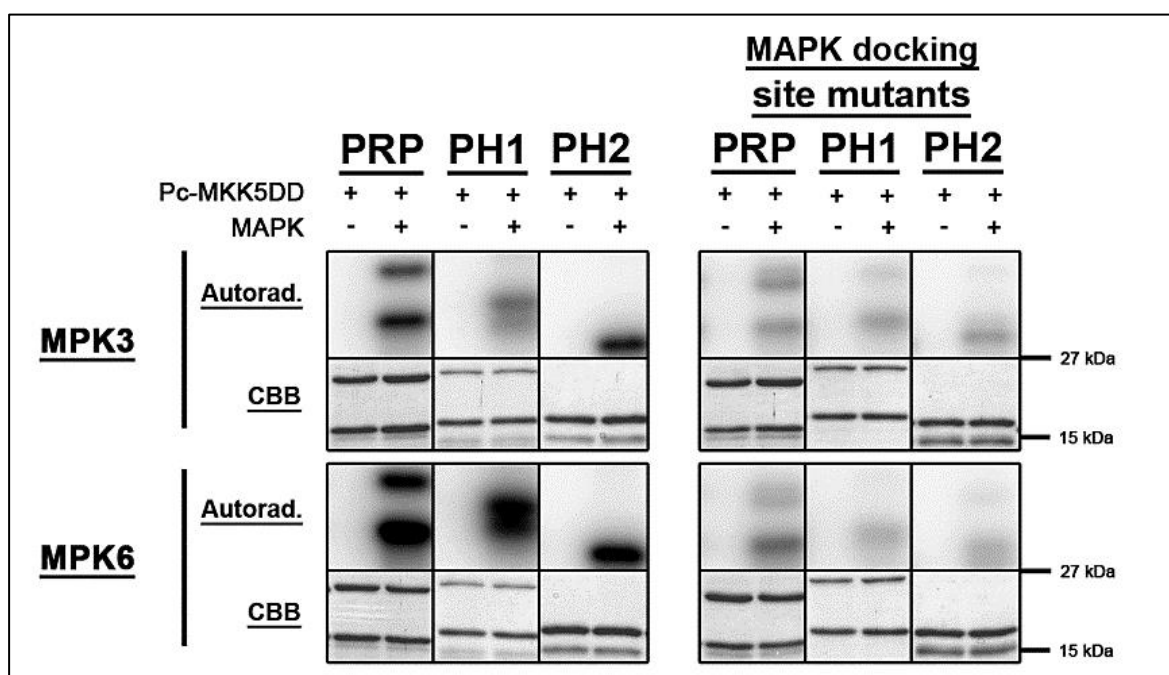


Fig. 6B: Autoradiographs of PRP, PH1 and PH2 wild type proteins along with the docking site mutated versions after *in vitro* phosphorylation by MPK3 and MPK6. The docking site in PRP (K26E, R27E, L31D, I33D), PH1 (R42E, R43E, L47D, I49D), and PH2 (R21E, R22E, L27D, I29E) were mutated, thereby changing the basic region to acidic, and the hydrophobic region to hydrophilic. MPK3 and MPK6 were activated by incubation with a constitutively active MKK from Parsley (Pc-MKK5DD). Equal sample loading was visualised with Coomassie brilliant blue (CBB) staining.

2. Gene expression profile of *PRP*, *PH1* and *PH2* in *A. thaliana*

Genevestigator is an online data mining tool for analysing global expression profile data. Expression patterns of genes can be visualised based on a selection of environmental conditions, growth stages, treatments etc. (Zimmermann et al., 2004). The “anatomy” data of *PRP* indicated that it was exceptionally highly expressed in pollen. The whole flower sample and stamen samples also showed high *PRP* expression but not as high as in the pure pollen sample. The remaining data showed low expression for *PRP* compared to the flower, stamen and pollen samples. *PH2* showed medium expression in embryo and endosperm samples and low expression in the other illustrated tissues and organs. In the case of *PH1*, there is no data set available as it is not covered in the Arabidopsis chipset. The eFP Browser, in addition to Genevestigator, was used to generate a pictographic representation of the microarray data discussed above as seen below in figure 7A (Winter et al., 2007).

To validate the expression levels of *PRP*, *PH1*, and *PH2*, RNA was extracted from various Arabidopsis organs and 14 day old seedlings, cDNA synthesised, and gene expression analysed by Real-time qPCR. In agreement with the microarray data (Fig. 7A), *PRP* expression levels were exceptionally high in pollen (Fig. 7B). *PRP*'s expression in flowers and siliques correlated to the microarray data examined. Expression levels for *PH2* (Fig. 7B) were high in mature siliques correlating well with the microarray data (Fig. 7A). *PH1* expression was highest in mature siliques compared to the other samples tested. As the same reference gene is used to normalize the expression of the tested genes, direct comparisons between the expression data for the investigated genes can be made. Therefore, the expression of *PH1* is generally much weaker in comparison to the expression levels observed for *PRP* and *PH2*.

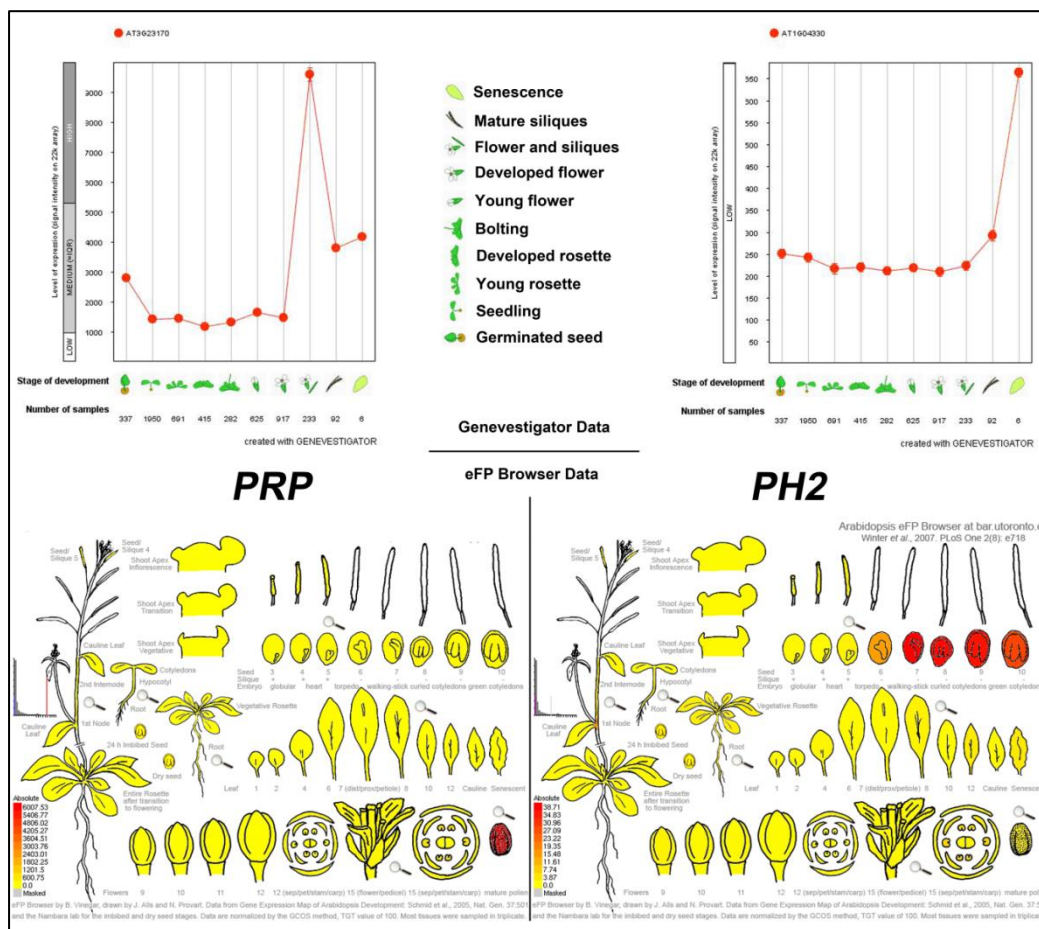


Fig. 7A: Genevestigator and eFP browser pictograph representation of the expression levels of *PRP* and *PH2* in various organs in *A. thaliana* (Col-0) based on the *ATH1* microarray data set. Expression levels for eFP browser are colour coded for low (yellow) to high (red).

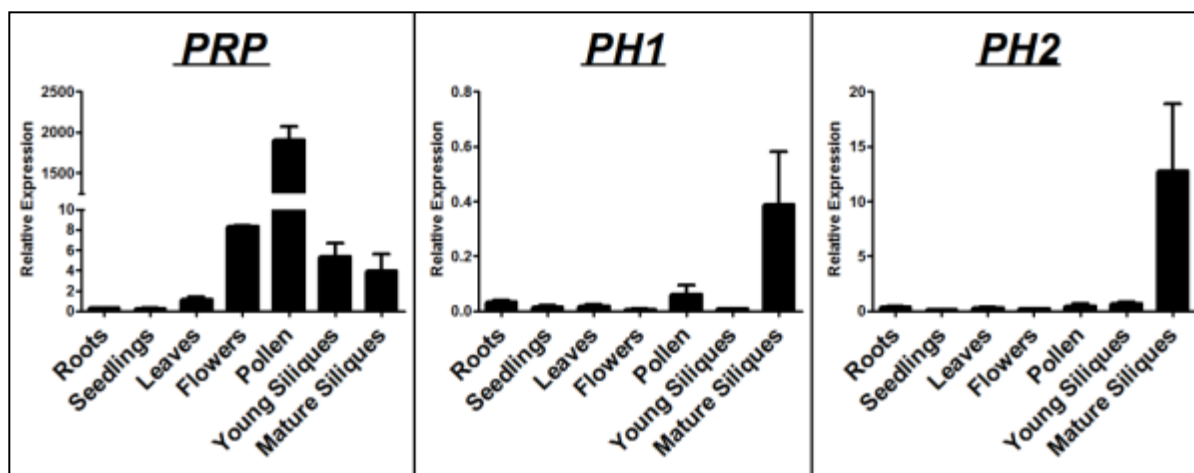


Fig. 7B: Real-time qPCR analysis of *PRP*, *PH1* and *PH2* expression in various organs and seedlings of *A. thaliana* (Col-0). The relative expression of each gene was normalized to the reference gene *PP2A* (At1g13320).

2.1 Effect of MAMP treatment on expression of *PRP*-like genes

The application of MAMPs such as flg22 and elf18, to trigger immune responses has been used extensively to study plant immunity (Fiil et al., 2009). To analyse the stress-responsiveness of the *PRP*-like genes, Arabidopsis seedlings were grown for two weeks in MS media before elicitation with flg22 and elf18 [100nM]. Material was harvested at multiple time points to generate gene expression kinetics for each treatment. RNA was extracted and cDNA synthesised before analysis by Real-time qPCR. *PRP* gene expression rapidly increased (Fig. 8A) 10-30min after flg22 treatment before reverting to basal level expression at 60min. A significant increase was also observed after elf18 treatment (Fig. 8B) at 20 and 30min before returning to basal level expression.

The expression of *PH1* was significantly increased transiently from 20-90min after flg22 and elf18 treatment (Fig. 8A, B). Compared to *PRP*, *PH1* expression in the flg22-treated samples was higher. In the elf18-treated samples, the expression of *PRP* was higher than *PH1*'s. *PRP* expression in both flg22- and elf18-treated samples was rapidly down regulated after 30min while *PH1* was down regulated more gradually in both MAMP treatments. In summary, for both *PRP* and *PH1*, expression was rapidly increased after MAMP perception, whereas *PH2* was unresponsive to both MAMP treatments (Fig. 8A, B). To exclude any osmotic and unintended stress during the handling of the seedlings, a water control was included where *PRP*, *PH1* and *PH2* gene expression was unaffected (Fig.8C).

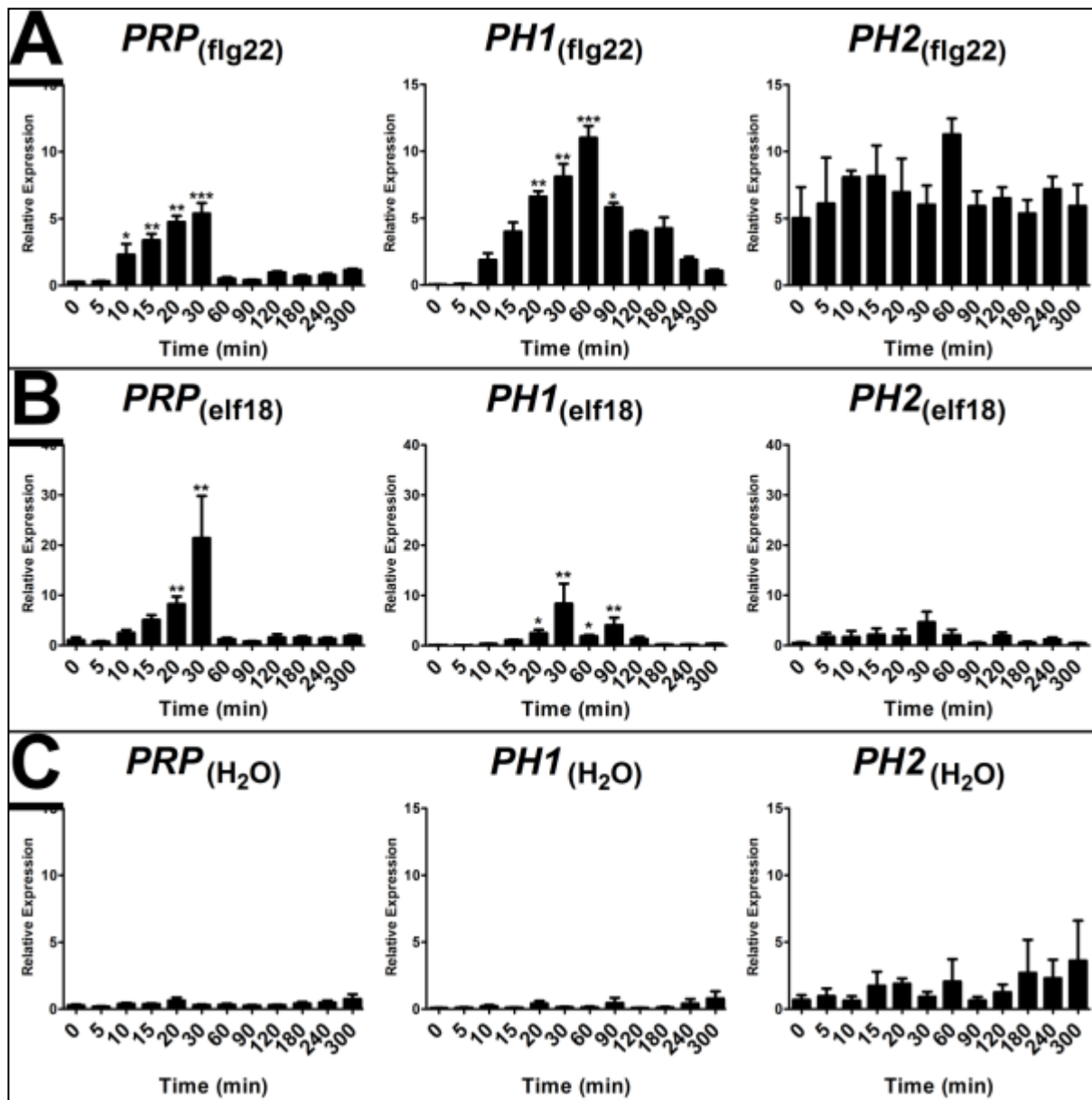


Fig.8: Relative gene expression of *PRP*, *PH1* and *PH2* in seedlings after treatment with (A) flg22 [100nM], (B) elf18 [100nM] and (C) H₂O. Expression values were normalised to the expression of *PP2A*. Statistically significant time points are marked with an asterisk (One-way ANOVA with Dunns post-test; * = $p < 0.05$; ** = $p < 0.01$; *** = $p < 0.001$) and all experiments were performed with $n \geq 2$ along with two biological replicates.

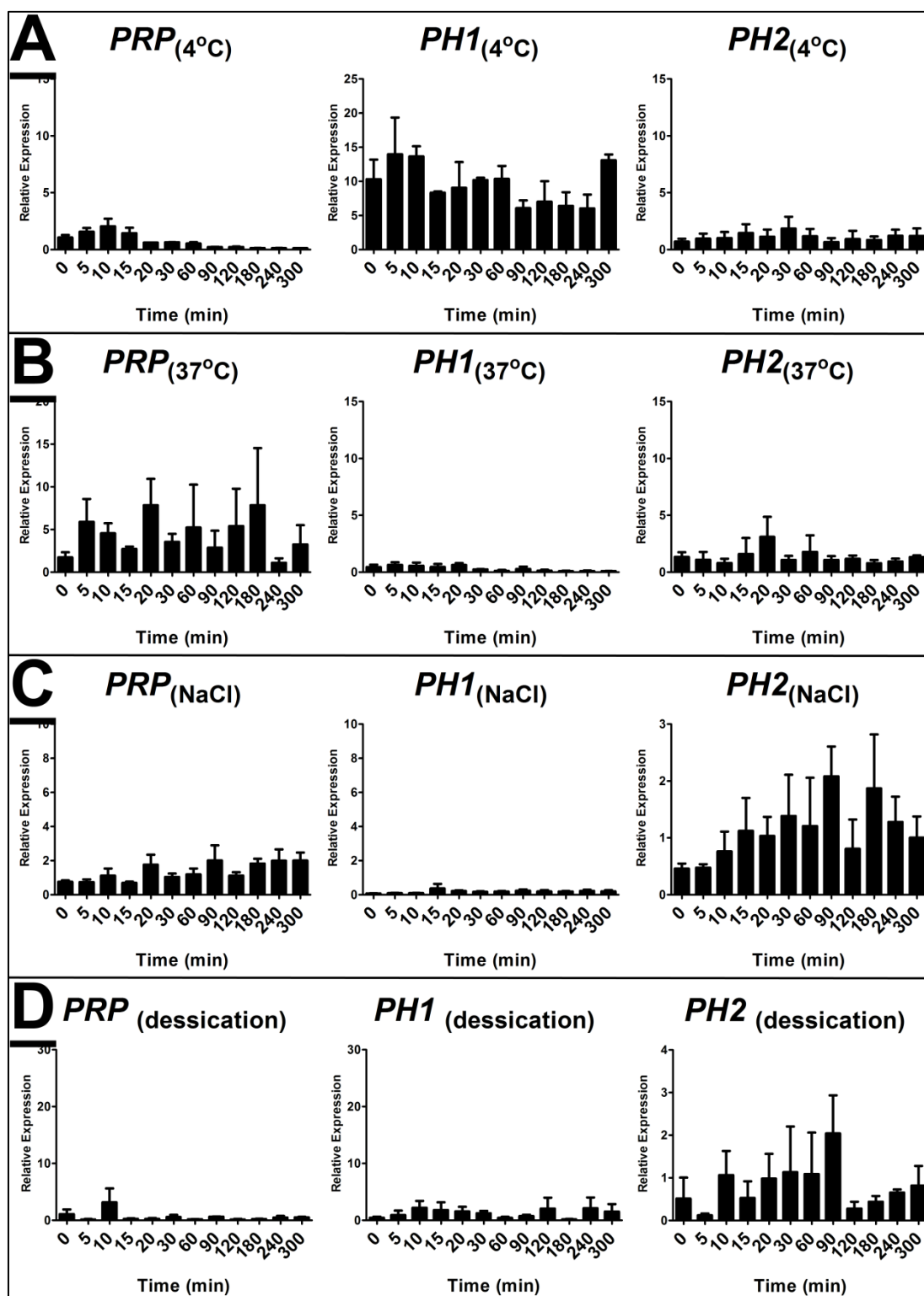


Fig. 9: Relative gene expression of *PRP*, *PH1* and *PH2* in seedlings after treatment incorporating (A) 4°C, (B) 37°C, (C) NaCl [250mM], and (D) desiccation. Expression values were normalised to the expression of *PP2A*. Statistically significant time points are marked with an asterisk (One-way ANOVA with Dunns post-test; * = $p < 0.05$; ** = $p < 0.01$; * = $p < 0.001$) and all experiments were performed with $n \geq 2$ and two biological replicates.**

2.2 Effect of abiotic stresses on expression of *PRP-like* genes

Arabidopsis seedlings were grown for two weeks in MS media before applying abiotic stresses. Conditions tested included cold (4°C), heat (37°C), salt [250nM] and desiccation. The four abiotic treatments (Fig. 9A, B, C, and D) did not significantly affect the gene expression of *PRP*, *PH1* and *PH2*. From this data and that shown in figures 8A and 8B, it is clear that *PRP* and *PH1* are only up-regulated by MAMPs and therefore possibly involved in the early responses of the defence related pathway. *PH2* expression was unaffected by biotic and abiotic stresses tested.

3. Promoter Analysis

3.1 Analysis of *PRP*, *PH1* and *PH2* promoter activity in response to flg22 or elf18 treatments

To validate the MAMP induced gene expression of *PRP*, *PH1* and *PH2* in seedlings, the respective promoters were tested for responsiveness to MAMP treatments. The promoters of *PRP* (1139bp upstream from the ATG start codon), *PH1* (1868bp) and *PH2* (1470bp) were individually fused to a *luciferase* (*LUC*) reporter gene and transfected into mesophyll protoplasts of *Arabidopsis thaliana* (Col-0). The protoplasts were treated with either flg22 or elf18 and the resulting luminescence from the *LUC* reporter measured continuously for 180min. This system has been used to analyse defence-related promoter activity (Shan et al., 2008; Ranf et al., 2011).

In figure 10, we can see that *pPRP* and *pPH1* activity transiently increases in response to treatment with flg22 and elf18 in comparison to water. *pPH2* activity remains unaffected by both elicitors. Transcript accumulation of *PRP* and *PH1* in seedlings (Fig. 8A, B) occurs within 30min after MAMP treatment, and as seen in figure 10 below, the increase of promoter activity visibly increases from 30min onward. There is a strong correlation between the results seen in the two systems, while the slight delay in the protoplast system could be due to the lengths of the promoters selected for the analysis.

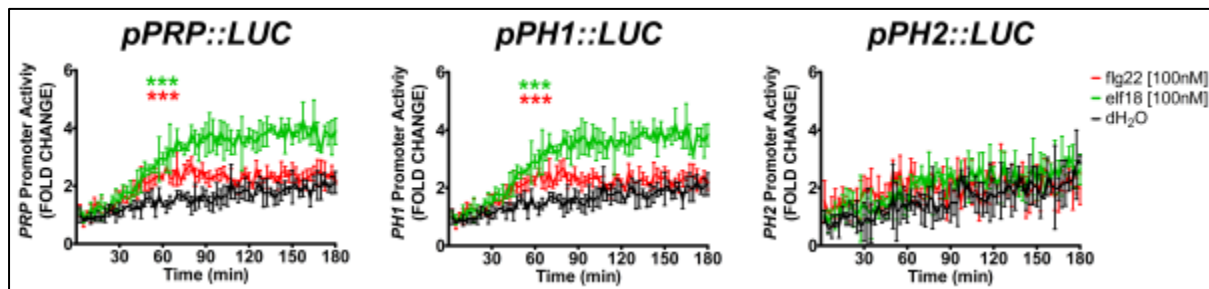


Fig. 10: Promoter activity of PRP, PH1 and PH2 after treatment with flg22 [100nM], elf18 [100nM] and dH₂O. The figure depicts representative data seen in three independent experiments (n=3). *Promoter::luciferase* fusion constructs were co-transformed with a *pUBQ10::GUS* construct into mesophyll protoplasts from *A. thaliana* (Col-0). Promoter activity is represented as LUC activity normalised to GUS activity. One-way ANOVA was performed and statistically significant differences to the water-treated samples are indicated (***) = p<0.001).

3.2 Effect of PRP-like proteins on the MAMP-responsive promoter *FRK1*

Activation of MPK3 and MPK6 after flg22 perception is followed by transcriptional activation of several genes including the *flg22-induced receptor like kinase 1* (*FRK1*) (Asai et al., 2002). *PRP* and *PH1* show transcriptional activation by flg22/elf18 (Fig. 10) and their respective gene products are phosphorylated by MPK3 and MPK6 (Fig. 3). Therefore, we investigated if these MAPK substrates might influence the *FRK1* promoter activity. The *FRK1* promoter was fused to a luciferase reporter gene and used as a reporter for promoter activity to easily monitor any potential influence on *FRK1* transcription. The respective phosphosite mutants PRP^{S51A}, PH1^{S65A} and PH2^{S44A} were also tested to determine if phosphorylation could additionally influence any potential effect on the *FRK1* promoter. Figures 11 and 12 show the promoter activity of *FRK1* after treatment of transfected mesophyll protoplasts with either flg22 (Fig. 11A-F) or elf18 (Fig. 12A-F).

The basal *FRK1* promoter activities (water-treated samples) were higher with expression of PRP (Fig. 11A, p<0.001), PH1 (Fig. 11C, p<0.001) or PH2 (Fig. 11E, p<0.01) compared to expression of the cyan fluorescent protein (CFP) transfected control. Transfection with CFP is routinely used in our promoter

assays to show that overexpression of an unrelated protein has no impact on the promoters being studied. In fact, the basal level promoter activities in the protoplasts overexpressing the PRP-like proteins were analogous to the level observed for the flg22 elicited samples (blue versus red lines in Fig. 11A, C, and E respectively). Overexpression of the phosphosite mutants PRP^{S51A} (Fig. 12A, $p \leq 0.001$), PH1^{S65A} (Fig. 11C, $p \leq 0.001$), or PH2^{S44A} (Fig. 11E, $p \leq 0.001$) accentuated the basal level of *FRK1* promoter activities even further than their wild type counterparts (green lines in Fig. 11). This would suggest that phosphorylation of these proteins by MAPKs negatively regulates the stimulation of the *FRK1* promoter.

Flg22 treatment of the samples overexpressing PRP (Fig. 11B, $p \leq 0.01$), PH1 (Fig. 11D, $p \leq 0.001$), or PH2 (Fig. 11F, $p \leq 0.001$) further enhanced *pFRK1* activity far above the levels observed for the CFP-transfected protoplasts, leading to additive and, in part, synergistic effects. Treatment of the samples with flg22-expressing phosphosite mutants PRP^{S51A} (Fig. 11B, $p \leq 0.001$), PH1^{S65A} (Fig. 11D, $p \leq 0.001$), or PH2^{S44A} (Fig. 11F, $p \leq 0.001$) displayed a stronger influence on *FRK1* promoter activity than their respective wild type proteins. PRP^{S51A} expression resulted in a continuous higher level of *FRK1* promoter activity compared to wild-type PRP overexpression for the duration of the experiment. The PH1 phosphosite mutant PH1^{S65A} affected the promoter activity similarly to the wild-type PH1, before leading to higher promoter activity post 60 min (Fig. 11D). PH2's phosphosite mutant PH2^{S44A} increased *FRK1* promoter activity more between 30 and 60 min (Fig. 11F) after which its promoter activity levels resembled those seen where wild-type PH2 was overexpressed.

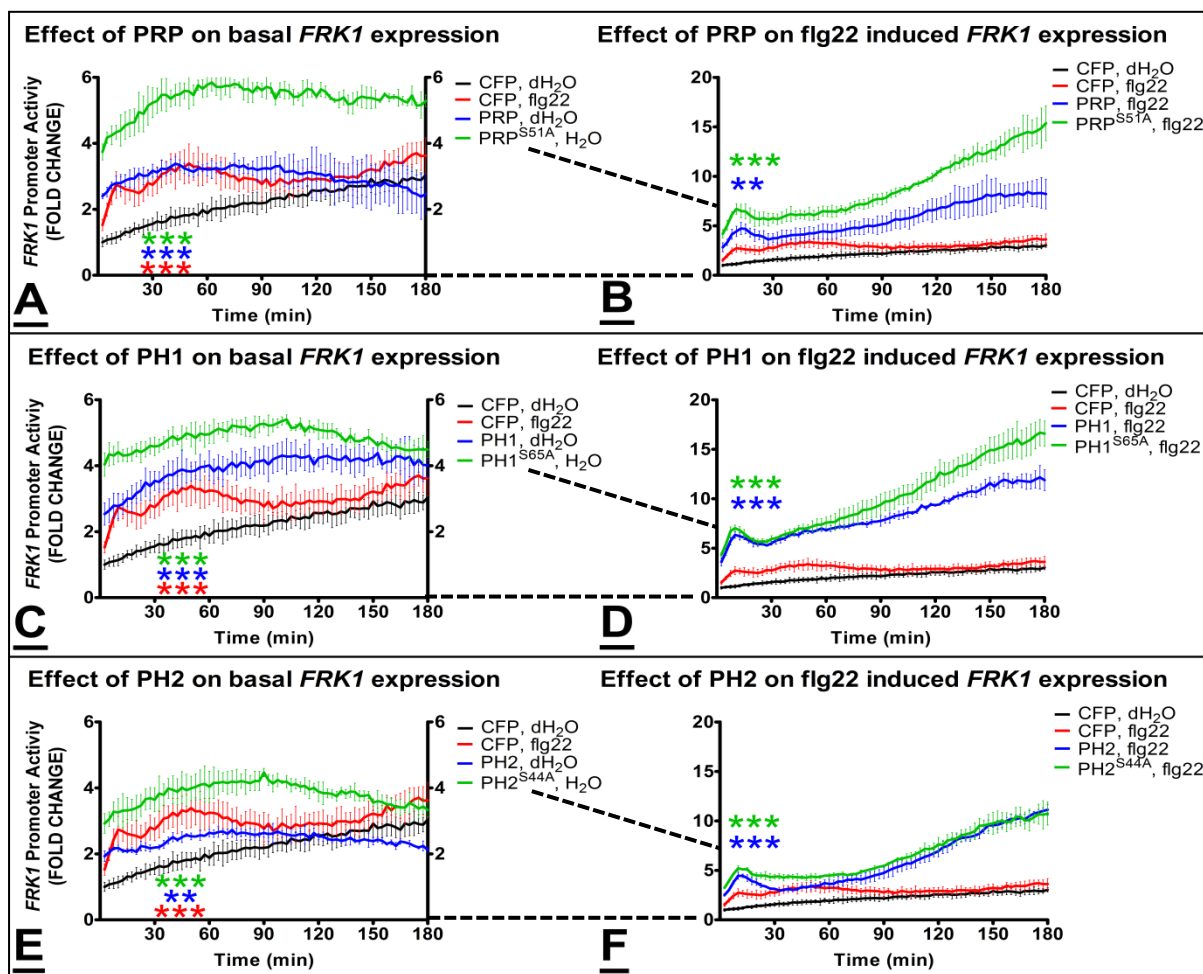


Fig. 11: Impact of PRP-like proteins on basal and flg22-induced *FRK1* expression. In the left panels, the basal *pFRK1* activities (in water-treated samples) are compared between protoplasts overexpressing either (A) PRP or its phosphosite mutant (PRP^{S51A}), (C) PH1, or its phosphosite mutant (PH1^{S65A}), or (E) PH2, or its phosphosite mutant (PH2^{S44A}). The corresponding effect(s) on the flg22-induced *pFRK1* activities, when the indicated proteins are overexpressed, are shown in the right panels (B, D and F). As a transfection control, CFP was used. Note that the basal (black line) and flg22-induced (red line) activities are identical in all the figures and depicted – as indicated by the dashed lines between the graphs on the left and the right – with a different range for better visualization. Promoter activities are presented as LUC activity normalized to *pUBQ10::GUS* activity and represented as fold change, with the water-treated control (Time = 0; transfected with CFP) set as a reference value of one. Error bars indicate the standard error of triplicate measurements. Two-way ANOVA was performed (Bonferroni post-test) on the raw data and only the statistically significant differences are highlighted with asterisks (** = $p \leq 0.01$; *** = $p \leq 0.001$), which are color-coded according to the curves being compared. In (A), (C) and (E), the statistical test was calculated against the water-treated protoplasts overexpressing CFP (i.e. testing if they were significantly different from the basal level promoter activity). For testing if the overexpression of the PRP-like proteins significantly affected the flg22-induced promoter activity (in B, D and F), the indicated statistics were calculated relative to CFP-transfected protoplasts after flg22 elicitation. The figure is representative of three independent experiments with similar outcome.

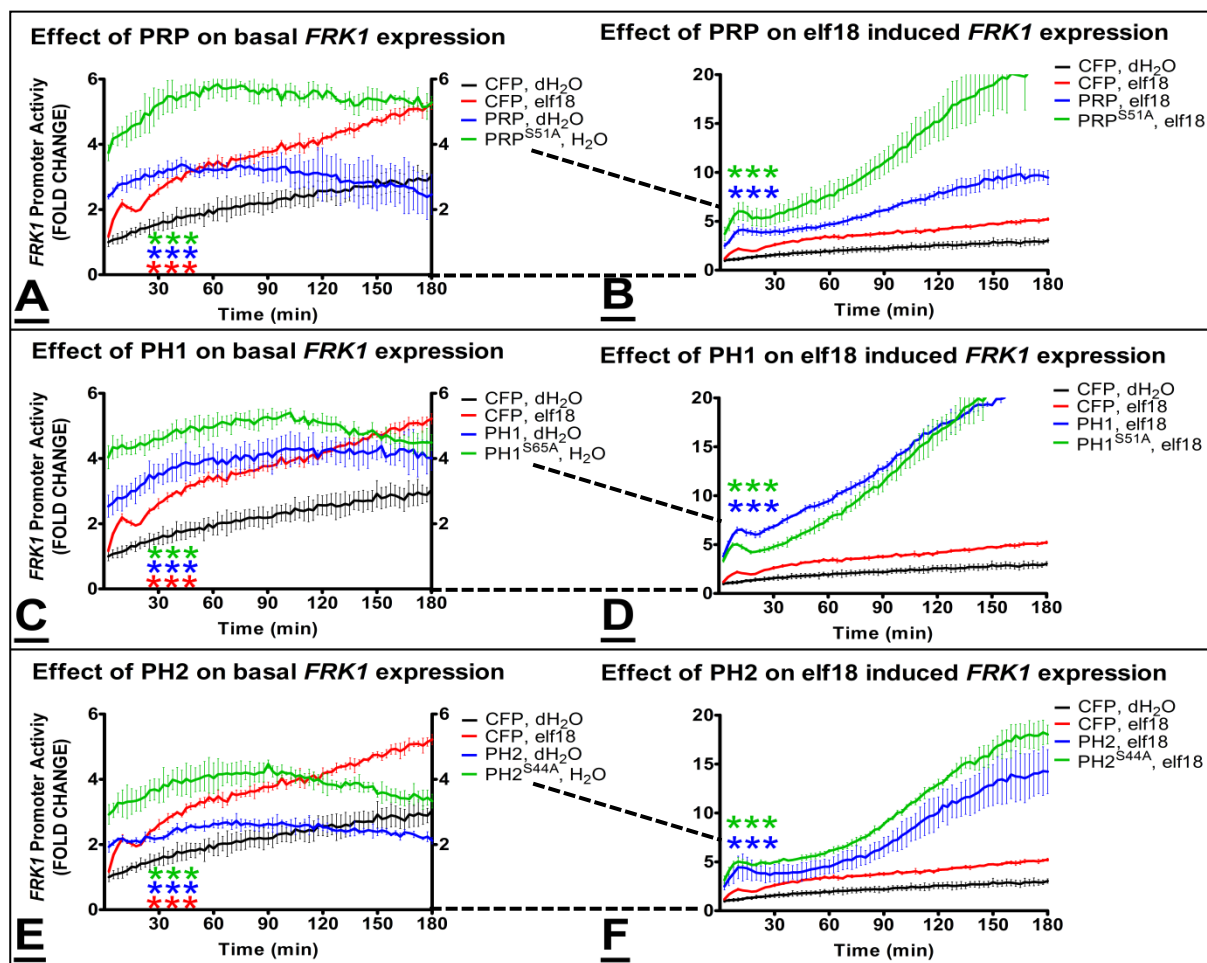


Fig. 12: Impact of PRP-like proteins on basal and elf18-induced *FRK1* expression. In the left panels, the basal *pFRK1* activities (in water-treated samples) are compared between protoplasts overexpressing either (A) PRP or its phosphosite mutant (PRP^{S51A}), (C) PH1, or its phosphosite mutant (PH1^{S65A}), or (E) PH2, or its phosphosite mutant (PH2^{S44A}). The corresponding effect(s) on the elf18-induced *pFRK1* activities, when the indicated proteins are overexpressed, are shown in the right panels (B, D and F). As a transfection control, CFP was used. Note that the basal (black line) and elf18-induced (red line) activities are identical in all the figures and depicted – as indicated by the dashed lines between the graphs on the left and the right – with a different range for better visualization. Promoter activities are presented as LUC activity normalized to *pUBQ10::GUS* activity and represented as fold change, with the water-treated control (Time = 0; transfected with CFP) set as a reference value of one. Error bars indicate the standard error of triplicate measurements. Two-way ANOVA was performed (Bonferroni post-test) on the raw data and only the statistically significant differences are highlighted with asterisks (***) = $p \leq 0.001$), which are color-coded according to the curves being compared. In (A), (C) and (E), the statistical test was calculated against the water-treated protoplasts overexpressing CFP (i.e. testing if they were significantly different from the basal level promoter activity). For testing if the overexpression of the PRP-like proteins significantly affected the elf18-induced promoter activity (in B, D and F), the indicated statistics were calculated relative to CFP-transfected protoplasts after elf18 elicitation. The figure is representative of three independent experiments with similar outcome.

For comparison, the effect of the PRP-like proteins on the elf18-induced *FRK1* expression was also tested. Unlike the transient flg22-induced *FRK1* expression, the elf18 induced response of *FRK1* is typically more pronounced with a sustained response within the tested time period (Fig. 12A, C, E). The enhancement of *FRK1* basal level activity by the PRP-like proteins did not surpass the levels observed for elf18-induced levels of *FRK1*. The phosphosite mutants did however enhance the level of *FRK1* promoter activity above that observed for elf18-induced promoter activity.

FRK1 promoter activity in response to elf18 treatment was significantly stronger in the samples overexpressing the PRP-like proteins compared to the CFP-transfected elf18-treated control samples (Fig. 12B, D, F; $p \leq 0.001$). A differential influence on *FRK1* promoter activity was once again observed between the PRP-like proteins and their phosphosite mutant proteins at various time points ($p \leq 0.05$).

In summary, the substantial increase of basal *pFRK1* activity by PRP, PH1, or PH2 indicates that some transcriptional regulation could be occurring. *FRK1* promoter activities were higher with the phosphosite mutants PRP^{S51A}, PH1^{S65A}, or PH2^{S44A} compared to their wild type counterparts, suggesting that the phosphorylation status of the PRP-like proteins has an impact on the level with which the PRP-like proteins can augment *FRK1* promoter activity.

3.3 Effect of PRP-like proteins on the *NHL10* MAMP-responsive promoter

The augmenting effect of PRP, PH1, and PH2 on the defence promoter activity of *FRK1* raised the question of whether this enhanced response to MAMP treatments could be seen in another defence-related promoter. The *NHL10* (*NDR1/HIN1-like 10*) promoter was selected as it has been reported to be activated early in the defence response by flg22 and elf18 (Boudsocq et al., 2010; Ranf et al., 2011).

The overexpression of the PRP-like proteins or their respective phosphosite mutants in water-treated samples resulted in a prodigious increase (≥ 8 fold increase) of the basal *NHL10* promoter activity (Fig. 13A, C, E; $p \leq 0.001$). This augmented basal level activity by the PRP-like proteins far surpassed the levels observed for flg22-induced *NHL10* promoter activity (CFP-transfected) samples (≥ 2 fold increase). The PRP-like proteins augmented *pNHL10* activity equally to their phosphosite mutants. Hence, unlike their impact on the *FRK1* promoter, phosphorylation status of the PRP-like proteins does not influence *NHL10* promoter activity.

Flg22-treatment of protoplasts expressing the PRP-like proteins and their respective phosphosite mutants led to a 10-20 fold increase of *pNHL10* activity (Fig. 13B, D, F; $p \leq 0.001$). The phosphosite mutant PRP^{S51A} displayed slightly weaker *pNHL10* activation compared to PRP after flg22 treatment (Fig. 13B; $p \leq 0.001$). The phosphosite mutant PH2^{S44A} displayed a two-fold decrease in *pNHL10* activity after flg22-treatment compared to levels observed for PH2 (Fig. 13F; $p \leq 0.001$).

The augmentation of *pNHL10* basal level activity by the PRP-like proteins did not surpass the elf18-induced *pNHL10* activity (Fig. 14A, C, E; $p \leq 0.001$), unlike that observed in the flg22 data set (Fig. 13). In fact, the elf18-induced *pNHL10* activity was up to two-fold higher than the augmented basal level activity of *pNHL10*. Only elf18-elicited protoplasts expressing either the phosphosite mutant PRP^{S51A} (Fig. 14B; $p \leq 0.001$) or PH2 (Fig. 14F; $p \leq 0.001$) increased the level of *pNHL10* activity above the levels observed for elf18-induced *pNHL10* activity (CFP-transfected control). The absence of phosphorylation sites in PH2^{S44A} (Fig. 14F; $p \leq 0.001$) appeared to negatively regulate *pNHL10* activity. Interestingly, both the presence and absence of phosphorylation sites in PH1 (Fig. 14D; $p \leq 0.001$) and PH1^{S65A} (Fig. 14D; $p \leq 0.05$) respectively, displayed differential negative regulation of *pNHL10* after elf18 elicitation at various time points compared to the wild type *pNHL10* promoter response (CFP-transfected control).

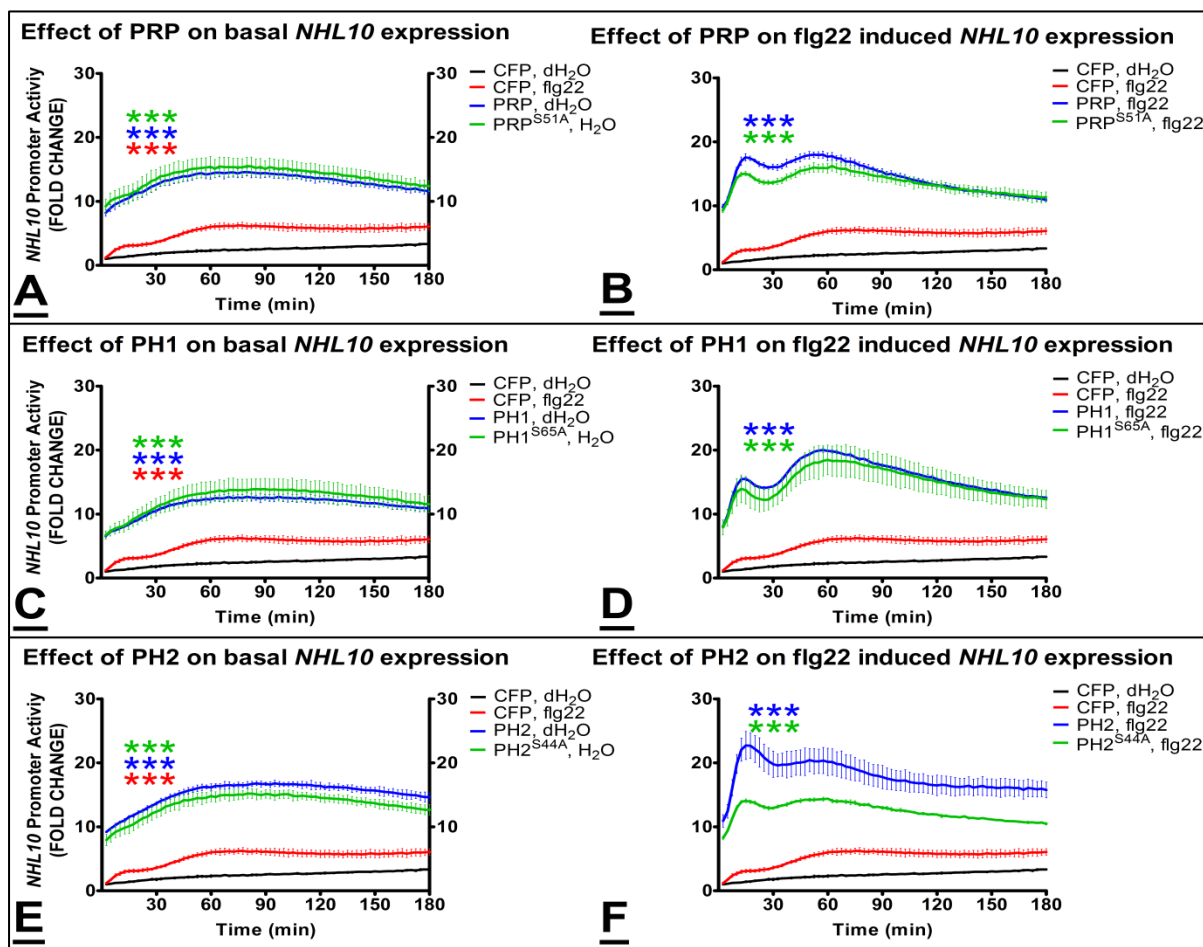


Fig. 13: Impact of PRP-like proteins on basal and flg22-induced *NHL10* expression.

In the left panels, the basal *pNHL10* activities (in water-treated samples) are compared between protoplasts overexpressing either (A) PRP or its phosphosite mutant (PRP^{S51A}), (C) PH1, or its phosphosite mutant (PH1^{S65A}), or (E) PH2, or its phosphosite mutant (PH2^{S44A}). The corresponding effect(s) on the flg22-induced *pNHL10* activities, when the indicated proteins are overexpressed, are shown in the right panels (B, D and F). As a transfection control, CFP was used. Note that the basal (black line) and flg22-induced (red line) activities are identical in all the figures and depicted – as indicated by the dashed lines between the graphs on the left and the right – with a different range for better visualization. Promoter activities are presented as LUC activity normalized to *pUBQ10::GUS* activity and represented as fold change, with the water-treated control (Time = 0; transfected with CFP) set as a reference value of one. Error bars indicate the standard error of triplicate measurements. Two-way ANOVA was performed (Bonferroni post-test) on the raw data and only the statistically significant differences are highlighted with asterisks (***) = $p \leq 0.001$, which are color-coded according to the curves being compared. In (A), (C) and (E), the statistical test was calculated against the water-treated protoplasts overexpressing CFP (i.e. testing if they were significantly different from the basal level promoter activity). For testing if the overexpression of the PRP-like proteins significantly affected the flg22-induced promoter activity (in B, D and F), the indicated statistics were calculated relative to CFP-transfected protoplasts after flg22 elicitation. The figure is representative of three independent experiments with similar outcome.

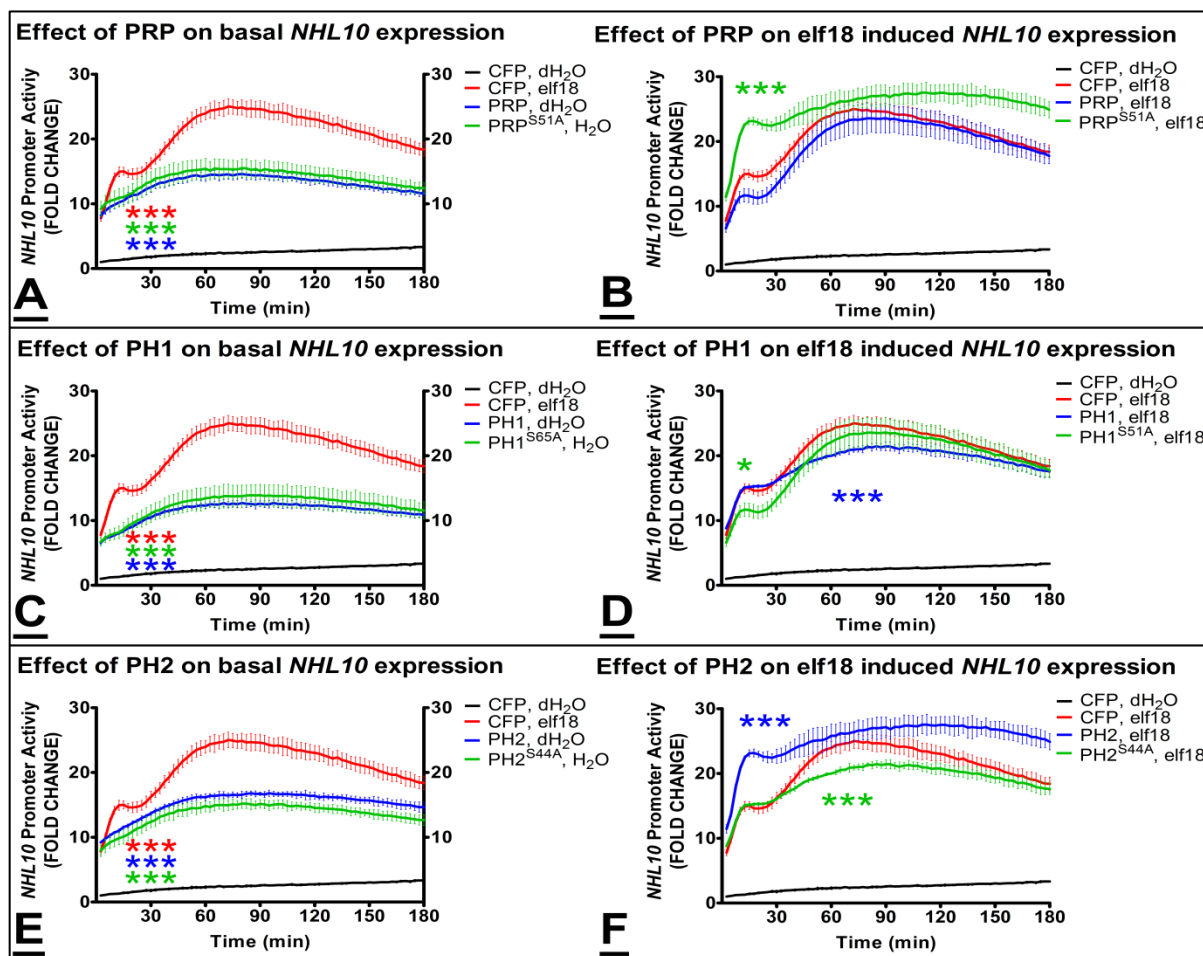


Fig. 14: Impact of PRP-like proteins on basal and elf18-induced *NHL10* expression.

In the left panels, the basal *pNHL10* activities (in water-treated samples) are compared between protoplasts overexpressing either (A) PRP or its phosphosite mutant (PRP^{S51A}), (C) PH1, or its phosphosite mutant (PH1^{S65A}), or (E) PH2, or its phosphosite mutant (PH2^{S44A}). The corresponding effect(s) on the elf18-induced *pNHL10* activities, when the indicated proteins are overexpressed, are shown in the right panels (B, D and F). As a transfection control, CFP was used. Note that the basal (black line) and elf18-induced (red line) activities are identical in all the figures and depicted – as indicated by the dashed lines between the graphs on the left and the right – with a different range for better visualization. Promoter activities are presented as LUC activity normalized to *pUBQ10::GUS* activity and represented as fold change, with the water-treated control (Time = 0; transfected with CFP) set as a reference value of one. Error bars indicate the standard error of triplicate measurements. Two-way ANOVA was performed (Bonferroni post-test) on the raw data and only the statistically significant differences are highlighted with asterisks (* = $p \leq 0.05$; *** = $p \leq 0.001$), which are color-coded according to the curves being compared. In (A), (C) and (E), the statistical test was calculated against the water-treated protoplasts overexpressing CFP (i.e. testing if they were significantly different from the basal level promoter activity). For testing if the overexpression of the PRP-like proteins significantly affected the elf18-induced promoter activity (in B, D and F), the indicated statistics were calculated relative to CFP-transfected protoplasts after elf18 elicitation. The figure is representative of three independent experiments with similar outcome.

In summary, expression of PRP, PH1, or PH2 enhanced the basal level promoter activities of both *FRK1* and *NHL10* defence-related promoters. Enhancement of the basal promoter activities reached (or in certain instances, even surpassed) the expression levels observed for the MAMP-treated samples. Upon elicitation of flg22 or elf18, additive and partially synergistic increases in promoter activities were observed when expressing the PRP-like proteins or their phosphosite mutants PRP^{S51A}, PH1^{S65A}, and PH2^{S44A}, with the only exception being for *NHL10* promoter activity when treated with elf18. Differences in promoter activities were also observed depending on whether the PRP-like proteins possessed their MAPK phosphorylation sites, indicating some regulation due to phosphorylation state. A visible difference was observed in the augmentation and response of the defence related promoters *FRK1* and *NHL10* to MAMP treatments depending on whether the FLS2 or EFR pathway was triggered. This demonstrates that the responses seen are not ubiquitous, but specific depending on MAMP treatment and which promoters are targeted.

3.4 Are PRP and PH1 able to augment their promoter activity?

We demonstrated that the PRP-like proteins were capable of augmenting the promoter activity of two defence-related genes, namely, *FRK1* and *NHL10*. As the promoters of *PRP* and *PH1* were also MAMP responsive (Section 3.1), they were selected to determine whether PRP, PH1, or their phosphosite mutants could similarly affect their own promoter activity to that observed for the promoters of *FRK1* and *NHL10* (Section 3.2 and 3.3).

PRP, PH1, and their respective phosphosite mutants PRP^{S51A} and PH1^{S65A} were co-expressed in mesophyll protoplasts along with their respective promoters (Fig. 15). Overexpression of CFP was once again used as a control that exerts no influence on promoter activity. The basal activity of the *PRP* promoter in the water-treated protoplasts was weakly suppressed ($p \leq 0.001$) by overexpression of PRP (Fig.15A, graph on the right). In contrast, PRP^{S51A}, the phosphosite mutant of PRP, did not exhibit the same suppression of the

basal promoter activity. Instead, *pPRP* activity while expressing PRP^{S51A} was similar to the CFP control, suggesting that phosphorylation of PRP does influence regulation of its own promoter.

This auto-suppression of *pPRP* activity by PRP was also visible upon treatment with flg22 ($p \leq 0.001$), while the phosphosite mutant PRP^{S51A} suppressed the promoter activity ($p \leq 0.01$) to a lesser degree (Fig. 15A, graph in the middle). A similar trend could be seen for the elf18 treatment, but with a weaker effect influencing only the initial rate of promoter activity (Fig. 15A, right graph). Elicitation by elf18 typically shows a stronger induction of *PRP* expression (Fig. 10). Therefore, it may mask the suppression effects of the co-expressed PRP and PRP^{S51A} . In summary, *PRP*'s promoter can be negatively regulated by PRP overexpression and that phosphorylation of PRP affects the strength of its promoter regulation. It is also interesting that the regulation of *pPRP* activity by PRP is significantly stronger when the FLS2 pathway is triggered but not as much in the EFR triggered pathway.

Notably, PRP or its phosphosite mutant, PRP^{S51A} , did not augment the basal level promoter activity as it did for *pFRK1* and *pNHL10* (Fig. 11-14). In contrast, co-expression of PRP or PRP^{S51A} weakly suppressed the MAMP-induced activity of the *PRP* promoter (Fig. 15A, middle and right graphs). This means that the augmentation and amplification seen for the *FRK1* and *NHL10* promoter activities upon overexpression of PRP and PRP^{S51A} is not a general phenomenon of any MAMP responsive promoter.

The co-expression of *PH1* suppressed its own promoter activity during water ($p \leq 0.01$) and flg22 ($p \leq 0.001$) treatments (Fig. 15B, left and middle graphs, respectively). No statistically significant suppression of promoter activity during elf18 treatment could be determined (Fig. 15B, right graph). Thus, as described above for PRP, the stronger elf18 induction compared to flg22 can presumably negate the suppression effect of PH1 on its own promoter. The PH1 phosphosite mutant, $PH1^{S65A}$, exhibited the same inhibition capacity as the wild type PH1 protein. Therefore, unlike PRP, PH1 phosphorylation

appears to have no impact on the auto-regulation of its own promoter. Decisively, PH1 and its phosphosite mutant also did not augment or increase its promoter activity in the manner observed for *pFRK1* and *pNHL10* activity. This reveals that its influence is specific, albeit varied.

In conclusion, both PRP and PH1 were able to suppress their respective promoters with varying degrees of strength. The presence or absence of the putative main phosphosite affected this activity partially for PRP but not for PH1, and a differential impact on the promoter suppression effect was observed for the elicitors used (Fig. 15A, B). Taken together this data supports the idea that the PRP-like proteins influence specific promoters in very different ways, and that its influence is far from generic.

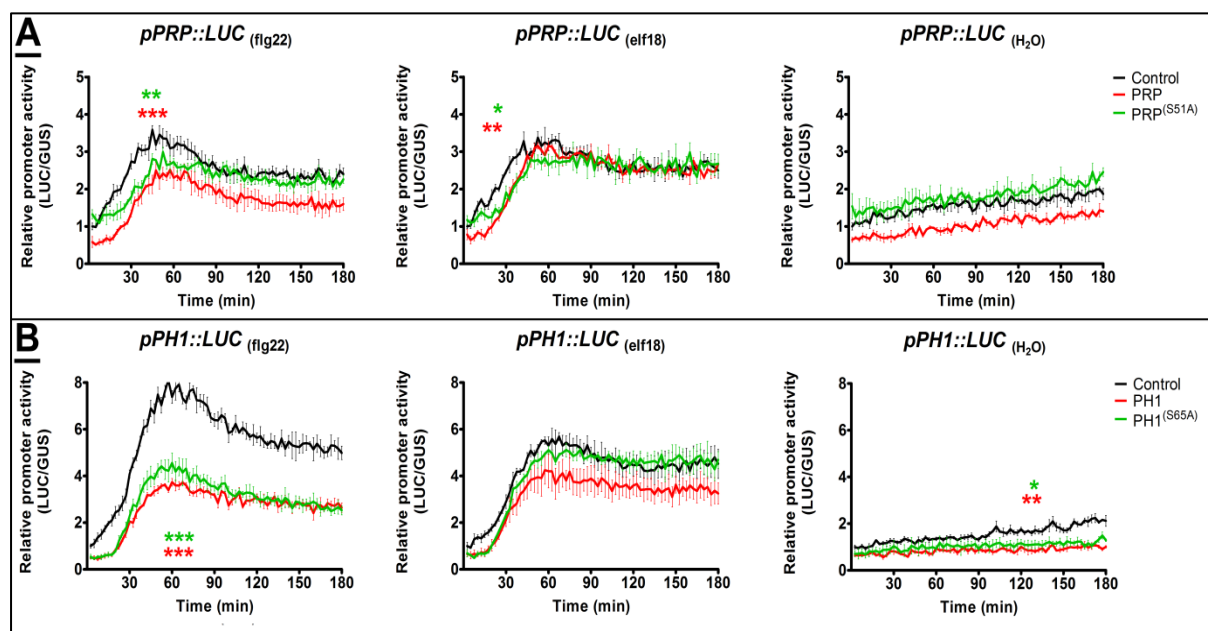


Fig. 15: Promoter activity of *PRP* and *PH1* after treatment with flg22 [100nM], elf18 [100nM], and dH₂O and co-expressing different constructs. In panel (A), *pPRP* activity is shown when PRP, its phosphosite mutant (PRP^{S51A}), or a CFP protein is constitutively overexpressed. Panel (B) shows *pPH1* activity when PH1, its phosphosite mutant (PH1^{S65A}), or CFP is constitutively overexpressed. The figure depicts the representative data of three independent experiments (n=3). Promoter activity is represented as LUC activity normalised to GUS activity (pUBQ10::GUS). Two-way ANOVA (Bonferroni post-test) was performed with sample versus control and statistically significant data indicated (* = p ≤ 0.05; ** = p ≤ 0.01; *** = p ≤ 0.001). Statistically significant data are colour coded and correspond to similar coloured curves.

3.5 Are PRP-like proteins able to bind the investigated promoters?

An electrophoretic mobility shift assay (EMSA) is used to study protein–DNA interactions that involve separation of free DNA from DNA-protein complexes based on differences in their electrophoretic mobility (Garner and Revzin, 1981). There are a number of classes of proteins that are able to bind DNA, i.e. transcription factors, that can regulate the expression of genes by binding to their respective target promoters.

An EMSA assay was performed to determine whether PRP-like proteins could auto-regulate their activities through direct DNA-binding activity of their promoters. The EMSA assay was performed in which each protein was incubated with DNA fragments containing either the *PRP*, *PH1*, or *PH2* promoter. PRP and PH2 retarded the electrophoretic mobility of all promoters and therefore indicated that DNA-protein interactions were occurring (Fig. 16A). PH1 was unable to bind any of the three promoters and therefore did not possess any DNA binding ability.

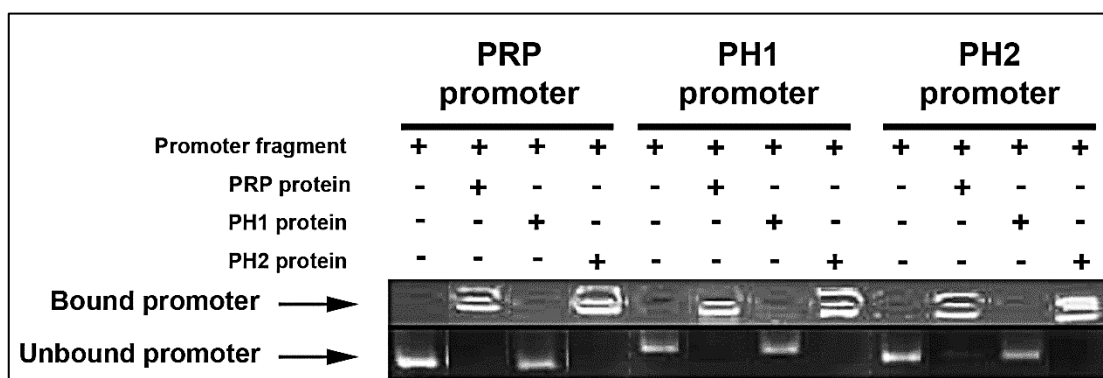


Fig. 16A: Electrophoretic mobility shift assay (EMSA) to investigate DNA-protein interactions between PRP-like proteins and their promoters. Positive binding is revealed as ethidium bromide-staining of the DNA in or around the loading wells, i.e. failure of the DNA-protein complex in entering the gel matrix.

The DNA-binding activity of the PRP-like proteins was also analysed for the promoters of *FRK1* and *NHL10* with another EMSA assay. Each protein was incubated with DNA fragments containing either the *FRK1* or *NHL10* promoter. PRP and PH2 retarded the electrophoretic mobility of both the *FRK1* and *NHL10* promoters, therefore indicating that DNA-protein interactions were occurring (Fig. 16B). PH1 was unable to bind either of the two promoters and therefore did not possess the DNA binding ability demonstrated by PRP and PH2.

As only PRP and PH2 demonstrated DNA-binding activity for all the promoters investigated, and not PH1, it is unlikely that the augmentation of promoter activity observed for *FRK1* and *NHL10* is due to direct DNA-binding of the PRP-like proteins to the promoters.

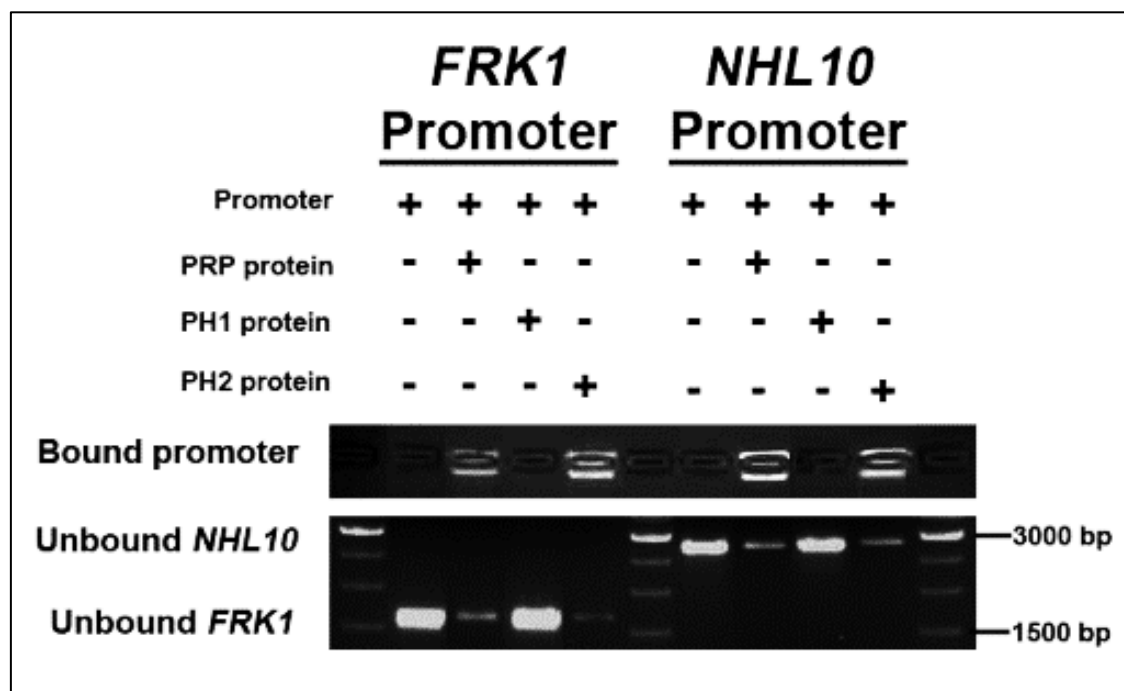


Fig. 16B: Electrophoretic mobility shift assay (EMSA) to investigate DNA-protein interactions between PRP-like proteins and *FRK1* or *NHL10* defence-related promoters. Positive binding is revealed as ethidium bromide-staining of the DNA in or around the loading wells, i.e. failure of the DNA-protein complex in entering the gel matrix. DNA marker lanes are denoted by M.

4. Effects of MAMP-treatments on the stability of PRP-like proteins

An important regulatory mechanism in plants is the degradation of proteins. One such example is that of the FLS2 receptor that is subjected to endocytosis following flg22 perception and then degraded (Robatzek et al., 2006), which may allow the activation of flg22-mediated pathway to be attenuated. Similarly, MPK6-mediated phosphorylation of the transcription factor ERF104, increases the stability of ERF104 thereby controlling the protein's levels after flg22 treatment (Bethke et al., 2009).

In order to investigate protein stability *in vivo*, the HA-epitope tagged PRP-like proteins were individually overexpressed in Arabidopsis mesophyll protoplasts, which were treated with flg22, elf18, or H₂O over a period of time. In figure 17, PRP appeared as a double band prior to elicitation (at t=0), and these double bands remained after the protoplasts were treated with H₂O. However, the lower PRP band disappeared 30min after flg22 or elf18 treatment. Further, the remaining upper band, observed for PRP after elf18 treatment, diminished in strength after 30min. The upper band observed for PRP, was completely absent in the protoplasts overexpressing its phosphosite mutant, PRP^{S51A}, irrespective of treatment administered. From this data, we can see that a band shift occurs for PRP after MAMP treatments, and that elf18 treatment eventually leads to lower PRP levels, which is presumably caused by degradation.

PH1 also appeared as a double band, and after either flg22 or elf18 treatment, there was a slight decrease in band strength for all time points. PH1^{S65A}, the phosphosite mutant of PH1, exhibited the same trend as its wild type counterpart PH1, but no reduction of protein levels post MAMP application was observed. For PH2 and its phosphosite mutant, PH2^{S44A}, no influence of MAMP treatment was observed at any time points. Further, no double band was observed for PH2 or its phosphosite mutant, PH2^{S44A}. In summary,

although all three proteins were *in vitro* substrates of MAPKs, only PRP and PH1 (but not PH2) showed phospho-modification-dependent regulation of protein levels after MAMP treatment.

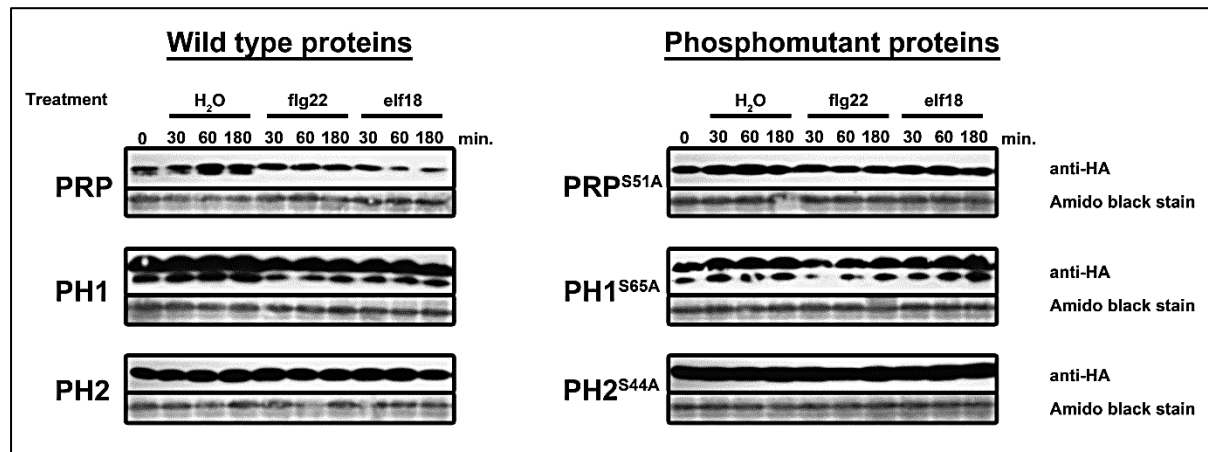


Fig. 17: Influence of MAMP treatment on protein stability. PRP, PH1, PH2, and their respective phosphosite mutants, PRP^{S51A}, PH1^{S65A}, and PH2^{S44A} were expressed as HA-epitope-tagged proteins in *A. thaliana* mesophyll protoplasts. Samples were harvested at the indicated time points after treatment with either dH₂O, flg22 [100nM], or elf18 [100nM]. Protein expression was investigated by western blot analysis with α -HA11 primary antibody.

5. Subcellular localization of PRP-like proteins

To determine the subcellular localization of the PRP-like proteins, *PRP*, *PH1* and *PH2* were fused to GFP under the control of the 35S promoter and transfected into *Nicotiana benthamiana* (Fig. 18). The PRP-like proteins were all localized to the nucleus and cytoplasm. Similarly, these GFP fusion proteins were then placed under the control of a weaker *ubiquitin10* promoter and transfected into Arabidopsis protoplasts (Fig. 19A, B). In the mesophyll protoplasts (Fig. 19A), visualization of the nuclei are often impeded by the large amount of chloroplasts; hence, cell-culture-derived protoplasts (Fig. 19B) were also tested. The localization of the PRP-like proteins in the nuclei can be clearly seen in the cell-culture-derived protoplasts. Therefore, localization of these proteins is the same as observed in tobacco with GFP fluorescence localized to the nucleus and cytoplasm.

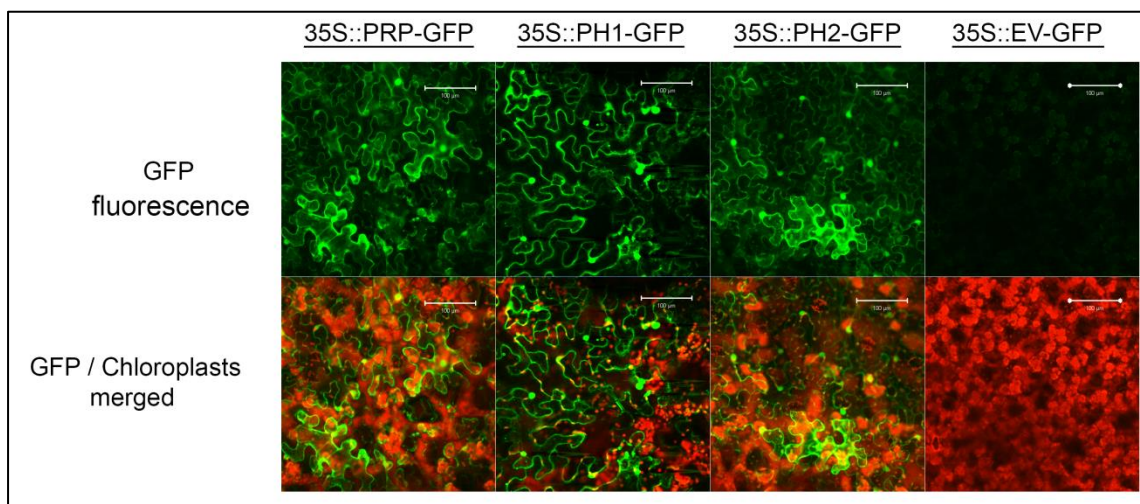


Fig. 18: Subcellular localization of PRP, PH1, and PH2 in *Nicotiana benthamiana*.

PRP, PH1, and PH2 were fused to a C-terminal GFP fragment (pEARLEYGATE103) and expressed in *N. benthamiana* after *A. tumefaciens*-mediated transformation. Infiltrated leaves were analysed for GFP fluorescence (Excitation: 489nm, Emission: 509nm) by confocal fluorescence microscopy. Scale bars are 100µm

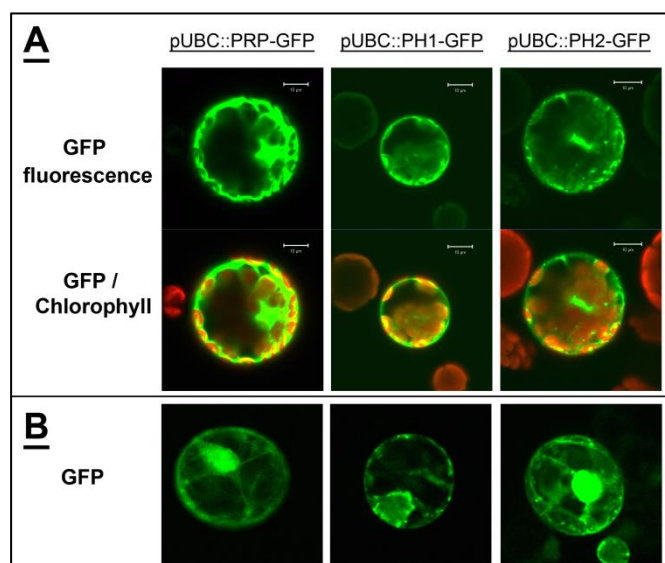


Fig. 19: Subcellular localization of PRP, PH1, and PH2 in *Arabidopsis thaliana* (Col-0)

protoplasts. Localisation studies were performed in (A) mesophyll protoplasts and (B) in cell-culture-derived protoplasts. PRP, PH1, and PH2 were fused to a C-terminal GFP fragment (pUBC-GFP) and analysed for GFP fluorescence (Excitation: 489nm, Emission: 509nm) by confocal fluorescence microscopy. Scale bars are 10µm.

5.1 Subcellular localization of PRP-like proteins after MAMP treatment

As two of the *PRP*-like genes, *PRP* and *PH1*, are transcriptionally up-regulated after MAMP treatment, we sought to determine if MAMPs could affect the localisation of the *PRP*-like proteins. The *PRP*-like proteins were transfected into *Arabidopsis* mesophyll protoplasts, which were treated with H₂O, flg22 or elf18 for one hour and observed in order to determine if localisation was affected. In all three cases, the *PRP*-like proteins localisation were unaffected by MAMP treatment, i.e. they remained in the nucleus and cytoplasm (Fig. 20).

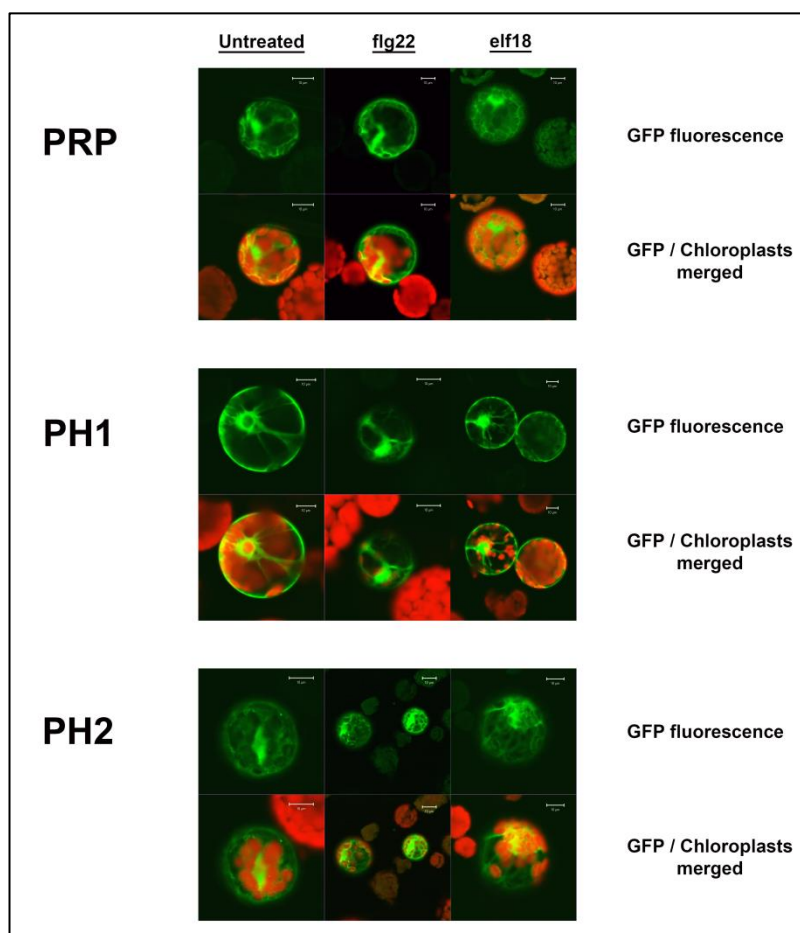


Fig. 20: Subcellular localization in response to MAMP treatment of PRP, PH1 and PH2 in *Arabidopsis thaliana* (Col-0). PRP, PH1, and PH2 were fused to a C-terminal GFP fragment (pUBC-GFP), transfected into mesophyll protoplasts and treated with H₂O, flg22, or elf18 for one hour. GFP fluorescence (Excitation: 489nm, Emission: 509nm) was detected by confocal fluorescence microscopy. Scale bars are 10µm.

6. Phenotypic Analysis

6.1 Developmental effects of overexpressing PRP-like proteins

To further elucidate possible functions of the PRP-like proteins, we created transgenic plants overexpressing native and phosphosite mutated variants of the PRP-like proteins. No obvious growth phenotype was seen in these plants. However, in rosette leaves of mature (4 weeks or older) plants, an altered developmental phenotype was observed in independent lines overexpressing PRP under short day conditions (Fig. 21A). The leaves of the PRP overexpressing lines were smaller and curved inward along the midrib. The overexpression of PRP's phosphosite mutant, PRP^{S51A}, displayed a weaker phenotype than the PRP lines. Leaves were only slightly curved but intermediate in size between the transgenic PRP lines and the wild type plants. The results suggest that the phosphorylation of PRP impacts the leaf phenotype in the overexpressing lines. Overexpressing line of PH1 and its phosphosite mutant, PH1^{S65A} (Fig. 21B), did not display an altered leaf phenotype compared to wild type lines. The overexpressing lines of PH2 (Fig. 21C) displayed an altered leaf phenotype compared to wild type leaves. The phenotype resembled that observed for the lines overexpressing PRP (Fig. 21A) with the leaves being smaller and curling inward along the midrib. The overexpressing lines of PH2's phosphosite mutant, PH2S44A, did not display the altered phenotype, but resembled the wild type plants.

6.2 Root growth inhibition assay of PRP-like overexpressing lines

Flg22 treatment of *Arabidopsis* stimulates the innate immune response that leads to multiple changes, including callose deposition, *PR* gene expression, and seedling growth inhibition (Felix et al., 1999). To determine whether the overexpression of the PRP-like proteins or their respective phosphosite mutant proteins could have an effect on the inhibition of growth after treatment with flg22, the overexpressing lines were grown for 14 days on plates with

either MS media or MS media supplemented with flg22. No statistically significant differences were observed between wild type line and those lines overexpressing PRP, PH1, or PH2 (Fig. 22).

Similarly, there was no difference between the wild type controls and the phosphosite mutants, with the exception of one line from PRP^{S51A} OE2 and PH1^{S65A} OE1. The observed effect is however only observed in one of the two transgenic lines, so the marginal difference is likely due to an insertion effect of the transgene.

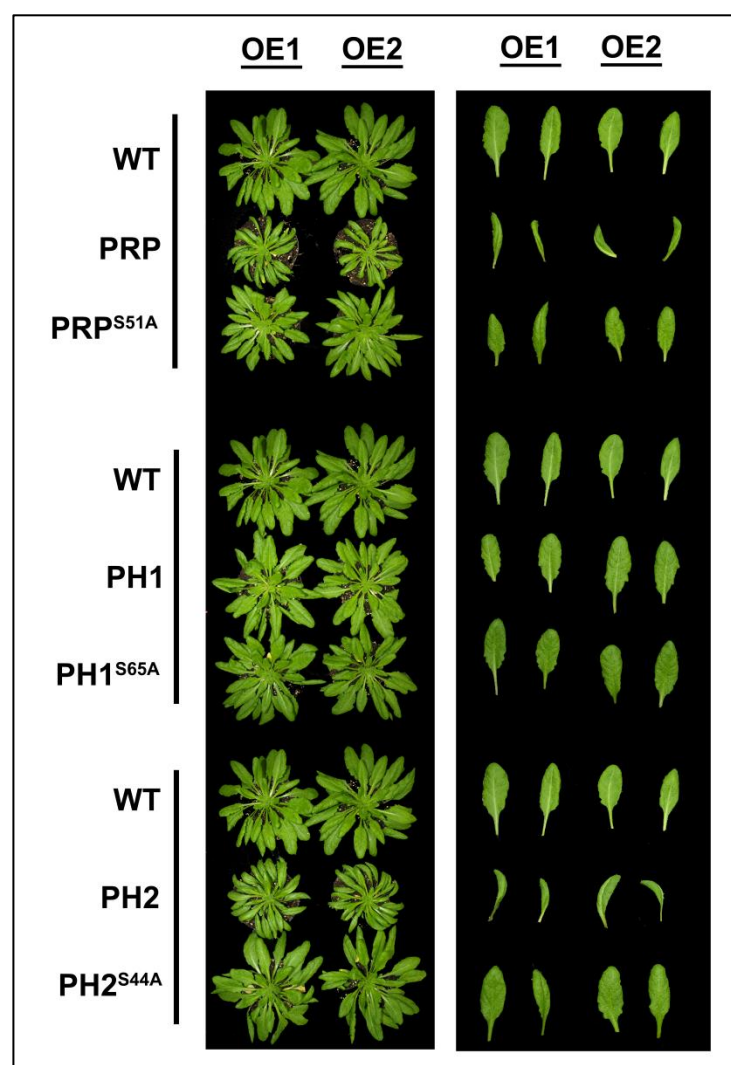


Fig. 21: Developmental phenotype observed in two independent lines overexpressing PRP-like proteins. (A) Lines overexpressing either PRP or its phosphosite mutant (PRP^{S51A}) compared to wild type (WT). (B) Lines overexpressing either PH1 or its phosphosite mutant (PH1^{S65A}) compared to wild type (WT). (C) Lines overexpressing either PH2 or its phosphosite mutant (PH2^{S44A}) compared to wild type (WT).

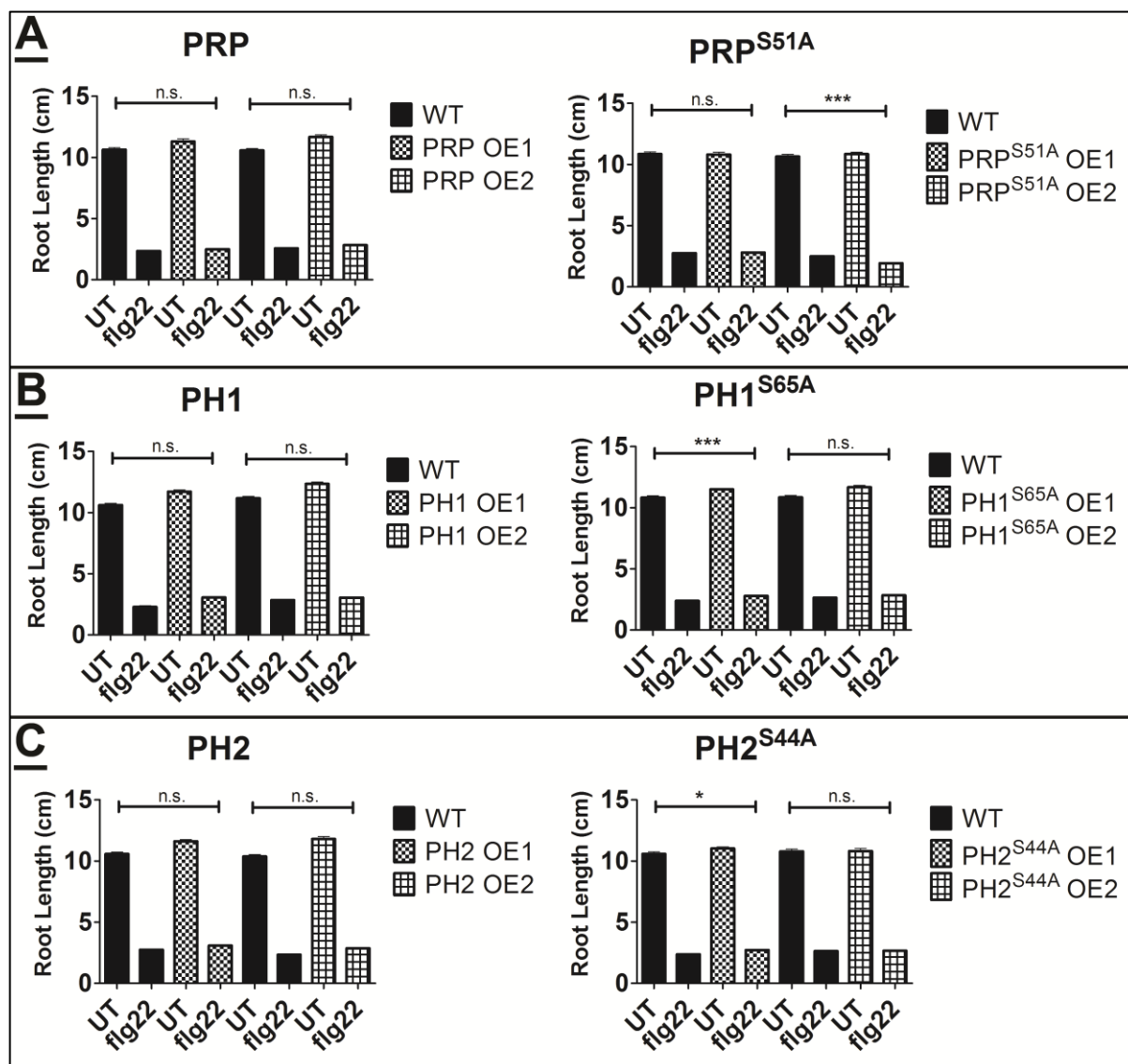


Fig. 22: Root length of untreated and flg22 [1 μ M] treated PRP-like overexpressing lines at 14 days. Growth inhibition for (A) PRP and phosphosite mutant, PRP^{S51A}, (B) PH1 and phosphosite mutant, PH1^{S65A}, and (C) PH2 and phosphosite mutant, PH2^{S44A} were calculated relative to respective wild type control lines. UT = untreated (i.e. growth on normal MS media). Statistical analysis was performed on log₂ transformed data combined from 2 independent experiments (n \geq 20) by two-way ANOVA (n.s. = not significant; *** = p \leq 0.001).

6.3 *Pst* DC3000 growth assay with PRP-like overexpressing lines

The *Arabidopsis-Pseudomonas syringae* interaction is a well investigated plant-pathogen model system (Zeng and He, 2010). *Pseudomonas syringae* is a Gram negative bacterium that typically enters plants through their stomata or wounds, and replicates into high numbers within intercellular spaces. Water-soaked patches, necrotic lesions, and chlorosis are visible in plants that are susceptible to *P. syringae* pv. *tomato* (*Pst*) infection. Resistant plants with corresponding cognate resistance genes respond with a rapid localised cell death, also known as the hypersensitive response (HR), which prevents the high levels of *Pst* replication (Katagiri et al., 2002). As two of the three PRP-like (*PRP*, *PH1*) genes respond to MAMP treatment, we wanted to investigate whether the overexpression of their gene products could lead to an enhanced response to infection with *Pst* DC3000.

Of all the PRP-like proteins, only lines overexpressing PRP or its phosphosite mutant, PRP^{S51A} (Fig. 23A), demonstrated increased resistance to *Pst* DC3000 growth. Although the increased resistance level seems marginal, it could be reproduced in five independently performed experiments. The absence of the main phosphorylation site in PRP^{S51A} did not affect the ability of PRP^{S51A} overexpression to confer increased resistance to *Arabidopsis* towards *Pst*.

The levels of bacterial growth between PH1 and PH1^{S65A} were not significantly different from that of the WT lines (Fig. 23C) and disease symptoms resembled that observed for the wild type plants. Bacterial growth in the lines overexpressing PH2 and its phosphosite mutant PH2^{S44A} also did not differ significantly from WT lines (Fig. 23C). Chlorosis and water soaked patches were visible in lines overexpressing PH2 and PH2^{S44A} to a similar degree as observed in the WT lines (Fig. 23F).

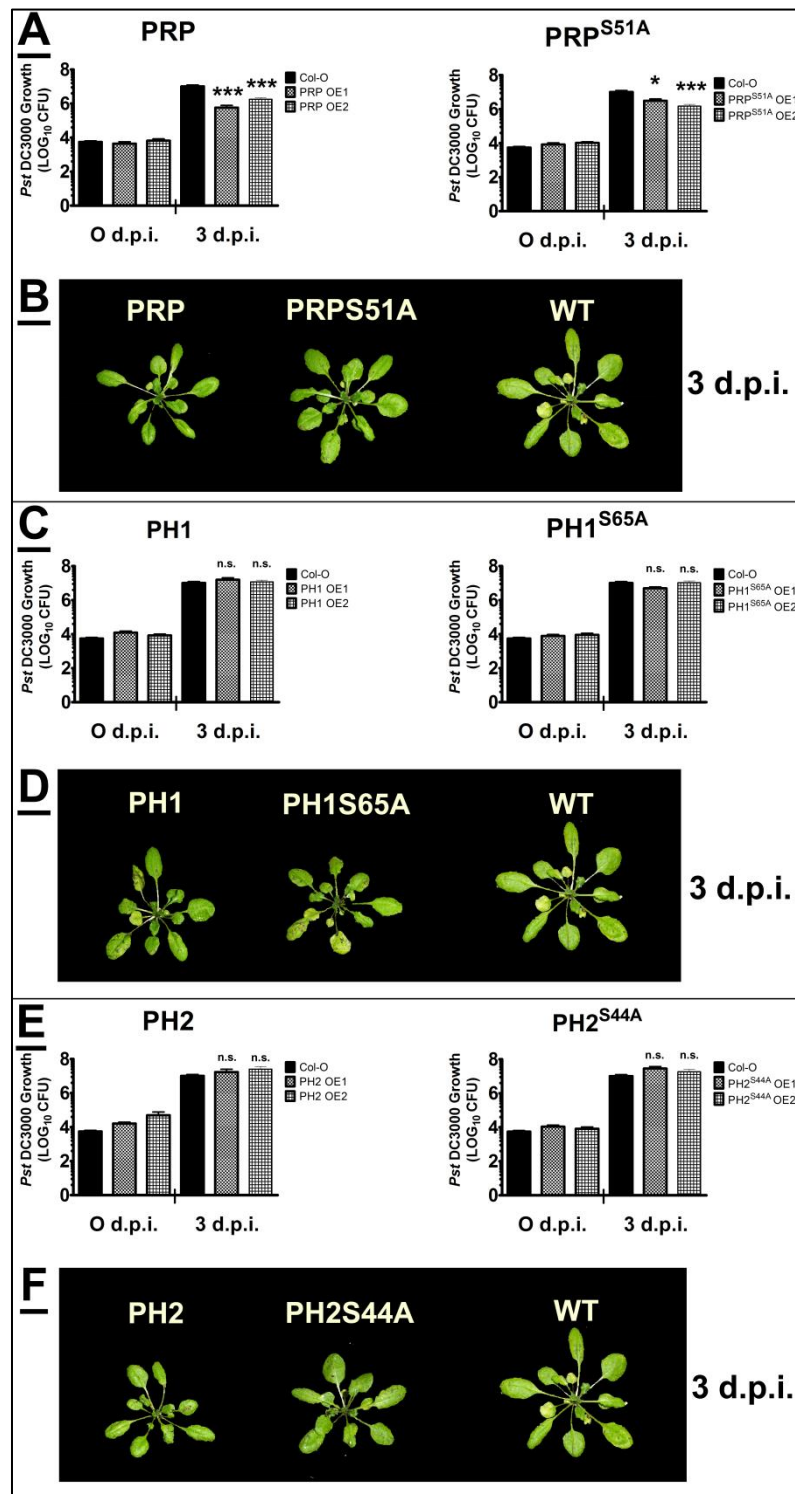


Fig. 23: Bacterial growth assay with *P. syringae* pv. *tomato* DC3000 (*Pst*). Bacterial growth at 0 and 3 days post infection in lines overexpressing (A) PRP and phosphosite mutant, PRP^{S51A}, (C) PH1 and phosphosite mutant, PH1^{S65A}, or (E) PH2 and phosphosite mutant, PH2^{S44A}. *Pst* spray inoculated lines of (B) PRP, PRP^{S51A}, WT, (D) PH1, PH1^{S65A}, WT and (F) PH2, PH2^{S44A}, WT three days post inoculation (3 d.p.i.). Statistical significance was calculated with the t-test from the combination of 5 independent experiments (n≥3) by comparing the bacterial growth at day 3 for each overexpressing line to the corresponding wild type control (* = p≤0.05; ***= p≤0.001).

IV. Discussion

1. PRP-like proteins interact with stress-activated MAPKs

The aim of this study was to investigate and characterise the function of the PRP-like proteins. PRP was originally identified as an interactor of MPK6 and MPK11 *via* a Y2H assay. To confirm this interaction, and to identify potential MAPK interactors of PRP's homologs, PH1 and PH2, another Y2H screen was performed against all 20 MAPKs from Arabidopsis.

The Y2H analysis identified only five MAPKs (MPK3/4/6/8/11), that interacted in various combinations with the PRP-like proteins. These five MAPKs have all been identified as stress-activated MAPKs. MPK3, MPK4, and MPK6 are activated by a variety of biotic and abiotic stress such as pathogen/MAMP, osmotic, cold, salt, and oxidative stress (Desikan et al., 2001; Asai et al., 2002; Droillard et al., 2002; Teige et al., 2004; Zipfel et al., 2006). Recently, MPK8 was shown to be activated by wounding and implicated in oxidative stress through the negative regulation of RbohD (Takahashi et al., 2011). MPK11 was also confirmed to be stress-activated by various MAMPs (Bethke et al., 2012; Eschen-Lippold et al., 2012). The stress related phytohormone ET is able to activate MPK3 and MPK6 (Yoo et al., 2008) whereas MPK4 negatively regulates SA and co-activates ET/JA-related defence signalling (Brodersen et al., 2006).

BiFC was employed to determine whether the Y2H results could be confirmed *in vivo* in Arabidopsis protoplasts. PRP and PH2 were able to interact with MPK3/4/6/11 *in vivo* but not MPK8 (Fig. 2). The interaction of PH1 with MPK6/8 identified in the Y2H screen was not observed in the BiFC screen. The lack of visible interaction of PH1 in the BiFC system may reflect that it interacts very transiently or weakly with the MAPKs tested, as the strength of *in vitro* phosphorylation of PH1, in general, is much weaker than that observed for PRP and PH2 (Fig. 3).

The Y2H and BiFC screen did not yield completely identical results. Both Y2H and BiFC assays are protein fragment complementation assays, requiring not only proximity of components, but also the correct reconstitution and folding of components to ensure functional reporters. Even though both systems can lead to false positives or false negatives (Fields, 2005; Kerppola, 2006), they are valuable tools for initial identification of putative proteins interactions. The data obtained from these two screens indicates that there is a bias towards interaction of stress-activated MAPKs with the PRP-like proteins, thereby implying these proteins are involved in stress-related responses.

The hypothesis that they are involved in stress-related responses is strengthened by the fact that induction of *PRP* and *PH1* occurs after MAMP treatment. We demonstrated transcript accumulation of *PRP* and *PH1* after MAMP treatment by qPCR. *PRP* is transiently induced four-fold stronger by elf18 treatment than flg22 treatment at 30min. The transient induction of *PH1* by flg22 and elf18 treatment is similar in strength to *PRP*, but displays a slightly more stable and prolonged response after elf18 treatment (Fig. 8). We could also demonstrate that the promoters of *PRP* and *PH1* were also MAMP responsive (Fig. 10), and that they are indeed transcriptionally regulated.

Transcriptional regulation is vital for plants in order to respond to changes in their environment, so that genes can be expressed only when they are needed to mount the appropriate stress response (Singh, 1998). The transcriptional regulation of *PRP* and *PH1* provides an insight into their possible functional roles in MAMP responses. However, it is not always a prerequisite. For example, *MPK3* and *MPK11* are both transcriptionally up-regulated by MAMPs, whereas *MPK4* and *MPK6* display no change in mRNA level after MAMP treatment, however the activities of all four MAPKs are stress activated (Bethke et al., 2012; Eschen-Lippold et al., 2012). In many instances, post-translational modification such as phosphorylation is additionally required for regulation of stress responses (Colcombet and Hirt, 2008).

2. Post-translational modification by MAPKs and target specificity for PRP-like proteins

Phosphorylation is a reversible modification regulating everything from substrate specificity, complex formation, to protein stability/degradation, ensuring functioning of important processes for the plants survival (Reinders and Sickmann, 2005). To confirm the interaction between MAPKs and the PRP-like proteins, an *in vitro* kinase assay was performed, which confirmed that the PRP-like proteins were indeed phosphorylated by MPK3 and MPK6 and therefore substrates. We concentrated on interactions with MPK3 and MPK6 as we could produce highly active kinases (Bethke et al., 2009). We attempted to see if MPK4 and MPK11 could also phosphorylate the PRP proteins, but we were unable to activate them like we did using the constitutively active parsley MKK5 for MPK3 and MPK6, despite trying several MKKs. Recently, it was shown that a constitutively activated MAPK can be created by mutating specific amino acids (Berriri et al., 2012). This would be useful in generating active MPK4 and MPK11 in the future to test if they too can phosphorylate the PRP-like proteins.

As MAPKs are proline-directed kinases and target serine/threonine that precedes a proline (S/T-P), we mutated all putative MAPK-targeted phosphosites within the PRP-like proteins from S/T to alanine (A) using a rapid and novel mutagenesis approach (Palm-Forster et al., 2012). We successfully identified and mapped the phosphorylation sites targeted by MPK3 and MPK6 (Fig. 5) and demonstrated that the PRP-like proteins possessed a singular phosphorylation site that was specifically targeted by these two kinases. As MPK3 and MPK6 did not indiscriminately phosphorylate any of the other potential sites available on the PRP-like proteins, it adds further evidence to the selective nature of MPK3/6 towards the PRP-like proteins. It is interesting to note that the main phosphosite targeted by both MPK3 and MPK6 is conserved in all three homologs (Fig. 4).

Additionally we mutated the MAPK docking site (D domain) with a (R/K)₁₋₂-(X)₂₋₆-Φ-X-Φ motif that was present in the PRP-like proteins. The mutation of the D domain in the PRP-like proteins abolished all interactions between the MAPKs and PRP-like proteins in the Y2H screen (Fig. 6A) and strongly reduced *in vitro* phosphorylation of the PRP-like proteins by MPK3 and MPK6 (Fig. 6B).

The D domain is ubiquitous in all MAPK substrates (Holland and Cooper, 1999) and could function to increase the local concentration of the substrate around a MAPK, similar to the way bi-phosphorylated SIC1 (CDK INHIBITOR p40) induces proximity to CDC4 (CELL DIVISION CONTROL PROTEIN 4). This is achieved by first binding one phosphorylation site thereby increasing the effective concentration allowing binding to the secondary site (Deshaies and Ferrell Jr, 2001). This binding model is only possible if there is flexibility in the region between either, the docking site and phosphorylation site of the substrate, the docking site and the kinase catalytic site, or both.

Alternatively, the D domain docking site may simply serve to align the MAPK with the substrate, enhancing the rate of phosphorylation. Peptides containing the D domain can stimulate MAPK activity, cause auto-phosphorylation or even negatively regulate kinase activity by allosteric inhibition through interference with ATP binding (Chang et al., 2002; Heo et al., 2004). Many of the known MAPK substrates contain the D domain, but that does not mean they are targeted by multiple MAPKs. For example, VIP1 is specifically phosphorylated by MPK3, MKS1 by MPK4, and ERF104 exclusively by MPK6 (Andreasson et al., 2005; Djamei et al., 2007; Bethke et al., 2009), supporting the idea that there are other factors determining specificity by individual MAPKs. In summary, the phosphorylation of a specific phosphosite and occurrence of the D domain in the PRP-like proteins supports the specificity of the interaction with MPK3 and MPK6. However, the exact role of the D domain and whether the PRP-like proteins are targeted by other MAPKs remains to be tested.

The successful mapping of the phosphosites and *in vitro* phosphorylation of the PRP-like proteins were subjected to *in vivo* validation in Arabidopsis mesophyll protoplasts. PRP is visible as a double band *in vivo* (Fig. 17). MAMP treatment with flg22 results in PRP's lower band to shift upward without a change in protein level, whereas after elf18 treatment, the mobility shift is accompanied with a decrease in protein level (Fig. 17). Treatment of PRPs phosphosite mutant, PRP^{S51A}, with flg22 and elf18 confirmed that phosphorylation of the main phosphosite was responsible for the observed band shift and decrease in protein levels. These data suggest a de-stabilising effect due to phosphorylation. In the case of PH1, the MAMP-induced reduction is not visible in its phosphosite mutated variant, thus suggesting a phospho-dependent regulation of protein levels.

In summary, the mobility shift after MAMP treatment observed for PRP, as well as changes in protein levels for PRP and PH1 support the *in vitro* data and additionally confirm that the proteins are post-translationally regulated after MAMP treatment. The MAPK substrate ACS6, is stabilised by phosphorylation through MPK6 that leads to protein accumulation and induction of ET (Joo et al., 2008). ACS6 is a good example of post-translational regulation by MAPKs through phosphorylation. In fact, the absence of the negative charge introduced on the C-terminus of ACS6 by phosphorylation, is what leads to its targeted degradation by the 26S proteasome (Joo et al., 2008). Phosphorylation can also increase protein stability, i.e. the phosphorylation of ERF104 by MAMP activated MPK6 confers stability to the protein substrate (Bethke et al., 2009).

Post-translational regulation by phosphorylation extends beyond protein stability/degradation (ACS6/ERF104) or increased activity of a MAPK substrate such as NIA2 (Wang et al., 2010) to effect a response. In a broader context, it regulates defence responses through interaction of protein complexes and altering subcellular localisation of proteins. A prime example of this is the negative regulation of pathogen response through the

MPK4/MKS1/WRKY33 interaction. Perception of flg22 results in the phosphorylation of MKS1 by MPK4, releasing the MKS1/WRKY33 complex from MPK4 allowing re-localisation of the complex to the nucleus, and subsequently inducing the transcription of the *PAD3* defence gene (Andreasson et al., 2005; Qiu et al., 2008; Petersen et al., 2010).

These results demonstrate that PRP and PH1 can be added to the known list of post-translationally regulated MAPK substrates. More specifically, they are post-translational regulated by MAMPs, which may imply a role in innate immunity. They can also be placed downstream of the FLS2/EFR receptors and MKK4/5-MPK3/6 signalling cascades that have been shown to be central in the response to pathogen invasion (Asai et al., 2002; Zipfel et al., 2006). Further experimentation incorporating proteasome inhibitors needs to be performed in order to determine if phosphorylation, or lack thereof, is potentially responsible for targeting these MAPK substrates for protein degradation through the 26S proteasome.

Additionally, protein-protein interaction and co-immunoprecipitation experiments need to be performed to identify any additional proteins that may interact in a complex with the PRP-like proteins. If any are identified, it would help illuminate the effect of phosphorylation on the PRP-like proteins within the framework of protein binding, as phosphorylation may modulate the strength of such interactions, provide diversity of recognition patterns, and/or present recognition sites for binding certain domains and motifs (Nishi et al., 2011). This may help explain the differential effect observed for PRP when treated with flg22 versus elf18 (Fig. 17). These two different MAMP responsive pathways may need PRP to interact with one or several proteins in the one pathway, thereby stabilising or preventing its degradation in e.g. the FLS2 pathway, but not in the other e.g. the EFR pathway.

3. Potential functions of PRP-like proteins in innate immunity

The overexpression of PRP-like proteins is able to strongly augment the basal promoter activity of two defence-related genes, *FRK1* and *NHL10*. This observed enhancement was equal to, and in certain circumstances surpassed the MAMP-induced *FRK1* and *NHL10* promoter activity. Furthermore, the enhancement of the defence-related promoter activities is affected by the post-translational modification state of the PRP-like proteins.

It is conceivable that the augmentation of promoter activity is due to the DNA-binding ability of PRP and PH2. The EMSA assay (Fig. 16B) merely demonstrated the direct DNA-binding ability of these two proteins, but not the specificity thereof. Further, EMSA assays should be performed with truncated promoter fragments in order to determine if PRP and PH2 are able to target specific regulatory regions that are contained within particular sections of the promoters, or if the DNA-binding is non-specific. *In silico* analysis predicted that the promoters of both *FRK1* and *NHL10* share a number of regulatory motifs that include W-box motifs for WRKY binding, LFY motif for LEAFY (LFY) protein binding, RAV11 motifs for ABI3VP1 (ABA INSENSITIVE 3/PPASE1) transcription family, HSE motifs for HSF (HEAT SHOCK FACTOR) binding, as well as binding sites for Homeobox and bZIP (BASIC LEUCINE-ZIPPER) transcription factors (Palaniswamy et al., 2006).

The data from the promoter activity studies suggest that the PRP-like proteins act as transcriptional activators of both *FRK1* and *NHL10*, regulating rate and intensity of promoter activation. The DNA-binding activity of PRP and PH2 is not shared by PH1, yet all three proteins are able to influence the transcription of the two defence related promoters. This, together with the effect of post-translational regulation of the PRP-like proteins on *pFRK1* and *pNHL10*, implies that the promoter activity augmentation is likely not due to DNA-binding of one the regulatory domains mentioned above. Perhaps it is due to the interaction with a large complex of proteins, such as the preinitiation complex necessary for transcription of protein coding genes in eukaryotes

(Lee and Young, 2000). Possibly, the DNA-binding ability of PRP and PH2 could add target specificity in a similar manner as enhancer-binding proteins, like the Arabidopsis NB-Y (NUCLEAR BINDING-Y) family, recognises CCAAT-boxes to aid transcription (Edwards et al., 1998).

The promoters of both *FRK1* and *NHL10* contain W-boxes for WRKY binding, and WRKY29 strongly activates the *FRK1* promoter after flg22 treatment (Asai et al., 2002). Conceivably, the PRP-like proteins may be able to interact with transcription factors such as the WRKYs to increase *FRK1/NHL10* transcription in a similar manner to the MKS1/WRKY33 interaction leading to *PAD3* transcription initiation (Qiu et al., 2008). Alternatively, there may be other proteins with which regulatory complexes could be formed. Two proteins from Arabidopsis, the 12 kDa KIWI (putative transcriptional co-activator) and 19 kDa KELP (transcriptional co-activator), were identified as putative plant transcriptional co-activators that could associate both hetero- and homomericly (Cormack et al., 1998). These two proteins are believed to play a role in plant development and pathogen defence. KELP was also shown to bind various viral movement proteins of *Tomato mosaic virus*, and in this manner could interfere with host defence responses by limiting the number of co-activators available (Matsushita et al., 2001).

The PRP-like proteins only augmented the activities of the defence-related promoters *FRK1* and *NHL10*, but repressed their own promoter activities. This differential effect is indicative that they are not merely general transcription enhancers, but seem to target defence-related promoters. This result adds credence to the idea that the PRP-like proteins could be a novel class of MAMP responsive transcriptional co-activators similar to KIWI and KELP. Fine regulation of its effect, however, is context-dependent, i.e. the effect is conditional on the target promoter and on possible protein partners.

As mentioned previously, further experimentation is necessary to determine if there are other *in vivo* binding partners for the PRP-like proteins and whether the DNA-binding ability of PRP and PH2 targets specific DNA motifs. This

would help to elucidate whether they form part of some transcriptional co-regulatory complexes. Finally, it would be invaluable to perform more expansive profiling of various defence-related promoters to determine if the influence of the PRP-like proteins is general to all defence-related promoters, or a specific subset.

4. The localisation of the PRP-like proteins

Besides expression patterns, subcellular localisation of a protein can provide hints on its function. *In silico* predictions in SUBA (Arabidopsis Subcellular Database) for the subcellular localisation of the PRP-like proteins were however inconclusive, with possible localisation suggested in the nucleus, plastids, mitochondria, and chloroplasts with low confidence scores (Heazlewood et al., 2007). Using GFP-tagged proteins, we saw that the PRP-like proteins were localised in the nucleus and in the cytoplasm in both Arabidopsis mesophyll protoplasts (Fig. 19) and in Tobacco leaves (Fig. 18).

Due to the very small sizes of the PRP-like proteins, they may diffuse freely in or out of the nucleus. In an attempt to prevent this, they were tagged with a C-terminal tandem EOS fluorescent protein, which should increase fusion protein size beyond the size of nuclear pores and prevent passive diffusion. Unfortunately, all that was observed were random fluorescent specks (data not shown), possibly due to protein aggregation and/or misfolding.

Since MAMP treatments produced changes in PRP and PH1 levels, and a phosphorylation dependent band shift in PRP (Fig. 17), a stimuli-dependent effect on protein localisation was investigated. However, there was no visible effect on the localisation of the PRP-like proteins *in vivo* for the first hour after MAMP treatment (Fig. 20). If there is any influence on the localisation of the PRP-like proteins after MAMP treatment, it may be masked due to the strong overexpression of the promoters that were utilised. Thus, in the future, native promoters may be used to drive the expression of the PRP-like proteins and

also a more extensive time course of MAMP treatments may be necessary to investigate possible transient changes in protein localisation.

Hence, despite the inconclusive localisation of PRP-like proteins, the presence of GFP signals in the nucleus correlates with their ability to influence defence related promoter activities with the potential ability to interact with nucleic acids (and/or the speculated ability to interact with transcription factors).

5. Potential functions inferred from the expression patterns of *PRP*-like genes

PRP, *PH1* and *PH2* are highly and exclusively expressed in pollen, mature siliques, and ovules, respectively (Fig. 7A, B). This implies that they have roles in reproductive processes. Several CDPKs (CALCIUM DEPENDENT PROTEIN KINASE) are implicated in the regulation of pollen tube function and the MAMP responsive gene *NHL10* is also induced by CDPKs (Zhou et al., 2009b; Boudsocq et al., 2010). As PRP is sufficient to stimulate *pNHL10* activities, perhaps there is a correlation between PRP and pollen tube function as the pollen phosphoproteome displays an almost overabundant amount of motifs specific for Ca²⁺/calmodulin-dependent protein kinases and MAPKs (Mayank et al., 2012).

Examination of knockout mutant or RNAi silencing lines is necessary to determine the function of the PRP-like proteins. Interestingly, we were not able to generate RNAi lines for *PH2*. The expression data (Fig. 7A) shows that it is highly expressed in ovules, and along with the lack of RNAi lines, supports the hypothesis that it is required for plant reproduction. No knock-out plants for the PRP-like proteins were available from the SALK T-DNA insertion mutant database. This could be because the PRP-like proteins are necessary for reproduction (pollen viability?) or as they are encoded by such small genes, they have not yet been successfully targeted by the random T-DNA insertion mutations. Further analysis of pollen from *PRP* overexpressing/silencing lines

and ovules from *PH2* overexpressing/DEX-induced silencing lines would assist in elucidating the potential roles of PRP and PH2 in reproduction.

Similar to PRP and PH1, the protein KIWI shows high expression levels in late stage ovule development and in pollen (Craigon et al., 2004). It is also a small protein present in reproductive tissues that is implicated in defence response (Cormack et al., 1998). Thus, it is not uncommon for proteins with roles in defence responses to be present in reproductive organs. The PRP-like proteins may additionally have roles in other stress-related responses. BLAST analysis revealed homologous sequences only in dicotyledonous plants (not shown), suggesting evolutionary divergence of some function/s specific for dicotyledonous plants.

The developmental phenotype observed in the mature rosettes of lines overexpressing PRP and PH2 is not shared by the overexpression of PH1. The protein overexpression of AS2 (ASSYMMETRICAL LEAVES 2) gives rise to leaves that are upwardly curled while the loss-of-function lines display the opposite effect of downward curled leaves (Iwakawa et al., 2002). The protein AS1 is expressed in leaf founder cells and additional to its developmental role, loss-of-function mutants of AS1 increase resistance against necrotrophic fungi. AS1 is therefore a negative regulator of pathogen response by binding the promoters of JA-controlled genes (Nurmburg et al., 2007). This illustrates the complexity and versatility of proteins that have roles in development and disease resistance.

Only PRP and PH2 overexpressing plants displayed altered leaf morphology and also only these two proteins were able to bind DNA directly (Fig. 16 A, B). Conceivably the overexpression of PRP and PH2 interferes with nucleic acid binding proteins (perhaps AS1/2) that are responsible for correct leaf development and thereby resulting in the prominent curved leaf morphology that was observed (Fig. 21).

6. Resistance phenotype of PRP-overexpressing plants

The overexpression of the PRP-like proteins and their phosphosite mutants did not display any altered growth effect due to perception of flg22 in the root growth inhibition assay (Felix et al., 1999). The overexpressing lines were equally sensitive to flg22 treatment as the wild type Col-0 lines.

However, overexpressing lines of PRP and its phosphosite mutant, PRP^{S51A}, displayed a moderate but statistically significant resistance phenotype to infection with *Pseudomonas syringae* pv. *tomato* DC3000 (Fig. 23A). What could be the mechanism behind the decrease of bacterial growth observed? Is it as straight forward as perception of *Pst* by FLS2/EFR and activating the MKK4/MKK5-MPK3/6-PRP signalling cascade? Does PRP then enhance the transcription of defence-related genes such as *FRK1* and *NHL10*, to strengthen PTI?

Most likely, the resistance phenotype due to PRP overexpression is not solely dependent on, or is completely independent of *FRK1* and *NHL10* expression, as it is not the only PRP-like protein to augment the promoter activities (Fig. 11-14). Therefore, the PRP-like proteins also possess very distinct functions. Overall, the mechanism behind the increased resistance of the PRP-overexpressing lines remains to be uncovered. Utilising the *Pseudomonas* genetic toolbox to express various bacterial effector genes targeting specific resistance mechanisms e.g. HopAI1 targeting MPK3/4/6 (Zhang et al., 2007; Zhang et al., 2012) or AvrPto targeting RLKs like FLS2 and EFR directly (Xiang et al., 2008) etc., could provide valuable insight towards elucidating the mode of action of PRP.

In conclusion, the data presented support roles for the members of the PRP-like proteins in plant defence responses. Additionally, the expression patterns also hint at roles in pollen and reproductive organs. Thus, the same MAPK cascade component(s) functionally overlap in both defence and developmental processes. This leads to the fundamental question of how

MAPK cascades determine signal specificity when common MAPK elements are shared. A common conception is that this is mediated by temporal and spatial expression of pathway-specific scaffold proteins or MAPK targets. In this work, three novel MAPK substrates were identified. This adds to the list of plant MAPK substrates identified to-date and may contribute to the dissection of MAPK signal transduction specificity.

V. Summary

Plants continuously face an ever changing environment that influences their development and survival. A mechanism ensuring their continued survival is the ability to detect adverse conditions, like invading pathogens, to mount an appropriate defence response. The MAPK signalling cascade is an integral part of this response, conveying signals after perception of pathogens to downstream substrates that affect the defence response. Only a handful of plant substrates have been discovered and characterised to-date (Colcombet and Hirt, 2008).

In this work, three novel proline-rich proteins (PRP, PH1 and PH2) from *Arabidopsis thaliana* were identified as *in vitro* phospho-targets of MPK3 and MPK6. Accordingly, mutation of a predicted MAPK-docking site eliminated interaction with and phosphorylation by MAPKs. Using site-directed mutagenesis, the targeted phospho-sites in these substrates could be localised. The phosphorylation states of PRP and PH1 affect protein levels after PAMP treatment (presumably via regulation of targeted degradation). Additionally, phosphorylation differentially influences the enhancement effects of the PRP-like proteins on *FRK1* and *NHL10* promoter activities. This suggests that functions of the PRP-like proteins may be fine-tuned through phosphorylation dependent regulation. The ability of these PRP-like proteins to modulate defence-gene expression and the enhanced resistance to *Pseudomonas syringae* in PRP-overexpressing transgenic plants suggest roles in plant immunity of these MAPK substrates. Further, roles in reproduction and development are implicated since the PRP-like proteins are highly expressed in reproductive organs of Arabidopsis, and older leaves of PRP- and PH2-overexpressing plants having slightly modified leaf morphology. These findings are in line with involvement of MAPKs in both development processes (e.g. stomatal patterning, ovule, anther and inflorescence development; Bush and Krysan, 2007; Wang et al., 2007; Wang et al., 2008) and defense responses (PTI and ETI; Tena et al., 2011).

The maintenance of signal specificity, without aberrant signal crosstalk between pathways, is still poorly elucidated for plant MAPK cascades. Factors such as temporal and spatial expression of genes for pathway-specific scaffolding proteins and MAPK targets facilitate this intricate response control to specific stimuli. In conclusion, this work has successfully identified a novel class of MPK3 and MPK6 substrates. These proteins add to the catalogue of plant MAPK substrates, which will contribute to the attempts of the MAPK research community in dissecting fidelity of MAPK signal transduction in defence and developmental pathways.

VI. Appendix

Table 2: Vector list

Vector	Selection		Cloning sites	Structure	Source
	Bacteria / Yeast	Plant			
<u>Entry Vector</u>					
pENTR /D-TOPO	Kan	-	Gateway	attL1-TOPO-attL2	Invitrogen
<u>Yeast-2-Hybrid</u>					
pDEST32	Gent/Leu2	-	Gateway	pADH1-Gal4 DBD-GW	Invitrogen
pDEST22	Amp/Trp	-	Gateway	pADH1-Gal4 AD-GW	Invitrogen
<u>Recombinant Overexpression</u>					
pDEST-N110	Amp	-	Gateway	pT7-lacO-SD-His10-GW	(Dyson et al., 2004)
pJC40	Amp	-	Classic	pT7-SD-His10-MCS	(Clos and Brandau, 1994)
pGEX-4T-1	Amp	-	Classic	pTaq-GST-MCS	GE
<u>BiFC</u>					
pUC-SPYCE-GW	Amp	-	Gateway	35S::GW myc-nYFP-nosT	(Walter et al., 2004)
pUC-SPYNE-GW	Amp	-	Gateway	35S::GW HA-cYFP-nosT	(Walter et al., 2004)
<u>Localisation</u>					
pUBC-GFP-Dest	Spec	Bar	Gateway	pUBQ10--GW-GFP-T35	(Grefen et al., 2010)
<u>Stable RNAi silencing <i>in planta</i></u>					
pHellsgate8	Spec	Kan	Gateway		(Helliwell and Waterhouse, 2003)
<u>Stable overexpression <i>in planta</i></u>					
pEarleygate 203	Kan	Bar	Gateway	35S-cMyc-GW-OCS	(Earley et al., 2006)
<u>Transient overexpression <i>in planta</i></u>					
pUGW14-kpnl	Amp	-	Gateway	35S::GW-kpnl-3xHA nosT	(Nakagawa et al., 2007)
<u>Promoter Activity</u>					
pPROMOTER-LUC	Amp	-	Gateway	pPROM::LUC	(Shan et al., 2008)

Table 3: Primer and probe list

<u>Primers for TOPO cloning</u>	<u>Sequence</u>
PRP_F_cacc	5' -CAC CAT GTC GAC GAC GAT GAA GAG -3'
PRP_R_stop	5' -CTA AAC CGG AAC AAA CGG TG -3'
PRP_R_nostop	5' -AAC CGG AAC AAA CGG TG-3'
PH1_F_cacc	5' -CAC CAT GTT CTT TGA TAC AAA AGT ACT CAA
PH1_R_stop	5' -CTA AAC CTG GAT GAA CGG TG -3'
PH1_R_nostop	5' -AAC CTG GAT GAA CGG TG-3'
PH2_F_cacc	5' -CAC CAT GTC GTC CAC GGC GAG A-3'
PH2_R_stop	5' -TTA ATT TGG CCA TGC AAA CG -3'
PH2_R_nostop	5' -ATT TGG CCA TGC AAA CG- 3'
<u>Real time PCR primers</u>	
PRP_probe_5	5'- GTG GCG GTT GAG AAA AGA -3'
PRP_probe_3	5'- GAA CAA ACG TCG ATG ACT CG-3'
PH1_probe_5	5'- GGT GAAGAA GAC ACC AGT TTT CA-3'
PH1_probe_3	5'- GTT GTT GGC TCG TAG CAG AA-3'
PH2_probe_5	5'- GTC GCC ACC ACA AAA ACC-3'
PH2_probe_3	5'- GCT TCT CCG CCT CTT TAC C-3'
FRK1_5	5'- GAG ACT ATT TGG CAG GTA AAA GGT -3'
FRK1_3	5'- AGG AGG CTT ACA ACC ATT GTG -3'
NHL10_5	5'- ACG CCG GAC AGT CTA GGA -3'
NHL10_3	5'- CCC TAA GCC TGA ACT TGA TCT C -3'
PP2A_5	5'- GAC CGG AGC CAA CTA GGA C -3'
PP2A_3	5'- AAA ACT TGG TAA CTT TTC CAG CA -3'
<u>Tagman probes</u>	
PRP_probe_145	FAM- ATG GCA ACA TCC CGC GGC GC -BHQ1
PH1_probe_145	FAM- TGG CAA CAT CCC GCG TCG CC -BHQ1
PH2_probe_52	FAM- TGA AGA GGG AGG AGC AAC GGT GG -BHQ1
FRK1_probe_145	FAM- TCT TGA GCT GGG AAG AGA GGT TGA AG -BHQ1
NHL10_probe_55	FAM- ACG CGG AGA GGA TAT CCG GTG T -BHQ1
PP2A_probe_28	CY5- GAT CTG GTG CCT GCA TAT GCT CGT C -BBQ
<u>Promoter primers</u>	
PRP promotorF	5'- GGA TCC TCA TCG CTT CTT TTC TTC TTT GT -3'
PRP promotorR	5'- CCA TGG AAA CGC GAA AGA AAT CGA GTT -3'
PH1 promotorF	5'- GGA TCC GGT GCG TAC GTT AAG GAC TTA CT -3'
PH1 promotorR	5'- CCA TGG AAT AT GAT GTT GGT GTG TGA TGT -3'
PH2 promotorF	5'- GGA TCC AGT TCT TCT CTT CTC CTC CAC ACA -3'
PH2 promotorR	5'- CCA TGG AGC AGG ATC TTG TTG TAT TAA TTT-3'

Table 4: Site directed mutagenesis primer list

<u>PRP phosphosite mutations</u>		
<u>Amino Acid</u>	<u>Oligoname</u>	<u>Sequence</u>
S37A_F	ggm1Fwt	5'- AAG GTC TCG GCG CCG GCG GCG AAT AAC TGG -3'
S37A_R	ggm1Rwt	5'- AAG GTC TCG GCG CCG CCG GAA CGA TTT TTA ACG -3'
S51A_F	ggm2Fwt	5'- AAG GTC TCC GGC GCC GTT AGC TCT TTC TCC CG -3'
S51A_R	ggm2Rwt	5'- AAG GTC TCC CGC CAG GAG AGG TAT AGC CGT ATT CCA G -3'
S56A_F	ggm3Fwt	5'- AAG GTC TCT GGC GCC CGA ATC ATC ACC GGT AGA CC -3'
S56A_R	ggm3Rwt	5'- AAG GTC TCG CGC CAG AGC TAA CGG CGA GAG GAG -3'
S60A_F	ggm4Fwt	5'- AAG GTC TCA GGC GCC GGT AGA CCA ACC ACC GG -3'
S60A_R	ggm4Rwt	5'- AAG GTC TCG CGC CGA TTC GGG AGA AAG AGC TAA CG -3'
S80A_F	ggm5Fwt	5'- AAG GTC TCA GGC GCC GGT TTT CAA GAA ATG GC -3'
S80A_R	ggm5Rwt	5'- AAG GTC TCG CGC CTT CTC AAC CGC CAC CG -3'
S51A_F	GGm2_m3mutf	5'- AAG GTC TCC GGC GCC GTT AGC TCT TGC TCC CG -3'
S51A_R	GGm2_m3mutr	5'- AAG GTC TCC CGC CAG GAG AGG TAT AGC CGT ATT CCA G -3'
S56A_F	GGm3_m4mutf	5'- AAG GTC TCT GGC GCC CGA ATC AGC ACC GGT AGA CC -3'
S56A_R	GGm3_m4mutr	5'- AAG GTC TCG CGC CAG AGC TAA CGG CGC GAG GAG -3'
S60A_F	GGm4_m3mutf	5'- AAG GTC TCA GGC GCC GGT AGA CCA ACC ACC GG -3'
S60A_R	GGm4_m3mutr	5'- AAG GTC TCG CGC CGA TTC GGG AGC AAG AGC TAA CG -3'
<u>PH1 phosphosite mutations</u>		
S65A	GGm6F	5'- ATC CCG GTC TCT GCA CCG CT -3'
S65A	GGm6R	5'- GAA GGA GGT CTC GGT GCA AGG AG -3'
S99A	GGm7F	5'- AGG TGG TCT CGG CAC CAG TT -3'
S99A	GGm7R	5'- CTT GGG TCT CGG TGC CTT CTT C -3'
S110A	GGm8F	5'- GGC AAC AGG TCT CG GCG CCG TTC -3'
S110A	GGm8R	5'- CGT AGG GTC TCG GCG CCG CG -3'
<u>PH2 phosphosite mutations</u>		
S48A	ggm10Fmt	5'- AAG GTC TCG GCG CCA CCA CAA AAA CCA CC -3'
S48A	ggm10Rmt	5'- AAG GTC TCG GCG CCT CCG TAG GTG CTA GAA GAG G -3'
<u>MAPK docking site mutations</u>		
L26D I27D	PRPdockF	5'- AAG GTC TCC CCC CGG CGG ATA AAG ACG TTC -3'
K26D R27D	PRPdockR	5'-AAG GTC TCC GGG GGT TCT TCT AGT AGA CGA -3'
L47D I49D	PH1dockF	5'- AAG GTC TCC TCC GTC TGA TAT GGA CAA ACC -3'
R42D R43D	PH1dockR	5'- AAG GTC TCC GGA GCT TCT TCC TGT AGC TGG CTA AGT TGC C -3'
L27D I29D	PH2dockF	5'- AAG GTC TCC TCC ACC GCC TGA TAA GGA AAA CCC TTG CGA AGC G -3'
R21R 22D	PH2dockR	5'- AAG GTC TCT GGA GCT TCT TCC TGC AGC CTA -3'

VII. References

- AARTS, N., METZ, M., HOLUB, E., STASKAWICZ, B.J., DANIELS, M.J., AND PARKER, J.E.** (1998). DIFFERENT REQUIREMENTS FOR EDS1 AND NDR1 BY DISEASE RESISTANCE GENES DEFINE AT LEAST TWO R GENE-MEDIATED SIGNALING PATHWAYS IN ARABIDOPSIS. PROCEEDINGS OF THE NATIONAL ACADEMY OF SCIENCES **95**, 10306-10311.
- AHLFORS, R., LÅNG, S., OVERMYER, K., JASPERS, P., BROSCHE, M., TAURIAINEN, A., KOLLIST, H., TUOMINEN, H., BELLES-BOIX, E., PIIPPO, M., INZÉ, D., PALVA, E.T., AND KANGASJÄRVI, J.** (2004). ARABIDOPSIS RADICAL-INDUCED CELL DEATH1 BELONGS TO THE WWE PROTEIN-PROTEIN INTERACTION DOMAIN PROTEIN FAMILY AND MODULATES ABSCISIC ACID, ETHYLENE, AND METHYL JASMONATE RESPONSES. THE PLANT CELL ONLINE **16**, 1925-1937.
- ANDREASSON, E., JENKINS, T., BRODERSEN, P., THORGRIMSEN, S., PETERSEN, N.H.T., ZHU, S., QIU, J.-L., MICHEELSEN, P., ROCHER, A., PETERSEN, M., NEWMAN, M.-A., BJORN NIELSEN, H., HIRT, H., SOMSSICH, I., MATTSSON, O., AND MUNDY, J.** (2005). THE MAP KINASE SUBSTRATE MKS1 IS A REGULATOR OF PLANT DEFENSE RESPONSES. EMBO JOURNAL **24**, 2579-2589.
- ASAI, T., TENA, G., PLOTNIKOVA, J., WILLMANN, M.R., CHIU, W.-L., GOMEZ-GOMEZ, L., BOLLER, T., AUSUBEL, F.M., AND SHEEN, J.** (2002). MAP KINASE SIGNALLING CASCADE IN ARABIDOPSIS INNATE IMMUNITY. NATURE **415**, 977-983.
- BARDWELL, L.** (2006). MECHANISMS OF MAPK SIGNALLING SPECIFICITY. BIOCHEMICAL SOCIETY TRANSACTIONS **34**, 837-841.
- BERGMANN, D.C., LUKOWITZ, W., AND SOMERVILLE, C.R.** (2004). STOMATAL DEVELOPMENT AND PATTERN CONTROLLED BY A MAPKK KINASE. SCIENCE **304**, 1494-1497.
- BERRIRI, S., GARCIA, A.V., FREI DIT FREY, N., ROZHON, W., PATEYRON, S., LEONHARDT, N., MONTILLET, J.L., LEUNG, J., HIRT, H., AND COLCOMBET, J.** (2012). CONSTITUTIVELY ACTIVE MITOGEN-ACTIVATED PROTEIN KINASE VERSIONS REVEAL FUNCTIONS OF ARABIDOPSIS MPK4 IN PATHOGEN DEFENSE SIGNALING. THE PLANT CELL ONLINE. DOI:10.1105/TPC.112.101253.
- BETHKE, G., UNTHAN, T., UHRIG, J.F., PÖSCHL, Y., GUST, A.A., SCHEEL, D., AND LEE, J.** (2009). FLG22 REGULATES THE RELEASE OF AN ETHYLENE RESPONSE FACTOR SUBSTRATE FROM MAP KINASE 6 IN *ARABIDOPSIS THALIANA* VIA ETHYLENE SIGNALING. PROCEEDINGS OF THE NATIONAL ACADEMY OF SCIENCES **106**, 8067-8072.
- BETHKE, G., PECHER, P., ESCHEN-LIPPOLD, L., TSUDA, K., KATAGIRI, F., GLAZEBROOK, J., SCHEEL, D., AND LEE, J.** (2012). ACTIVATION OF THE *ARABIDOPSIS THALIANA* MITOGEN-ACTIVATED PROTEIN KINASE MPK11 BY THE FLAGELLIN-DERIVED ELICITOR PEPTIDE, FLG22. MOLECULAR PLANT-MICROBE INTERACTIONS **25**, 471-480.
- BOLLER, T.** (1995). CHEMOPERCEPTION OF MICROBIAL SIGNALS IN PLANT CELLS. ANNUAL REVIEW OF PLANT PHYSIOLOGY AND PLANT MOLECULAR BIOLOGY **46**, 189-214.
- BOUDSOCQ, M., WILLMANN, M.R., MCCORMACK, M., LEE, H., SHAN, L., HE, P., BUSH, J., CHENG, S.-H., AND SHEEN, J.** (2010). DIFFERENTIAL INNATE IMMUNE SIGNALLING VIA Ca^{2+} SENSOR PROTEIN KINASES. NATURE **464**, 418-422.
- BRADFORD, M.M.** (1976). A RAPID AND SENSITIVE METHOD FOR THE QUANTITATION OF MICROGRAM QUANTITIES OF PROTEIN UTILIZING THE PRINCIPLE OF PROTEIN-DYE BINDING. ANALYTICAL BIOCHEMISTRY **72**, 248-254.
- BRODERSEN, P., PETERSEN, M., BJØRN NIELSEN, H., ZHU, S., NEWMAN, M.-A., SHOKAT, K.M., RIETZ, S., PARKER, J., AND MUNDY, J.** (2006). ARABIDOPSIS MAP KINASE 4 REGULATES SALICYLIC ACID- AND JASMONIC ACID/ETHYLENE-DEPENDENT RESPONSES VIA EDS1 AND PAD4. THE PLANT JOURNAL **47**, 532-546.
- BUSH, S.M., AND KRYSAN, P.J.** (2007). MUTATIONAL EVIDENCE THAT THE ARABIDOPSIS MAP KINASE MPK6 IS INVOLVED IN ANther, INFLORESCENCE, AND EMBRYO DEVELOPMENT. JOURNAL OF EXPERIMENTAL BOTANY **58**, 2181-2191.
- CHAIWONGSAR, S., OTEGUI, M.S., JESTER, P.J., MONSON, S.S., AND KRYSAN, P.J.** (2006). THE PROTEIN KINASE GENES MAP3Kε1 AND MAP3Kε2 ARE REQUIRED FOR POLLEN VIABILITY IN *ARABIDOPSIS THALIANA*. THE PLANT JOURNAL **48**, 193-205.

- CHANDRA, S., MARTIN, G.B., AND LOW, P.S.** (1996). THE PTO KINASE MEDIATES A SIGNALING PATHWAY LEADING TO THE OXIDATIVE BURST IN TOMATO. PROCEEDINGS OF THE NATIONAL ACADEMY OF SCIENCES **93**, 13393-13397.
- CHANG, C.I., XU, B.E., AKELLA, R., COBB, M.H., AND GOLDSMITH, E.J.** (2002). CRYSTAL STRUCTURES OF MAP KINASE p38 COMPLEXED TO THE DOCKING SITES ON ITS NUCLEAR SUBSTRATE MEF2A AND ACTIVATOR MKK3B. MOLECULAR CELL **9**, 1241-1249.
- CHANG, L., AND KARIN, M.** (2001). MAMMALIAN MAP KINASE SIGNALLING CASCADES. NATURE **410**, 37-40.
- CHINCHILLA, D., ZIPFEL, C., ROBATZEK, S., KEMMERLING, B., NURNBERGER, T., JONES, J.D.G., FELIX, G., AND BOLLER, T.** (2007). A FLAGELLIN-INDUCED COMPLEX OF THE RECEPTOR FLS2 AND BAK1 INITIATES PLANT DEFENCE. NATURE **448**, 497-500.
- CHOMCZYNSKI, P., AND SACCHI, N.** (1987). SINGLE-STEP METHOD OF RNA ISOLATION BY ACID GUANIDINIUM THIOCYANATE-PHENOL-CHLOROFORM EXTRACTION. ANALYTICAL BIOCHEMISTRY **162**, 156-159.
- CLOS, J., AND BRANDAU, S.** (1994). pJC20 AND pJC40 - TWO HIGH-COPY-NUMBER VECTORS FOR T7 RNA POLYMERASE-DEPENDENT EXPRESSION OF RECOMBINANT GENES IN *ESCHERICHIA COLI*. PROTEIN EXPRESSION AND PURIFICATION **5**, 133-137.
- COLCOMBET, J., AND HIRT, H.** (2008). ARABIDOPSIS MAPS: A COMPLEX SIGNALLING NETWORK INVOLVED IN MULTIPLE BIOLOGICAL PROCESSES. BIOCHEMICAL JOURNAL **413**, 217-226.
- CORMACK, R.S., HAHLBROCK, K., AND SOMSSICH, I.E.** (1998). ISOLATION OF PUTATIVE PLANT TRANSCRIPTIONAL COACTIVATORS USING A MODIFIED TWO-HYBRID SYSTEM INCORPORATING A GFP REPORTER GENE. THE PLANT JOURNAL **14**, 685-692.
- CRAIGON, D.J., JAMES, N., OKYERE, J., HIGGINS, J., JOTHAM, J., AND MAY, S.** (2004). NASCARRAYS: A REPOSITORY FOR MICROARRAY DATA GENERATED BY NASC'S TRANSCRIPTOMICS SERVICE. NUCLEIC ACIDS RESEARCH **32**, D575-577.
- CUI, H., WANG, Y., XUE, L., CHU, J., YAN, C., FU, J., CHEN, M., INNES, R.W., AND ZHOU, J.M.** (2010). *PSEUDOMONAS SYRINGAE* EFFECTOR PROTEIN AVR-B PERTURBS ARABIDOPSIS HORMONE SIGNALING BY ACTIVATING MAP KINASE 4. CELL HOST MICROBE **7**, 164-175.
- CZECHOWSKI, T., STITT, M., ALTMANN, T., UDVARDI, M.K., AND SCHEIBLE, W.-R.** (2005). GENOME-WIDE IDENTIFICATION AND TESTING OF SUPERIOR REFERENCE GENES FOR TRANSCRIPT NORMALIZATION IN ARABIDOPSIS. PLANT PHYSIOLOGY **139**, 5-17.
- DESHAIES, R.J., AND FERRELL JR, J.E.** (2001). MULTISITE PHOSPHORYLATION AND THE COUNTDOWN TO S PHASE. CELL **107**, 819-822.
- DESIKAN, R., HANCOCK, J.T., ICHIMURA, K., SHINOZAKI, K., AND NEILL, S.J.** (2001). HARPIN INDUCES ACTIVATION OF THE ARABIDOPSIS MITOGEN-ACTIVATED PROTEIN KINASES ATMPK4 AND ATMPK6. PLANT PHYSIOLOGY **126**, 1579-1587.
- DI TOMMASO, P., MORETTI, S., XENARIOS, I., OROBITG, M., MONTANYOLA, A., CHANG, J.-M., TALY, J.-F., AND NOTREDAME, C.** (2011). T-COFFEE: A WEB SERVER FOR THE MULTIPLE SEQUENCE ALIGNMENT OF PROTEIN AND RNA SEQUENCES USING STRUCTURAL INFORMATION AND HOMOLOGY EXTENSION. NUCLEIC ACIDS RESEARCH **39**, W13-W17.
- DJAMEI, A., PITZSCHKE, A., NAKAGAMI, H., RAJH, I., AND HIRT, H.** (2007). TROJAN HORSE STRATEGY IN AGROBACTERIUM TRANSFORMATION: ABUSING MAPK DEFENSE SIGNALING. SCIENCE **318**, 453-456.
- DROILLARD, M., BOUDSOCQ, M., BARBIER-BRYGOO, H., AND LAURIERE, C.** (2002). DIFFERENT PROTEIN KINASE FAMILIES ARE ACTIVATED BY OSMOTIC STRESSES IN *ARABIDOPSIS THALIANA* CELL SUSPENSIONS. INVOLVEMENT OF THE MAP KINASES ATMPK3 AND ATMPK6. FEBS LETTERS **527**, 43-50.
- DURRANT, W.E., AND DONG, X.** (2004). SYSTEMIC ACQUIRED RESISTANCE. ANNUAL REVIEWS OF PHYTOPATHOLOGY **42**, 185-209.
- DYSON, M., SHADBOLT, S., VINCENT, K., PERERA, R., AND MCCAFFERTY, J.** (2004). PRODUCTION OF SOLUBLE MAMMALIAN PROTEINS IN *ESCHERICHIA COLI*: IDENTIFICATION OF PROTEIN FEATURES THAT CORRELATE WITH SUCCESSFUL EXPRESSION. BMC BIOTECHNOLOGY **4**, 1-18.
- EARLEY, K.W., HAAG, J.R., PONTES, O., OPPER, K., JUEHNE, T., SONG, K., AND PIKAARD, C.S.** (2006). GATEWAY-COMPATIBLE VECTORS FOR PLANT FUNCTIONAL GENOMICS AND PROTEOMICS. THE PLANT JOURNAL **45**, 616-629.

- EDWARDS, D., MURRAY, J.A.H., AND SMITH, A.G.** (1998). MULTIPLE GENES ENCODING THE CONSERVED CCAAT-BOX TRANSCRIPTION FACTOR COMPLEX ARE EXPRESSED IN ARABIDOPSIS. *PLANT PHYSIOLOGY* **117**, 1015-1022.
- ESCHEN-LIPPOLD, L., BETHKE, G., PALM-FORSTER, M., PECHER, P., BAUER, N., GLAZEBROOK, J., SCHEEL, D., AND LEE, J.** (2012). MPK11-A FOURTH ELICITOR-RESPONSIVE MITOGEN-ACTIVATED PROTEIN KINASE IN *ARABIDOPSIS THALIANA*. *PLANT SIGNALING AND BEHAVIOUR* **7**.
- FEILNER, T., HULTSCHIG, C., LEE, J., MEYER, S., IMMINK, R.G., KOENIG, A., POSSLING, A., SEITZ, H., BEVERIDGE, A., SCHEEL, D., CAHILL, D.J., LEHRACH, H., KREUTZBERGER, J., AND KERSTEN, B.** (2005). HIGH THROUGHPUT IDENTIFICATION OF POTENTIAL ARABIDOPSIS MITOGEN-ACTIVATED PROTEIN KINASES SUBSTRATES. *MOLECULAR AND CELLULAR PROTEOMICS* **4**, 1558-1568.
- FELIX, G., DURAN, J.D., VOLKO, S., AND BOLLER, T.** (1999). PLANTS HAVE A SENSITIVE PERCEPTION SYSTEM FOR THE MOST CONSERVED DOMAIN OF BACTERIAL FLAGELLIN. *THE PLANT JOURNAL* **18**, 265-276.
- FEYS, B.J., WIERMER, M., BHAT, R.A., MOISAN, L.J., MEDINA-ESCOBAR, N., NEU, C., CABRAL, A., AND PARKER, J.E.** (2005). ARABIDOPSIS SENESCENCE-ASSOCIATED GENE101 STABILIZES AND SIGNALS WITHIN AN ENHANCED DISEASE SUSCEPTIBILITY1 COMPLEX IN PLANT INNATE IMMUNITY. *THE PLANT CELL ONLINE* **17**, 2601-2613.
- FIELDS, S.** (2005). HIGH-THROUGHPUT TWO-HYBRID ANALYSIS. *FEBS JOURNAL* **272**, 5391-5399.
- FIL, B.K., PETERSEN, K., PETERSEN, M., AND MUNDY, J.** (2009). GENE REGULATION BY MAP KINASE CASCADES. *CURRENT OPINION IN PLANT BIOLOGY* **12**, 615-621.
- GARNER, M.M., AND REVZIN, A.** (1981). A GEL ELECTROPHORESIS METHOD FOR QUANTIFYING THE BINDING OF PROTEINS TO SPECIFIC DNA REGIONS: APPLICATION TO COMPONENTS OF THE *ESCHERICHIA COLI* LACTOSE OPERON REGULATORY SYSTEM. *NUCLEIC ACIDS RESEARCH* **9**, 3047-3060.
- GASSMANN, W., AND BHATTACHARJEE, S.** (2012). EFFECTOR-TRIGGERED IMMUNITY SIGNALING: FROM GENE-FOR-GENE PATHWAYS TO PROTEIN-PROTEIN INTERACTION NETWORKS. *MOLECULAR PLANT-MICROBE INTERACTIONS* **25**, 862-868.
- GÖHRE, V., SPALLEK, T., HÄWEKER, H., MERSMANN, S., MENTZEL, T., BOLLER, T., DE TORRES, M., MANSFIELD, J.W., AND ROBATZEK, S.** (2008). PLANT PATTERN-RECOGNITION RECEPTOR FLS2 IS DIRECTED FOR DEGRADATION BY THE BACTERIAL UBIQUITIN LIGASE AVRPTOB. *CURRENT BIOLOGY* **18**, 1824-1832.
- GÓMEZ-GÓMEZ, L., AND BOLLER, T.** (2000). FLS2: AN LRR RECEPTOR-LIKE KINASE INVOLVED IN THE PERCEPTION OF THE BACTERIAL ELICITOR FLAGELLIN IN ARABIDOPSIS. *MOLECULAR CELL* **5**, 1003-1011.
- GÓMEZ-GÓMEZ, L., FELIX, G., AND BOLLER, T.** (1999). A SINGLE LOCUS DETERMINES SENSITIVITY TO BACTERIAL FLAGELLIN IN ARABIDOPSIS THALIANA. *THE PLANT JOURNAL* **18**, 277-284.
- GRANT, M., AND LAMB, C.** (2006). SYSTEMIC IMMUNITY. *CURRENT OPINION IN PLANT BIOLOGY* **9**, 414-420.
- GRFEN, C., DONALD, N., HASHIMOTO, K., KUDLA, J., SCHUMACHER, K., AND BLATT, M.R.** (2010). A UBIQUITIN-10 PROMOTER-BASED VECTOR SET FOR FLUORESCENT PROTEIN TAGGING FACILITATES TEMPORAL STABILITY AND NATIVE PROTEIN DISTRIBUTION IN TRANSIENT AND STABLE EXPRESSION STUDIES. *THE PLANT JOURNAL* **64**, 355-365.
- GUTIERREZ, J.R., BALMUTH, A.L., NTOUKAKIS, V., MUCYN, T.S., GIMENEZ-IBANEZ, S., JONES, A.M.E., AND RATHJEN, J.P.** (2010). PRF IMMUNE COMPLEXES OF TOMATO ARE OLIGOMERIC AND CONTAIN MULTIPLE PTO-LIKE KINASES THAT DIVERSIFY EFFECTOR RECOGNITION. *THE PLANT JOURNAL* **61**, 507-518.
- HEAZLEWOOD, J.L., VERBOOM, R.E., TONTI-FILIPPINI, J., SMALL, I., AND MILLAR, A.H.** (2007). SUBA: THE ARABIDOPSIS SUBCELLULAR DATABASE. *NUCLEIC ACIDS RESEARCH* **35**, D213-218.
- HELLIWELL, C., AND WATERHOUSE, P.** (2003). CONSTRUCTS AND METHODS FOR HIGH-THROUGHPUT GENE SILENCING IN PLANTS. *METHODS* **30**, 289-295.
- HEO, Y.S., KIM, S.K., SEO, C.I., KIM, Y.K., SUNG, B.J., LEE, H.S., LEE, J.I., PARK, S.Y., KIM, J.H., HWANG, K.Y., HYUN, Y.L., JEON, Y.H., RO, S., CHO, J.M., LEE, T.G., AND YANG, C.H.** (2004). STRUCTURAL BASIS FOR THE SELECTIVE INHIBITION OF JNK1 BY THE SCAFFOLDING PROTEIN JIP1 AND SP600125. *EMBO JOURNAL* **23**, 2185-2195.

- HINDERHOFER, K., AND ZENTGRAF, U. (2001). IDENTIFICATION OF A TRANSCRIPTION FACTOR SPECIFICALLY EXPRESSED AT THE ONSET OF LEAF SENESCENCE. *PLANTA* **213**, 469-473.
- HOLLAND, P.M., AND COOPER, J.A. (1999). PROTEIN MODIFICATION: DOCKING SITES FOR KINASES. *CURRENT BIOLOGY* **9**, R329-R331.
- ICHIMURA, K., SHINOZAKI, K., TENA, G., SHEEN, J., HENRY, Y., CHAMPION, A., KREIS, M., ZHANG, S., HIRT, H., WILSON, C., HEBERLE-BORS, E., ELLIS, B.E., MORRIS, P.C., INNES, R.W., ECKER, J.R., SCHEEL, D., KLESSIG, D.F., MACHIDA, Y., MUNDY, J., OHASHI, Y., AND WALKER, J.C. (2002). MITOGEN-ACTIVATED PROTEIN KINASE CASCADES IN PLANTS: A NEW NOMENCLATURE. *TRENDS IN PLANT SCIENCE* **7**, 301-308.
- IWAKAWA, H., UENO, Y., SEMIARTI, E., ONOUCHI, H., KOJIMA, S., TSUKAYA, H., HASEBE, M., SOMA, T., IKEZAKI, M., MACHIDA, C., AND MACHIDA, Y. (2002). THE *ASYMMETRIC LEAVES2* GENE OF *ARABIDOPSIS THALIANA*, REQUIRED FOR FORMATION OF A SYMMETRIC FLAT LEAF LAMINA, ENCODES A MEMBER OF A NOVEL FAMILY OF PROTEINS CHARACTERIZED BY CYSTEINE REPEATS AND A LEUCINE ZIPPER. *THE PLANT CELL PHYSIOLOGY* **43**, 467-478.
- JAMES, P., HALLADAY, J., AND CRAIG, E.A. (1996). GENOMIC LIBRARIES AND A HOST STRAIN DESIGNED FOR HIGHLY EFFICIENT TWO-HYBRID SELECTION IN YEAST. *GENETICS* **144**, 1425-1436.
- JIN, Q., THILMONY, R., ZWIESLER-VOLLICK, J., AND HE, S.-Y. (2003). TYPE III PROTEIN SECRETION IN *PSEUDOMONAS SYRINGAE*. *MICROBES AND INFECTION* **5**, 301-310.
- JONAK, C., ÖKRÉSZ, L., BÖGRE, L., AND HIRT, H. (2002). COMPLEXITY, CROSS TALK AND INTEGRATION OF PLANT MAP KINASE SIGNALLING. *CURRENT OPINION IN PLANT BIOLOGY* **5**, 415-424.
- JONES, J.D.G., AND DANGL, J.L. (2006). THE PLANT IMMUNE SYSTEM. *NATURE* **444**, 323-329.
- JOO, S., LIU, Y., LUETH, A., AND ZHANG, S. (2008). MAPK PHOSPHORYLATION-INDUCED STABILIZATION OF ACS6 PROTEIN IS MEDIATED BY THE NON-CATALYTIC C-TERMINAL DOMAIN, WHICH ALSO CONTAINS THE CIS-DETERMINANT FOR RAPID DEGRADATION BY THE 26S PROTEASOME PATHWAY. *THE PLANT JOURNAL* **54**, 129-140.
- KATAGIRI, F., THILMONY, R., AND HE, S.Y. (2002). THE *ARABIDOPSIS THALIANA*-*PSEUDOMONAS SYRINGAE* INTERACTION. *THE ARABIDOPSIS BOOK*, E0039.
- KERPPOLA, T.K. (2006). DESIGN AND IMPLEMENTATION OF BIMOLECULAR FLUORESCENCE COMPLEMENTATION (BiFC) ASSAYS FOR THE VISUALIZATION OF PROTEIN INTERACTIONS IN LIVING CELLS. *NATURE PROTOCOLS* **1**, 1278-1286.
- KIM, Y.J., LIN, N.C., AND MARTIN, G.B. (2002). TWO DISTINCT *PSEUDOMONAS* EFFECTOR PROTEINS INTERACT WITH THE PTO KINASE AND ACTIVATE PLANT IMMUNITY. *CELL* **109**, 589-598.
- KUNZE, G., ZIPFEL, C., ROBATZEK, S., NIEHAUS, K., BOLLER, T., AND FELIX, G. (2004). THE N TERMINUS OF BACTERIAL ELONGATION FACTOR TU ELICITS INNATE IMMUNITY IN *ARABIDOPSIS* PLANTS. *THE PLANT CELL ONLINE* **16**, 3496-3507.
- LAEMMLI, U.K. (1970). CLEAVAGE OF STRUCTURAL PROTEINS DURING THE ASSEMBLY OF THE HEAD OF BACTERIOPHAGE T4. *NATURE* **227**, 680-685.
- LAMPARD, G.R., MACALISTER, C.A., AND BERGMANN, D.C. (2008). *ARABIDOPSIS* STOMATAL INITIATION IS CONTROLLED BY MAPK-MEDIATED REGULATION OF THE *bHLH* *SPEECHLESS*. *SCIENCE* **322**, 1113-1116.
- LEE, J., RUDD, J.J., MACIOSZEK, V.K., AND SCHEEL, D. (2004). DYNAMIC CHANGES IN THE LOCALIZATION OF MAPK CASCADE COMPONENTS CONTROLLING *PATHOGENESIS-RELATED (PR)* GENE EXPRESSION DURING INNATE IMMUNITY IN PARSLEY. *JOURNAL OF BIOLOGICAL CHEMISTRY* **279**, 22440-22448.
- LEE, J.S., AND ELLIS, B.E. (2007). *ARABIDOPSIS* MAPK PHOSPHATASE 2 (MKP2) POSITIVELY REGULATES OXIDATIVE STRESS TOLERANCE AND INACTIVATES THE MPK3 AND MPK6 MAPKS. *JOURNAL OF BIOLOGICAL CHEMISTRY* **282**, 25020-25029.
- LEE, T.I., AND YOUNG, R.A. (2000). TRANSCRIPTION OF EUKARYOTIC PROTEIN-CODING GENES. *ANNUAL REVIEW OF GENETICS* **34**, 77-137.
- LIU, Y., AND ZHANG, S. (2004). PHOSPHORYLATION OF 1-AMINOCYCLOPROPANE-1-CARBOXYLIC ACID SYNTHASE BY MPK6, A STRESS-RESPONSIVE MITOGEN-ACTIVATED PROTEIN KINASE, INDUCES ETHYLENE BIOSYNTHESIS IN *ARABIDOPSIS*. *THE PLANT CELL* **16**, 3386-3399.

- LOGEMANN, E., BIRKENBIHL, R., ULKER, B., AND SOMSSICH, I.** (2006). AN IMPROVED METHOD FOR PREPARING AGROBACTERIUM CELLS THAT SIMPLIFIES THE ARABIDOPSIS TRANSFORMATION PROTOCOL. *PLANT METHODS* **2**, 16.
- LOTZE, M.T., ZEH, H.J., RUBARTELLI, A., SPARVERO, L.J., AMOSCATO, A.A., WASHBURN, N.R., DEVERA, M.E., LIANG, X., TÖR, M., AND BILLIAR, T.** (2007). THE GRATEFUL DEAD: DAMAGE-ASSOCIATED MOLECULAR PATTERN MOLECULES AND REDUCTION/OXIDATION REGULATE IMMUNITY. *IMMUNOLOGICAL REVIEWS* **220**, 60-81.
- MACKAY, D., AND MCFALL, A.J.** (2006). MAMPS AND MIMPS: PROPOSED CLASSIFICATIONS FOR INDUCERS OF INNATE IMMUNITY. *MOLECULAR MICROBIOLOGY* **61**, 1365-1371.
- MAO, G., MENG, X., LIU, Y., ZHENG, Z., CHEN, Z., AND ZHANG, S.** (2011). PHOSPHORYLATION OF A WRKY TRANSCRIPTION FACTOR BY TWO PATHOGEN-RESPONSIVE MAPKs DRIVES PHYTOALEXIN BIOSYNTHESIS IN ARABIDOPSIS. *THE PLANT CELL ONLINE* **23**, 1639-1653.
- MAROIS, E., VAN DEN ACKERVEKEN, G., AND BONAS, U.** (2002). THE XANTHOMONAS TYPE III EFFECTOR PROTEIN AVRBS3 MODULATES PLANT GENE EXPRESSION AND INDUCES CELL HYPERTROPHY IN THE SUSCEPTIBLE HOST. *MOLECULAR PLANT-MICROBE INTERACTIONS* **15**, 637-646.
- MATSUSHITA, Y., DEGUCHI, M., YODA, M., NISHIGUCHI, M., AND NYUNOYA, H.** (2001). THE TOMATO MOSAIC TOBAMOVIRUS MOVEMENT PROTEIN INTERACTS WITH A PUTATIVE TRANSCRIPTIONAL COACTIVATOR KELP. *MOLECULES AND CELLS* **12**, 57-66.
- MAYANK, P., GROSSMAN, J., WUEST, S., BOISSON-DERNIER, A., ROSCHITZKI, B., NANNI, P., NÜHSE, T., AND GROSSNIKLAUS, U.** (2012). CHARACTERIZATION OF THE PHOSPHOPROTEOME OF MATURE ARABIDOPSIS POLLEN. *THE PLANT JOURNAL* **72**, 89-101.
- MERKOUROPOULOS, G., ANDREASSON, E., HESS, D., BOLLER, T., AND PECK, S.C.** (2008). AN ARABIDOPSIS PROTEIN PHOSPHORYLATED IN RESPONSE TO MICROBIAL ELICITATION, ATPHOS32, IS A SUBSTRATE OF MAP KINASES 3 AND 6. *JOURNAL OF BIOLOGICAL CHEMISTRY* **283**, 10493-10499.
- MIAO, Y., LAUN, T., SMYKOWSKI, A., AND ZENTGRAF, U.** (2007). ARABIDOPSIS MEKK1 CAN TAKE A SHORT CUT: IT CAN DIRECTLY INTERACT WITH SENESCENCE-RELATED WRKY53 TRANSCRIPTION FACTOR ON THE PROTEIN LEVEL AND CAN BIND TO ITS PROMOTER. *PLANT MOLECULAR BIOLOGY* **65**, 63-76.
- MIYA, A., ALBERT, P., SHINYA, T., DESAKI, Y., ICHIMURA, K., SHIRASU, K., NARUSAKA, Y., KAWAKAMI, N., KAKU, H., AND SHIBUYA, N.** (2007). CERK1, A LYSM RECEPTOR KINASE, IS ESSENTIAL FOR CHITIN ELICITOR SIGNALING IN ARABIDOPSIS. *PROCEEDINGS OF THE NATIONAL ACADEMY OF SCIENCES* **104**, 19613-19618.
- NAKAGAMI, H., SOUKUPOVÁ, H., SCHIKORA, A., ZÁRSKÝ, V., AND HIRT, H.** (2006). A MITOGEN-ACTIVATED PROTEIN KINASE KINASE KINASE MEDIATES REACTIVE OXYGEN SPECIES HOMEOSTASIS IN ARABIDOPSIS. *JOURNAL OF BIOLOGICAL CHEMISTRY* **281**, 38697-38704.
- NAKAGAWA, T., KUROSE, T., HINO, T., TANAKA, K., KAWAMUKAI, M., NIWA, Y., TOYOOKA, K., MATSUOKA, K., JINBO, T., AND KIMURA, T.** (2007). DEVELOPMENT OF SERIES OF GATEWAY BINARY VECTORS, pGWBS, FOR REALIZING EFFICIENT CONSTRUCTION OF FUSION GENES FOR PLANT TRANSFORMATION. *JOURNAL OF BIOSCIENCE AND BIOENGINEERING* **104**, 34-41.
- NEILL, S.J., DESIKAN, R., CLARKE, A., HURST, R.D., AND HANCOCK, J.T.** (2002). HYDROGEN PEROXIDE AND NITRIC OXIDE AS SIGNALLING MOLECULES IN PLANTS. *JOURNAL OF EXPERIMENTAL BOTANY* **53**, 1237-1247.
- NISHI, H., HASHIMOTO, K., AND PANCHENKO, ANNA R.** (2011). PHOSPHORYLATION IN PROTEIN-PROTEIN BINDING: EFFECT ON STABILITY AND FUNCTION. *STRUCTURE (LONDON, ENGLAND : 1993)* **19**, 1807-1815.
- NURMBERG, P.L., KNOX, K.A., YUN, B.-W., MORRIS, P.C., SHAFIEI, R., HUDSON, A., AND LOAKE, G.J.** (2007). THE DEVELOPMENTAL SELECTOR AS1 IS AN EVOLUTIONARILY CONSERVED REGULATOR OF THE PLANT IMMUNE RESPONSE. *PROCEEDINGS OF THE NATIONAL ACADEMY OF SCIENCES* **104**, 18795-18800.
- PALANISWAMY, S.K., JAMES, S., SUN, H., LAMB, R.S., DAVULURI, R.V., AND GROTEWOLD, E.** (2006). AGRIS AND ATREGNET. A PLATFORM TO LINK CIS-REGULATORY ELEMENTS AND TRANSCRIPTION FACTORS INTO REGULATORY NETWORKS. *PLANT PHYSIOLOGY* **140**, 818-829.

- PALM-FORSTER, M.A.T., ESCHEN-LIPPOLD, L., AND LEE, J.** (2012). A MUTAGENESIS-BASED SCREEN TO RAPIDLY IDENTIFY PHOSPHORYLATION SITES IN MITOGEN-ACTIVATED PROTEIN KINASE SUBSTRATES. *ANALYTICAL BIOCHEMISTRY* **427**, 127-129.
- PETERSEN, K., QIU, J.L., LUTJE, J., FIIL, B.K., HANSEN, S., MUNDY, J., AND PETERSEN, M.** (2010). ARABIDOPSIS MKS1 IS INVOLVED IN BASAL IMMUNITY AND REQUIRES AN INTACT N-TERMINAL DOMAIN FOR PROPER FUNCTION. *PLOS ONE* **5**, E14364.
- PETERSEN, M., BRODERSEN, P., NAESTED, H., ANDREASSON, E., LINDHART, U., JOHANSEN, B., NIELSEN, H.B., LACY, M., AUSTIN, M.J., PARKER, J.E., SHARMA, S.B., KLESSIG, D.F., MARTIENSSON, R., MATTSSON, O., JENSEN, A.B., AND MUNDY, J.** (2000). ARABIDOPSIS MAP KINASE 4 NEGATIVELY REGULATES SYSTEMIC ACQUIRED RESISTANCE. *CELL* **103**, 1111-1120.
- PETUTSCHNIG, E.K., JONES, A.M., SERAZETDINOVA, L., LIPKA, U., AND LIPKA, V.** (2010). THE LYSIN MOTIF RECEPTOR-LIKE KINASE (LYSM-RLK) CERK1 IS A MAJOR CHITIN-BINDING PROTEIN IN ARABIDOPSIS THALIANA AND SUBJECT TO CHITIN-INDUCED PHOSPHORYLATION. *JOURNAL OF BIOLOGICAL CHEMISTRY* **285**, 28902-28911.
- PIETERSE, C.M.J., LEON-REYES, A., VAN DER ENT, S., AND VAN WEES, S.C.M.** (2009). NETWORKING BY SMALL-MOLECULE HORMONES IN PLANT IMMUNITY. *NATURE CHEMICAL BIOLOGY* **5**, 308-316.
- PITZSCHKE, A., SCHIKORA, A., AND HIRT, H.** (2009). MAPK CASCADE SIGNALLING NETWORKS IN PLANT DEFENCE. *CURRENT OPINION IN PLANT BIOLOGY* **12**, 421-426.
- QIU, J.L., FIIL, B.K., PETERSEN, K., NIELSEN, H.B., BOTANGA, C.J., THORGRIMSEN, S., PALMA, K., SUAREZ-RODRIGUEZ, M.C., SANDBECH-CLAUSEN, S., LICHOTA, J., BRODERSEN, P., GRASSER, K.D., MATTSSON, O., GLAZEBROOK, J., MUNDY, J., AND PETERSEN, M.** (2008). ARABIDOPSIS MAP KINASE 4 REGULATES GENE EXPRESSION THROUGH TRANSCRIPTION FACTOR RELEASE IN THE NUCLEUS. *EMBO JOURNAL* **27**, 2214-2221.
- RANF, S., ESCHEN-LIPPOLD, L., PECHER, P., LEE, J., AND SCHEEL, D.** (2011). INTERPLAY BETWEEN CALCIUM SIGNALLING AND EARLY SIGNALLING ELEMENTS DURING DEFENCE RESPONSES TO MICROBE- OR DAMAGE-ASSOCIATED MOLECULAR PATTERNS. *THE PLANT JOURNAL* **68**, 100-113.
- REINDERS, J., AND SICKMANN, A.** (2005). STATE-OF-THE-ART IN PHOSPHOPROTEOMICS. *PROTEOMICS* **5**, 4052-4061.
- ROBATZEK, S., CHINCHILLA, D., AND BOLLER, T.** (2006). LIGAND-INDUCED ENDOCYTOSIS OF THE PATTERN RECOGNITION RECEPTOR FLS2 IN ARABIDOPSIS. *GENES & DEVELOPMENT* **20**, 537-542.
- ROBBINS, D.J., ZHEN, E., OWAKI, H., VANDERBILT, C.A., EBERT, D., GEPPERT, T.D., AND COBB, M.H.** (1993). REGULATION AND PROPERTIES OF EXTRACELLULAR SIGNAL-REGULATED PROTEIN KINASES 1 AND 2 *IN VITRO*. *JOURNAL OF BIOLOGICAL CHEMISTRY* **268**, 5097-5106.
- SAMBROOK, J., FRITSCH, E.F., AND MANIATIS, T.** (1989). *MOLECULAR CLONING : A LABORATORY MANUAL*, 2ND ED. (COLD SPRING HARBOR, N.Y. :: COLD SPRING HARBOR LABORATORY).
- SCHIELTL, R.H., AND GIETZ, R.D.** (1989). HIGH EFFICIENCY TRANSFORMATION OF INTACT YEAST CELLS USING SINGLE STRANDED NUCLEIC ACIDS AS A CARRIER. *CURRENT GENETICS* **16**, 339-346.
- SCHMITTGEN, T.D., AND LIVAK, K.J.** (2008). ANALYZING REAL-TIME PCR DATA BY THE COMPARATIVE CT METHOD. *NATURE PROTOCOLS* **3**, 1101-1108.
- SHAN, L., HE, P., LI, J., HESE, A., PECK, S.C., NÜRNBERGER, T., MARTIN, G.B., AND SHEEN, J.** (2008). BACTERIAL EFFECTORS TARGET THE COMMON SIGNALING PARTNER BAK1 TO DISRUPT MULTIPLE MAMP RECEPTOR-SIGNALING COMPLEXES AND IMPEDE PLANT IMMUNITY. *CELL HOST AND MICROBE* **4**, 17-27.
- SHANG, Y., LI, X., CUI, H., HE, P., THILMONY, R., CHINTAMANANI, S., ZWIESLER-VOLLICK, J., GOPALAN, S., TANG, X., AND ZHOU, J.-M.** (2006). RAR1, A CENTRAL PLAYER IN PLANT IMMUNITY, IS TARGETED BY *PSEUDOMONAS SYRINGAE* EFFECTOR AVR-B. *PROCEEDINGS OF THE NATIONAL ACADEMY OF SCIENCES* **103**, 19200-19205.
- SHIU, S.-H., AND BLEECKER, A.B.** (2001). RECEPTOR-LIKE KINASES FROM ARABIDOPSIS FORM A MONOPHYLETIC GENE FAMILY RELATED TO ANIMAL RECEPTOR KINASES. *PROCEEDINGS OF THE NATIONAL ACADEMY OF SCIENCES* **98**, 10763-10768.
- SINGH, K.B.** (1998). TRANSCRIPTIONAL REGULATION IN PLANTS: THE IMPORTANCE OF COMBINATORIAL CONTROL. *PLANT PHYSIOLOGY* **118**, 1111-1120.
- SONG, W.-Y., WANG, G.-L., CHEN, L.-L., KIM, H.-S., PI, L.-Y., HOLSTEN, T., GARDNER, J., WANG, B., ZHAI, W.-X., ZHU, L.-H., FAUQUET, C., AND RONALD, P.** (1995). A RECEPTOR

- KINASE-LIKE PROTEIN ENCODED BY THE RICE DISEASE RESISTANCE GENE, XA21. *SCIENCE* **270**, 1804-1806.
- SUAREZ-RODRIGUEZ, M.C., PETERSEN, M., AND MUNDT, J.** (2010). MITOGEN-ACTIVATED PROTEIN KINASE SIGNALING IN PLANTS. *ANNUAL REVIEW OF PLANT BIOLOGY* **61**, 621-649.
- TAKAHASHI, F., MIZOGUCHI, T., YOSHIDA, R., ICHIMURA, K., AND SHINOZAKI, K.** (2011). CALMODULIN-DEPENDENT ACTIVATION OF MAP KINASE FOR ROS HOMEOSTASIS IN ARABIDOPSIS. *MOLECULAR CELL* **41**, 649-660.
- TEIGE, M., SCHEIKL, E., EULGEM, T., DÓCZI, R., ICHIMURA, K., SHINOZAKI, K., DANGL, J.L., AND HIRT, H.** (2004). THE MKK2 PATHWAY MEDIATES COLD AND SALT STRESS SIGNALING IN ARABIDOPSIS. *MOLECULAR CELL* **15**, 141-152.
- TENA, G., BOUDSOCQ, M., AND SHEEN, J.** (2011). PROTEIN KINASE SIGNALING NETWORKS IN PLANT INNATE IMMUNITY. *CURRENT OPINION IN PLANT BIOLOGY* **14**, 519-529.
- UBERSAX, J.A., AND FERRELL JR, J.E.** (2007). MECHANISMS OF SPECIFICITY IN PROTEIN PHOSPHORYLATION. *NATURE REVIEWS MOLECULAR CELL BIOLOGY* **8**, 530-541.
- WALTER, M., CHABAN, C., SCHÜTZE, K., BATISTIC, O., WECKERMANN, K., NÄKE, C., BLAZEVIC, D., GREFFEN, C., SCHUMACHER, K., OECKING, C., HARTER, K., AND KUDLA, J.** (2004). VISUALIZATION OF PROTEIN INTERACTIONS IN LIVING PLANT CELLS USING BIMOLECULAR FLUORESCENCE COMPLEMENTATION. *THE PLANT JOURNAL* **40**, 428-438.
- WAN, J., ZHANG, S., AND STACEY, G.** (2004). ACTIVATION OF A MITOGEN-ACTIVATED PROTEIN KINASE PATHWAY IN ARABIDOPSIS BY CHITIN. *MOLECULAR PLANT PATHOLOGY* **5**, 125-135.
- WAN, J., ZHANG, X.C., AND STACEY, G.** (2008A). CHITIN SIGNALING AND PLANT DISEASE RESISTANCE. *PLANT SIGNALING AND BEHAVIOUR* **3**, 831-833.
- WAN, J., ZHANG, X.-C., NEECE, D., RAMONELL, K.M., CLOUGH, S., KIM, S.-Y., STACEY, M.G., AND STACEY, G.** (2008B). A LYSM RECEPTOR-LIKE KINASE PLAYS A CRITICAL ROLE IN CHITIN SIGNALING AND FUNGAL RESISTANCE IN ARABIDOPSIS. *THE PLANT CELL ONLINE* **20**, 471-481.
- WANG, H., NGWENYAMA, N., LIU, Y., WALKER, J.C., AND ZHANG, S.** (2007). STOMATAL DEVELOPMENT AND PATTERNING ARE REGULATED BY ENVIRONMENTALLY RESPONSIVE MITOGEN-ACTIVATED PROTEIN KINASES IN ARABIDOPSIS. *THE PLANT CELL ONLINE* **19**, 63-73.
- WANG, H., LIU, Y., BRUFFETT, K., LEE, J., HAUSE, G., WALKER, J.C., AND ZHANG, S.** (2008). HAPLO-INSUFFICIENCY OF MPK3 IN MPK6 MUTANT BACKGROUND UNCOVERS A NOVEL FUNCTION OF THESE TWO MAPKS IN ARABIDOPSIS OVULE DEVELOPMENT. *THE PLANT CELL* **20**, 602-613.
- WANG, P., DU, Y., LI, Y., REN, D., AND SONG, C.-P.** (2010). HYDROGEN PEROXIDE-MEDIATED ACTIVATION OF MAP KINASE 6 MODULATES NITRIC OXIDE BIOSYNTHESIS AND SIGNAL TRANSDUCTION IN ARABIDOPSIS. *THE PLANT CELL ONLINE* **22**, 2981-2998.
- WIEMER, M., FEYS, B.J., AND PARKER, J.E.** (2005). PLANT IMMUNITY: THE EDS1 REGULATORY NODE. *CURRENT OPINION IN PLANT BIOLOGY* **8**, 383-389.
- WINTER, D., VINEGAR, B., NAHAL, H., AMMAR, R., WILSON, G.V., AND PROVART, N.J.** (2007). AN "ELECTRONIC FLUORESCENT PICTOGRAPH" BROWSER FOR EXPLORING AND ANALYZING LARGE-SCALE BIOLOGICAL DATA SETS. *PLOS ONE* **2**, E718.
- XIANG, T., ZONG, N., ZOU, Y., WU, Y., ZHANG, J., XING, W., LI, Y., TANG, X., ZHU, L., CHAI, J., AND ZHOU, J.-M.** (2008). *PSEUDOMONAS SYRINGAE* EFFECTOR AVRPTO BLOCKS INNATE IMMUNITY BY TARGETING RECEPTOR KINASES. *CURRENT BIOLOGY* **18**, 74-80.
- XING, Y., JIA, W., AND ZHANG, J.** (2008). ATMKK1 MEDIATES ABA-INDUCED *CAT1* EXPRESSION AND H₂O₂ PRODUCTION VIA ATMPK6-COUPLED SIGNALING IN ARABIDOPSIS. *THE PLANT JOURNAL* **54**, 440-451.
- YOO, S.-D., CHO, Y.-H., AND SHEEN, J.** (2007). ARABIDOPSIS MESOPHYLL PROTOPLASTS: A VERSATILE CELL SYSTEM FOR TRANSIENT GENE EXPRESSION ANALYSIS. *NATURE PROTOCOLS* **2**, 1565-1572.
- YOO, S.D., CHO, Y.H., TENA, G., XIONG, Y., AND SHEEN, J.** (2008). DUAL CONTROL OF NUCLEAR EIN3 BY BIFURCATE MAPK CASCADES IN C₂H₄ SIGNALING. *NATURE* **451**, 789-795.
- YOSHIOKA, K.** (2004). SCAFFOLD PROTEINS IN MAMMALIAN MAP KINASE CASCADES. *JOURNAL OF BIOCHEMISTRY* **135**, 657-661.
- ZENG, Q., CHEN, J.-G., AND ELLIS, B.E.** (2011). ATMPK4 IS REQUIRED FOR MALE-SPECIFIC MEIOTIC CYTOKINESIS IN ARABIDOPSIS. *THE PLANT JOURNAL* **67**, 895-906.

- ZENG, W., AND HE, S.Y.** (2010). A PROMINENT ROLE OF THE FLAGELLIN RECEPTOR FLAGELLIN-SENSING2 IN MEDIATING STOMATAL RESPONSE TO *PSEUDOMONAS SYRINGAE* PV. *TOMATO DC3000* IN ARABIDOPSIS. *PLANT PHYSIOLOGY* **153**, 1188-1198.
- ZHANG, J., SHAO, F., LI, Y., CUI, H., CHEN, L., LI, H., ZOU, Y., LONG, C., LAN, L., CHAI, J., CHEN, S., TANG, X., AND ZHOU, J.M.** (2007). A *PSEUDOMONAS SYRINGAE* EFFECTOR INACTIVATES MAPKs TO SUPPRESS PAMP-INDUCED IMMUNITY IN PLANTS. *CELL HOST MICROBE* **1**, 175-185.
- ZHANG, Z., WU, Y., GAO, M., ZHANG, J., KONG, Q., LIU, Y., BA, H., ZHOU, J., AND ZHANG, Y.** (2012). DISRUPTION OF PAMP-INDUCED MAP KINASE CASCADE BY A *PSEUDOMONAS SYRINGAE* EFFECTOR ACTIVATES PLANT IMMUNITY MEDIATED BY THE NB-LRR PROTEIN SUMM2. *CELL HOST MICROBE* **11**, 253-263.
- ZHOU, C., CAI, Z., GUO, Y., AND GAN, S.** (2009A). AN ARABIDOPSIS MITOGEN-ACTIVATED PROTEIN KINASE CASCADE, MKK9-MPK6, PLAYS A ROLE IN LEAF SENESCENCE. *PLANT PHYSIOL* **150**, 167-177.
- ZHOU, L., FU, Y., AND YANG, Z.** (2009B). A GENOME-WIDE FUNCTIONAL CHARACTERIZATION OF ARABIDOPSIS REGULATORY CALCIUM SENSORS IN POLLEN TUBES. *JOURNAL OF INTEGRATIVE PLANT BIOLOGY* **51**, 751-761.
- ZIMMERMANN, P., HIRSCH-HOFFMANN, M., HENNIG, L., AND GRUISSEM, W.** (2004). GENEVESTIGATOR. ARABIDOPSIS MICROARRAY DATABASE AND ANALYSIS TOOLBOX. *PLANT PHYSIOLOGY* **136**, 2621-2632.
- ZIPFEL, C., ROBATZEK, S., NAVARRO, L., OAKELEY, E.J., JONES, J.D.G., FELIX, G., AND BOLLER, T.** (2004). BACTERIAL DISEASE RESISTANCE IN ARABIDOPSIS THROUGH FLAGELLIN PERCEPTION. *NATURE* **428**, 764-767.
- ZIPFEL, C., KUNZE, G., CHINCHILLA, D., CANIARD, A., JONES, J.D.G., BOLLER, T., AND FELIX, G.** (2006). PERCEPTION OF THE BACTERIAL PAMP EF-TU BY THE RECEPTOR EFR RESTRICTS AGROBACTERIUM-MEDIATED TRANSFORMATION. *CELL* **125**, 749-760.

Declaration

I hereby declare that I have written this dissertation independently and the content contained within is solely based on my work as a Ph.D. student of Martin-Luther-Universität Halle-Wittenberg. All resources that were utilised during this study were cited and any assistance received is acknowledged accordingly.

I hereby submit this dissertation for examination for Dr.rer.nat. exclusively to the Martin-Luther-Universität Halle-Wittenberg. I also certify that it has never been submitted to other faculties or universities for examination.

Halle (Saale), February 2013

Mieder A. T. Palm-Forster

VIII. Erratum

- I. An error was observed for Fig. 10 (Page 44). The middle graph depicting the promoter activity of *PH1* was unintentionally duplicated from the graph on the left (*PRP* promoter activity). The figure below now displays the correct graph representing the promoter activity of *PH1*.

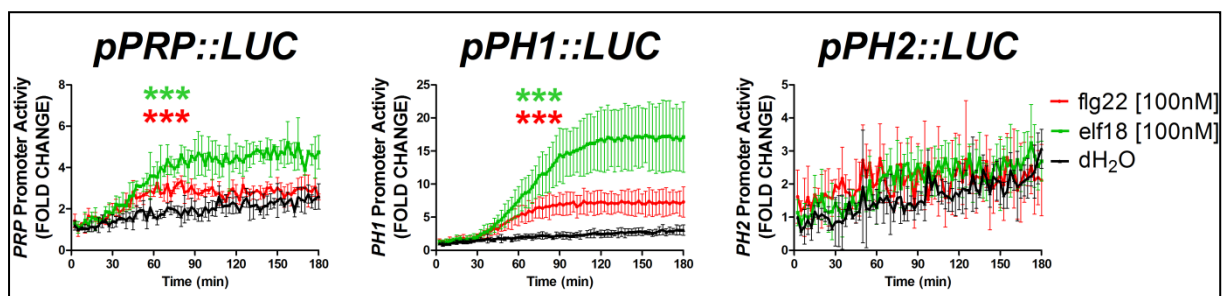


Fig. 10: Promoter activity of PRP, PH1 and PH2 after treatment with flg22 [100nM], elf18 [100nM] and dH₂O. The figure depicts representative data seen in three independent experiments (n=3). *Promoter::luciferase* fusion constructs were co-transformed with a *pUBQ10::GUS* construct into mesophyll protoplasts from *A. thaliana* (Col-0). Promoter activity is represented as LUC activity normalised to GUS activity. One-way ANOVA was performed and statistically significant differences to the water-treated samples are indicated (***) = p≤0.001).

- II. A method addendum to Section 3: Protein biochemical techniques (Page 23), is given below describing the *in vitro* phosphorylation assay.

3.7 *In vitro* phosphorylation assay

The *in vitro* phosphorylation assay was performed by incubating recombinant Pc-MKK5DD [0.025 µg], MPK3 or MPK6 [0.25 µg], and the putative substrates [2.5µg] in 20µl kinase reaction buffer (Hepes [20mM] at pH7.5; MgCl₂ [15mM]; EGTA [5mM]; DTT [1mM]; aprotinin [10µg/ml]; leupeptin [10ug/ml]; γATP [50µCi/ml]) for 30min at 37°C. The reaction was stopped by adding 5X SDS buffer to the reaction.

IX. Curriculum Vitae

Personal Information

Name	Mieder A. T. Palm-Forster
Date of birth	8 March 1982
Gender	Male
Nationality	South African
Address	2434 Forest Road., Lansing, Michigan, 48910, U.S.A.

Education

2001-2003	B.Sc. Biochemistry (2003). University of the Free State, Bloemfontein, South Africa.
2004	B.Sc.Hons. Biochemistry (2004). University of the Free State, Bloemfontein, South Africa.
2005-2008	M.Sc. Biochemistry (2008). University of the Free State, Bloemfontein, South Africa.
2008-2012	Ph.D. Plant Biology and Biochemistry (2012). Department of Stress and Developmental Biology, Leibniz Institute for Plant Biochemistry, Halle Saale, Germany

Publications

1. Palm-Forster, M.A.T., Eschen-Lippold, L., and Lee, J. (2012). A mutagenesis-based screen to rapidly identify phosphorylation sites in mitogen-activated protein kinase substrates. *Analytical Biochemistry* 427, 127-129.
2. Eschen-Lippold, L., Bethke, G., Palm-Forster, M., Pecher, P., Bauer, N., Glazebrook, J., Scheel, D., and Lee, J. (2012). MAPK11-a fourth elicitor-responsive mitogen-activated protein kinase in *Arabidopsis thaliana*. *Plant Signal Behav* 7.

Halle (Saale), February 2013

Mieder A. T. Palm-Forster